

Development of New Reactors for the Photocatalytic Treatment of Polluted Aquifers

Von der Naturwissenschaftlichen Fakultät
der Gottfried Wilhelm Leibniz Universität Hannover

zur Erlangung des Grades

Doktorin der Naturwissenschaften
(Dr. rer. nat.)

genehmigte Dissertation von

Lena Megatif, M. Sc. (Iran)

2019

Referent: apl. Prof. Dr. rer. nat. habil. Detlef W. Bahnemann

Korreferent: Prof. Dr. rer. nat. Jürgen Caro

Tag der Promotion: 17.10.2019

Acknowledgments

First and foremost I would like to sincerely thank Prof. Dr. Detlef Bahnemann for his support and supervision of this research and giving me absolute freedom for developing my ideas. I appreciate all his contributions of time and ideas to make my Ph.D. experience productive and stimulating.

I would also like to thank Dr. Ralf Dillert for his support, valuable guidance and the productive discussions.

I am thankful of Prof. Dr. Jürgen Caro for his time and kind acceptance of my PhD thesis revision and being my co-referee.

I would like to acknowledge Prof. Dr. Thomas Scheper as well for the opportunity to do my doctorate at the institute of technical chemistry and for being the head of my examination committee.

I also acknowledge the financial support of the Deutscher Akademischer Austausch Dienst (DAAD) by providing me a scholarship during my doctoral studies here in Germany. Also this thesis was printed with the support of the German Academic Exchange Service.

Many thanks go to the colleagues from the Institute of Technical Chemistry, specially the members of the Bahnemann research group for all the helpful discussions in our seminars and for the interesting talks in our office.

My special thanks go to my close friends here in TCI, Sona, Steffi, Carsten, Manuel, Christoph, Ana, Maryam, Camilla, and Fabian, who became my German family over the last few years and made my time in Hannover unforgettable. I will miss every single moment we laughed together.

I would like specially to thank Arsou for her support and standing by my side during all difficult moments throughout my PhD period. She was not only my best friend but also all I have here in Germany.

Finally, I would like to thank my parents for all their love and support throughout my entire study period. My heart is with my beloved father who left us last year. I miss him more than anything and wish he could still be here by my side. My thanks also go to

Mona, Hena, Jana, Amer, Alaa, Nicola, Arkan, Wael, Nael and of course Julia for their encouragements during my research period. This accomplishment would not have been possible without them.

Zusammenfassung

Eine Steigerung der Aktivität photokatalytischer Systeme erfordert eine effiziente Reaktorauslegung und eine geeignete Standardmethode, um die Leistung verschiedener Systeme zu vergleichen. Bei allen Methoden wird die Reaktionsgeschwindigkeit durch die optischen Eigenschaften von Photokatalysatoren durch Reflexion und Streuung beeinflusst. Darüber hinaus erfordert die quantitative Beurteilung der Leistung von photokatalytischen Systemen die Messung der Anzahl der im Reaktor absorbierten Photonen.

In der vorliegenden Arbeit wird ein Standardverfahren zum Vergleich verschiedener Photokatalysatoren unter Verwendung eines Schwarzkörperreaktors vorgeschlagen. In einem Schwarzkörperreaktor wird fast das gesamte in den Reaktor einfallende Licht von den Photokatalysatorpartikeln absorbiert. Daher ist die volumen-gemittelte Reaktionsgeschwindigkeit nahezu unabhängig von den Streuungseigenschaften des Photokatalysators und die photokatalytische Aktivität kann durch Messungen der Reaktionsgeschwindigkeit verglichen werden. Für diese Arbeit wurde Dichloressigsäure (DCA) als Modellschadstoff ausgewählt; Titandioxide und einige andere halbleitende Oxide wurden als Photokatalysatoren eingesetzt. Experimentelle Parameter einschließlich der Anfangskonzentration des Modellschadstoffs (C_0), der Beladung mit dem Photokatalysator (γ) und des Reaktionsvolumens (V) wurden variiert, um eine von den genannten Parametern unabhängige Methode für die vergleichende Bewertung von Photokatalysatoren bereitzustellen. Die Abbaurate von DCA, definiert als die umgewandelte Menge an Molekülen pro Zeiteinheit, erwies sich bei allen Reaktionsvolumina als konstant und unabhängig, wenn C_0 und γ größer als 5 mM bzw. 1 g L⁻¹ waren. Es wurde festgestellt, dass das vorgestellte Verfahren allgemein für verschiedene Photokatalysatoren auf Titan- und Nicht-Titanbasis anwendbar ist. Darüber hinaus wurde zur Ermittlung der Reaktionsgeschwindigkeit eine kinetische Untersuchung sowohl für den Zerfall der Reaktanten als auch für die Produkterzeugung durchgeführt.

Photonenfluss und Photonenflussdichte beeinflussen die Rekombination von Ladungsträgern sehr stark und haben somit auch Einfluss auf die Reaktionsgeschwindigkeit und die Quantenausbeute einer photokatalytischen Reaktion. Der Schwarzkörperreaktor wurde daher auch benutzt, um die Auswirkung der Geometrie des Lichteinlasses auf die Reaktionsgeschwindigkeit und die Quantenausbeute der

photokatalytischen DCA-Oxidation zu untersuchen. Mit einem Lichteinlass, der eine gleichmäßige Lichtverteilung und eine niedrige Photonenflussdichte ermöglichte, wurden konstante Quantenausbeuten ermittelt. Bei hoher Photonenflussdichte wurde jedoch eine Quadratwurzelkorrelation zwischen der Quantenausbeute und dem Photonenfluss beobachtet.

Schlüsselwörter: Schwarzkörperreaktor, Quantenausbeute, Kinetik, heterogenes photokatalytisches System, Dichloressigsäure

Abstract

An enhancement of the activity of photocatalytic systems requires an efficient reactor design and a suitable standard method to compare the performance of various systems. In almost all recommended measuring methods, the reaction rate is affected by the optical properties of photocatalysts through reflection and scattering. Moreover, the quantitative assessment of the performance of photocatalytic systems requires the determination of the amount of absorbed photons inside the photoreactor.

In the present work, a standard method for the comparison of different photocatalysts is proposed employing a black body reactor. In a black body reactor almost the entire incident light will be absorbed by the photocatalyst particles. Therefore, the volume-averaged reaction rate is almost independent from the scattering properties of the photocatalyst and the photocatalytic activity can be compared through reaction rate measurements. In this study, dichloroacetic acid (DCA) was chosen as the probe compound. Titanium dioxide and some other semiconducting oxides were applied as the photocatalysts. Variation of effecting parameters including the initial concentration of the probe molecule (C_0), the photocatalyst loading (γ), and the reaction volume (V) were studied in order to provide a comparison method which is independent from the mentioned parameters. The degradation rate of DCA defined as the converted amount of molecules per unit time was found to be constant at all reaction volumes and independent when C_0 and γ were larger than 5 mM and 1 g L⁻¹, respectively. The presented method was found to be generally applicable for different titanium and non-titanium based photocatalysts. Moreover, to determine the reaction rate, a kinetic study was performed for both, reactants decay and product generation.

Photon flux and photon flux density are known to strongly affect the charge carriers' recombination and, consequently, the reaction rate and the quantum yield. The black body reactor was employed to investigate the impact of the geometry of the light inlet on the reaction rate and on the quantum yield of a photocatalytic reaction. Accordingly, employing a hollow sphere light inlet providing uniform light distribution and low photon flux density, the quantum yield was constant and independent from the photon flux. However, in systems with high photon flux density, a square root correlation between the quantum yield and the photon flux was observed.

Keywords: Black body reactor, Quantum yield, Kinetic analysis, Heterogeneous photocatalytic systems, Dichloroacetic acid

**In Loving Memory of my Father
and my Brother**

Printed with the support of the German Academic Exchange Service

Table of Contents

Acknowledgments	I
Zusammenfassung	III
Abstract	V
1. Introduction and Objectives	1
References	21
2. Reactors for Artificial Photosynthesis in Heterogeneous Systems	27
2.1. Foreword	27
2.2. Introduction	27
2.3. Photoreactors for Heterogeneous Reactions	29
2.4. Reactors based on Mode of Operation	30
2.4.1. Batch Reactors	30
2.4.2. Continuous Reactors	31
2.4.2.1. Plug Flow Reactors	31
2.4.2.2. Continuous Stirred-Tank Reactor (CSTR)	32
2.5. Reactors based on State of the Photocatalyst	32
2.5.1. Slurry Reactors	32
2.5.2. Immobilized Reactors	33
2.6. Reactors Based on the Light Source	33
2.6.1. Solar Irradiation	33
2.6.1.1. Solar Photocatalytic Reactors	34
2.6.1.2. Examples of Solar Reactors	36
2.6.1.2.1. Compound Parabolic Concentrator	36
2.6.1.2.2. A Solar Concentrator for Carbon Dioxide Reduction	39
2.6.1.2.3. Single Bed Colloidal Suspension Reactor	40
2.6.1.2.4. Other Solar Reactors	41
2.6.1.3. Economic Analysis in Solar Photoreactors	43
2.6.2. Artificial light Sources	45
2.6.2.1. Slurry Photoreactors with Artificial Light Sources	45
2.6.2.2. Immobilized Photoreactor with Artificial Light Source	50
2.7. Photocatalytic Reactor Design	58
2.8. Conclusions	61

Table of Contents

2.9. Acknowledgments	62
2.10. References.....	62
3. A Method to Compare the Activities of Semiconductor Photocatalysts in Liquid-Solid Systems	71
3.1. Foreword.....	71
3.2. Abstract.....	72
3.3. Keywords.....	72
3.4. Manuscript.....	72
3.5. Experimental Procedure.....	77
3.6. Acknowledgements.....	78
3.7. References.....	78
4. Determination of the Quantum Yield of a Heterogeneous Photocatalytic Reaction Employing a Black Body Photoreactor	83
4.1. Foreword.....	83
4.2. Abstract.....	84
4.3. Keywords.....	84
4.4. Introduction.....	85
4.5. Materials	87
4.6. Experimental Procedure.....	87
4.7. Results.....	89
4.8. Discussion.....	92
4.9. Conclusions.....	96
4.10. Acknowledgements.....	97
4.11. Reference	97
5. Reaction Rate Study of Photocatalytic Degradation of Dichloroacetic Acid in a Black Body Reactor	101
5.1. Foreword.....	101
5.2. Abstract.....	101
5.3. Keywords.....	102
5.4. Introduction.....	102
5.5. Materials	105
5.6. Experimental Procedure.....	106
5.7. Results.....	106
5.8. Discussion.....	112

5.9. Conclusions	119
5.10. Acknowledgements	120
5.11. References	120
6. Summarizing Discussion	125
6.1. Mechanism of the Photocatalytic Degradation of DCA.....	126
6.2. Reaction Rate Study of Photocatalytic Degradation of DCA	131
6.3. Evaluation of the Quantum Yield in a Black Body Photoreactor	133
6.4. A Standard Method for the Comparison of the Photocatalytic Activities of Semiconducting Materials.....	139
6.5. Photocatalytic Reactor Design	143
6.6. Conclusions	148
6.7. References	151
Publications	159
Journal Publications	159
Oral Presentations	159
Poster Presentations	160
Curriculum Vitae	161

Table of Contents

1. Introduction and Objectives

The accelerated growth of the world's energy demand leading to an excessive consumption of fossil fuels and its disastrous effects on the environment, such as greenhouse gas emissions, global warming, and wastewater pollution have posed serious constraints in recent years. Consequently, concerns about alternative energy sources and attempts to move the world towards a green and sustainable energy pathway have increased during the past several decades. One of the most promising technologies considering green and renewable energy is photocatalysis, which represents a large potential in utilizing the abundant solar energy and addressing the environmental problems of fossil fuel combustion¹⁻³. Photocatalysis was defined by the International Union of Pure Applied Chemistry (IUPAC) as the “change in the rate of a chemical reaction or its initiation under the action of ultraviolet, visible, or infrared radiation in the presence of a substance, the photocatalyst, that absorbs light and is involved in the chemical transformation of the reaction partners”⁴. In heterogeneous photocatalysis, as shown in **Figure 1.1**, semiconductor photocatalysts absorb light within a specific wavelength range, resulting in the excitation of electrons from the valence band to the conduction band. Every excitation of an electron to the conduction band generates a positive hole in the valence band⁵. The photo-generated electrons and holes which act as reasonably reductants and oxidants, respectively, can independently participate in different chemical reactions⁶.

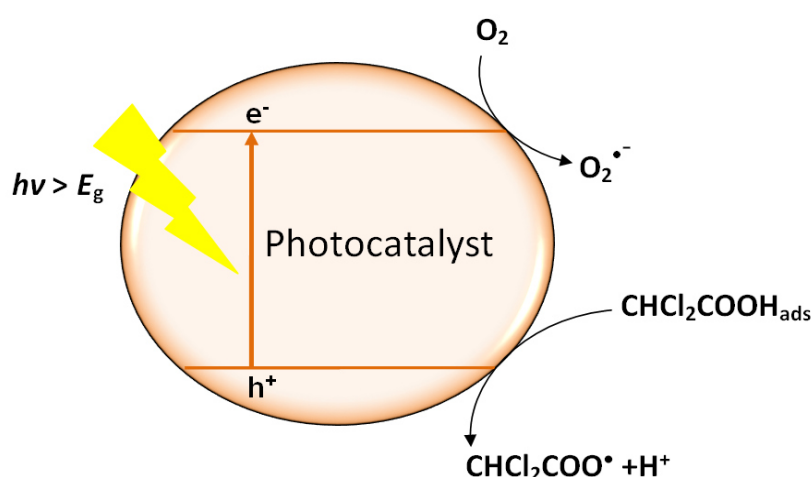


Figure 1.1. Schematic representation of semiconductor photo excitation

1. Introduction and Objectives

Generally, after generating the excited electrons and holes, a large number of electron-hole pairs recombine before migrating to the semiconductor's surface and dissipate the received energy in the form of heat or emitted light¹. This is mainly because of the short life time of the photo generated charge carriers due to the small hole diffusion length⁷. Therefore, in most cases a bare semiconductor is not favorable for the separation of electron-hole pairs. Consequently, co-catalyst nanostructures are commonly employed to enable the holes to migrate to the surface¹.

Pursuing the pioneering work of Fujishima and Honda in 1972⁸, who observed water splitting employing a TiO₂ electrode in a photo-electrochemical cell, photocatalysis gained considerable attention. Intense investigations on the different polymorphs of TiO₂ have been performed to investigate the fundamental principles of photocatalysis^{6,9} and to enhance the photocatalytic efficiency of this group of oxides. Considering the large band gap of TiO₂, UV radiation is required for its excitation. Since only 5 % of the sunlight consists of UV light, TiO₂ cannot utilize the solar illumination properly¹⁰. Therefore, huge efforts have been dedicated to modify TiO₂ and to increase its absorbance. Furthermore, a large number of studies have been carried out to apply the concept of photocatalysis in various areas¹¹. The investigations of the photocatalytic technology are not limited to water splitting and producing molecular hydrogen as a fuel. Photocatalysis is indeed widely discussed and applied for the photo-decomposition or the photo-oxidization of pollutants, for artificial photosynthesis, photo-induced super hydrophilicity, self-cleaning, and photo-electrochemical fuel synthesis¹. The potential applications of photocatalytic processes continue to grow with the increase of the photocatalytic studies dealing with the development of new photocatalysts¹²⁻¹⁵. Despite the significant progress in the development of new photocatalysts, the efficiencies of most photocatalytic processes are still low. Thus, any success to enhance the efficiency of heterogeneous photocatalytic processes will move the application of this technology one step forward as an alternative technology for water purification or energy conversion and storage.

The large scale application of photocatalysis is only achievable if an efficient photocatalyst can be merged with a proper photoreactor design. An ideal photoreactor should be able to harvest the light efficiently. Different types of photoreactors applied for heterogeneous systems are discussed in detail in **Chapter 2**. To be able to design a

photoreactor, initially, the catalyst's efficiency in utilizing the absorbed photons, known as the quantum yield (Φ), needs to be determined accurately.

The quantum yield of heterogeneous photochemical systems is described exactly following to the quantum yield definition in homogenous systems, as the number of defined events divided by the amount of photons absorbed by the catalyst at a specific wavelength (**Equation 1.1-a**)¹⁶.

$$\Phi = \frac{\text{Amount (mol) of conversion/ Stoichiometric coefficient}}{\text{Amount (mol) of monochromatic photons absorbed by the photocatalyst}} = \frac{\xi}{n_{\text{ph}}} \quad (1.1-a)$$

This equation can also be written as a kinetic definition. The quantum yield can be defined as the ratio of the rate of conversion of molecules relatives to the absorbed photon flux at one specific wavelength (**Equation 1.1-b**)¹⁶. This concept enables the evaluation of the catalyst's efficiency and the comparison of different photocatalysts.

$$\Phi = \frac{\text{Rate of conversion (mol/time)}}{\text{Rate of monochromatic photons absorbed by the reaction system (mol/time)}} = \frac{d\xi/dt}{dn_{\text{ph}}/dt} \quad (1.1-b)$$

The reaction rate can be easily determined experimentally by performing the reaction and following the concentration of reactants or products over time.

However, as most types of photoreactors especially solar photoreactors are illuminated from their outside, it is not possible to measure the number of absorbed photons in these heterogeneous systems directly and only the upper limit for the number of absorbed photons which is the number of incident photons is known. This is mainly due to the extinction of radiation through reflection and scattering of the light out of the reactor by the photocatalyst particles¹⁷.

Due to the above mentioned reasons, in addition to the quantum yield, the term photonic yield is used to determine the photocatalytic activity of the semiconductors. Photonic yield is defined in terms of the incident amount of photons of monochromatic light arriving at the internal surface of the irradiation window. In case of employing polychromatic light providing irradiation within a defined wavelength range, the term photonic efficiency is used. Therefore, according to IUPAC, photonic efficiency is defined as the "ratio of the rate of the photoreaction measured for a specified time interval (usually the initial conditions) to the rate of incident photons within a defined wavelength interval inside the irradiation window of the reactor"⁴.

1. Introduction and Objectives

On the other hand, in order to design a fully predictive photocatalytic reactor based on the lab-scale determinations, first the kinetic parameters of the proposed mechanistic model and the rate of photon absorption need to be calculated. Due to the noticeable variation of the rate of photon absorption along the photoreactor, in order to calculate the quantum yield (Φ) according to the **Equation 1.2** at any position of the photoreactor, the local volumetric rate of photon absorption at all positions inside the reactor must be known.

$$\Phi = \frac{r}{e_{\lambda}^a} \quad (1.2)$$

in which r is the reaction rate (mol s^{-1}) and e_{λ}^a is the local volumetric rate of photon absorption (mol s^{-1}). Therefore, solving the radiation transfer equation (RTE) is necessary. This equation considers the geometry and the boundary conditions corresponding to the power and the spectrum of the radiation source and the optical properties of the photocatalytically active material inside the reactor such as the spectral volumetric absorption coefficient, the spectral volumetric scattering coefficient, and the phase function¹⁷.

As shown in **Figure 1.2**, the RTE is the balance between the incident radiation and the rates of absorption, emission, and in and out scattered light (**Equation 1.3**)¹⁸. This equation will be discussed in more detail in **Chapter 2**. In a photoreactor, the number of absorbed photons at each position in the reactor is different. However, it can be calculated using the RTE, provided that the relevant parameters such as incident light intensity, rate of photon absorption, rate of photon emission, rate of photon in-scattering and rate of photon out-scattering per unit time, unit volume, unit solid angle, and unit frequency interval are known.

$$\frac{1}{c} \frac{\partial I_{\Omega,v}}{\partial t} + \nabla \cdot (I_{\Omega,v} \Omega) = -W_{\Omega,v}^{\text{absorption}} + W_{\Omega,v}^{\text{emission}} + W_{\Omega,v}^{\text{in-scattering}} - W_{\Omega,v}^{\text{out-scattering}} \quad (1.3)$$

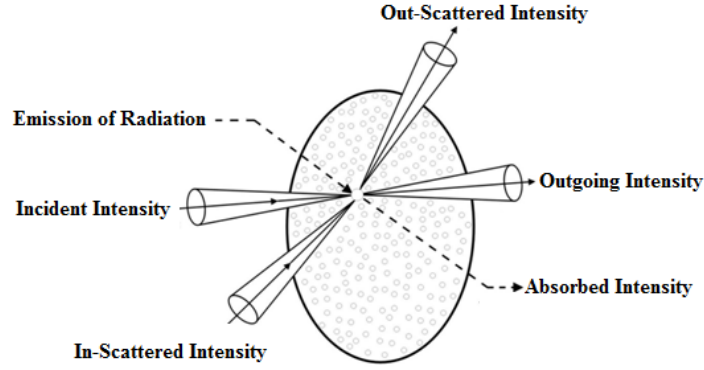


Figure 1.2. Schematic representation of the absorption, emission and scattering phenomena in radiation transport¹⁹. Adapted from Ref 19 Copyright (1993) with permission from Elsevier

All the mentioned source and sink terms are expressed by constitutive equations. To determine the absorption, the linear isotropic constitutive equations can be used:

$$W_{\Omega, \nu}^{\text{absorption}} = k_{\lambda}(x, t) I_{\lambda}(x, t) \quad (1.4)$$

where k_{λ} is the spectral volumetric absorption coefficient (length^{-1}), I_{λ} is the spectral radiation intensity defined as the amount of radiative energy per unit wavelength interval, per unit solid angle, per unit normal area, and per unit time, and λ , x and t represent the wavelength, position, and the time respectively.

The emission of radiation is related to planck's black-body radiation intensity²⁰:

$$W_{\Omega, \nu}^{\text{emission}} = k_{\lambda}(x, t) I_{\lambda}[T(x, t)] \quad (1.5)$$

Here k_{λ} is the spectral volumetric absorption coefficient (length^{-1}), I_{λ} is the black-body radiation intensity at temperature T .

Linear constitutive equation is also used to represent the out-scattering of radiation:

$$W_{\Omega, \nu}^{\text{out-scattering}} = \sigma_{\lambda}(x, t) I_{\lambda}(x, t) \quad (1.6)$$

where σ_{λ} is the spectral volumetric scattering coefficient and has the unit of length^{-1} . However, the directional distribution of scattered radiation is not considered in **Equation 1.6** and can be described by using a phase function. Finally, the in-scattering term which represents the scattered light inside the reactor in all directions according to the phase function can be written as:

1. Introduction and Objectives

$$W_{\Omega,\lambda}^{\text{in-scattering}} = \frac{1}{4\pi} \int_{4\pi} \sigma_{\lambda}(x, t) p_{\lambda}(\hat{\Omega} \rightarrow \Omega) I_{\hat{\Omega},\lambda}(x, t) d\hat{\Omega} \quad (1.7)$$

in which $p_{\lambda}(\hat{\Omega} \rightarrow \Omega)$ is the phase function describing the directional distribution of scattered radiation^{20,21}.

To simplify solving the RTE, it can be assumed that the factor $1/c$ is very low (in **Equation 1.3**), thus the first term on the left can be neglected. It can also be assumed that at a given time the radiation field reaches the steady state immediately²⁰:

$$\frac{1}{c} \frac{\partial I_{\Omega,\lambda}}{\partial t} \cong 0 \quad (1.8)$$

Moreover, the term $W_{\Omega,\nu}^{\text{emission}}$ can also be neglected since in general, the radiation emission is not so significant at low temperatures. With these assumptions, the RTE can be given as:

$$\frac{dI_{\Omega,\lambda}(s,t)}{ds} = [k_{\lambda}(s, t) + \sigma_{\lambda}(s, t)]I_{\Omega,\lambda}(s, t) + \frac{\sigma_{\lambda}(s,t)}{4\pi} \int_{4\pi} p_{\lambda}(\hat{\Omega} \rightarrow \Omega) I_{\hat{\Omega},\lambda}(s, t) d\hat{\Omega} \quad (1.9)$$

By determining the radiation field inside the reactor, the spectral incident radiation at any position of the system can be estimated. Through integration of these values along the whole photoreactor the volume-averaged values of the photon absorption in the reactor will be obtained which are then used to calculate the quantum yield. Therefore, in order to be able to design a photoreactor, having the volume-averaged values of quantum yield is essential. Considering the complexity and time consuming calculations of the volume-averaged quantum yield, discovering a simple method to determine this term is of great importance.

Moreover, enhancing the photocatalytic activity of photocatalysts initially requires a suitable way to compare the performance of different photocatalyst materials. Apart from the low photonic efficiency of the photocatalytic reactions (less than ~1 %)²², finding a standard method to compare the activity of photocatalytic nano materials is also a big challenge.

The international standards organisation (ISO) and European committee for standardization (CEN/TC 386) have introduced a series of standards for quantification of performance ability of the semiconductors²³⁻²⁹. These standards include: air purification (specifically, the removal of NO, acetaldehyde and toluene), water purification (the

photobleaching of methylene blue and oxidation of DMSO), self-cleaning surfaces (the removal of oleic acid and subsequent change in water droplet contact angle), photosterilisation (specifically probing the antibacterial action of semiconductor photocatalyst films), and UV light sources for semiconductor photocatalytic ISO work³⁰. CEN/TC 386 has also tried to address the need of evaluation of semiconductor photocatalysts by presenting irradiation conditions required for testing photocatalytic properties of semiconducting materials and for the measurement of these conditions³¹. These methods enable the quantitative measurement of photocatalytic activity of a material. However, each individual sub-test requires expensive analytical equipments³².

In photoelectrochemical (PEC) systems, the so-called solar-to-hydrogen conversion efficiency (STH), defined as the ratio of chemical energy of the generated molecular hydrogen to the total incident light energy, is the most important term to calculate the overall efficiency of PEC devices³³. The STH can, in principle, be obtained through integration of the respective quantum efficiencies over the entire wavelength range. Yet, significant attention should be paid to the fact that, depending on the incident wavelength, the values of energy efficiency and quantum efficiency do not provide the same information. As an example, in order to yield hydrogen (1.23 eV), more than half of the high energy of each UV photon (≥ 3.1 eV) will be dissipated³⁴. On the other hand, to check a material's intrinsic activities, applied bias photon to current efficiency (ABPE), external quantum efficiency expressed as the incident photon to current efficiency (IPCE) or internal quantum efficiency represented as the absorbed photon to current efficiency (APCE) are recommended to be measured^{33,35}.

The best practices for the determination of the intrinsic performance of photocatalysts are repeatedly discussed within the photocatalysis community. However, in heterogeneous photocatalytic systems, the comparison of the photocatalyst's performances is still complicated, due to the contradictions in the reported results. According to a recommendation published by the IUPAC, the quantum yield should be used to quantify the efficiency of photocatalytic processes⁴. The quantum yield is one of the fundamental quantities for the comparison of photochemical reactions and for the activity of various photocatalysts³⁶.

Due to the above mentioned difficulties regarding the quantum yield measurements, in a large number of publications only rate constants are reported. In this case, it is almost

1. Introduction and Objectives

impossible to compare the photoactivity of various photocatalysts. The rate constants measured in different laboratories are thus not comparable due to their dependency on the respective temperature, reactant and product concentrations, photon flux, light path, extinction and absorption coefficients³⁷. Presenting the photocatalytic activity alternatively as reaction rates per weight and surface area also does not reflect the true intrinsic photocatalytic activity of the materials. The rate per weight depends on the catalyst loading and it is not comparable even in the same photoreactor. The rate per surface area depends also on the catalyst loading. Although separation of charge carriers depends on the surface area, the rate per surface area does not yield the photocatalytic efficiency³⁴. The specific surface area can affect the reaction rate from two points of view. An increase in surface area enhances the adsorption of substrates at the surface of the photocatalyst hence increasing the reaction rate. However, often an increase of the surface area also results in an increase of the surface defects leading to an increase of the recombination rate of the charge carriers, thus decrease the photocatalytic reaction rate³⁸.

To solve this problem for heterogeneous photoreactions, Kisch and Bahnemann proposed a method for the comparison of photocatalytic activities. They recommended that “for solid/liquid systems, that is, suspensions of semiconductor powders in dissolved substrate, optimal reaction rates should be measured with the same type of photoreactor under identical irradiation conditions”³⁷. However, this proposed general procedure does not allow a comparison of data obtained in different laboratories with different experimental set-ups. Due to the difficulties of having the same external irradiation conditions, this method is actually only valid for the comparison of photocatalysts within one laboratory. Moreover, some factors such as effect of initial concentration of the probe molecule and reaction volume are still needed to be considered. Therefore, comparing the data obtained from different laboratories could be problematic.

A quantitative methods for the comparison of the activities of photocatalysts using the principle of the turnover number was proposed by Serpone *et al.*³⁹. The application of the turnover number and other related terms such as turnover rate and turnover frequency in heterogeneous catalysis was reported for the first time by Boudart *et al.* in 1966⁴⁰. In photocatalysis, the turnover number is defined as the number of photoinduced conversions for a given period of time related to the number of photocatalytic sites⁴¹. The turnover rate represents the ratio of the number of the reacted or produced molecules to

the number of photocatalytic active centers in a system per unit time, while the turnover frequency is the number of converted molecules per active sites per unit time^{41,42}. However, turnover quantities are not ideal parameters for the photoactivity comparison of different photocatalysts⁴¹ due to their dependency on temperature and concentration as mentioned by Laidler⁴³. Moreover, the determination of the number of photocatalytically active sites is complicated, since internal shading leads to some dark spots in the system. Consequently, the real operating surfaces are not easy to determine⁴. Furthermore, the number of active sites may change upon illumination and new active sites on the semiconductor particles can be generated. A change of the number of absorbed/desorbed probe molecules during the irradiation is also possible³⁹. Therefore, considering the light dependency of turnover terms, using this method to determine and compare the photocatalytic activities, requires light distribution calculations inside the photoreactor, which is time consuming.

Maschmeyer and Che have also suggested ranking the photocatalysts according to the turnover rate at their optimum capacity (non-diffusion-limited regime). This parameter can then be expressed as moles of molecular hydrogen per hour and gram or per hour and square meter of catalyst surface, from which the photonic efficiencies are derived. This simple method is recommended to be applied towards comparable data of photonic efficiencies for molecular hydrogen production through a photocatalytic process^{44,45}. They suggested to determine the photonic efficiency under a condition where the light absorption changes linearly with the catalyst loading (**Figure 1.3**, regime I)⁴⁶, because only under this condition the intrinsic activity (turnover rate) of the photocatalysts and the optimum activity of their catalytically active sites can be measured⁴⁶. In contrast, according to Kisch, the comparison of photocatalytic reactions at the onset range of the plateau region is more meaningful (**Figure 1.3**, regime II)⁴⁵. This region is assumed to be representing catalyst loadings assuring constant and optimal light absorption. As reported by Kisch, “the underlying premise that in any heterogeneous catalytic reaction a doubling of the catalyst concentration leads to a doubling of the observable rate in the non-diffusion-limited regime does not hold for a heterogeneous photocatalytic reaction”⁴⁵. Since both the reaction rate and the amount of absorbed light depend strongly on the catalyst concentration, the comparison of activities needs to be conducted at zero order conditions regarding the catalyst loading. Once the observed reaction rate is found to be independent from the catalyst concentration, it can be assumed that the system has

1. Introduction and Objectives

reached its maximal level of light absorption and is also not restricted by any diffusion limitations⁴⁵. Therefore, under these conditions the light absorption reaches an optimum point enabling the quantitative comparison of the photocatalytic activities of different catalysts.

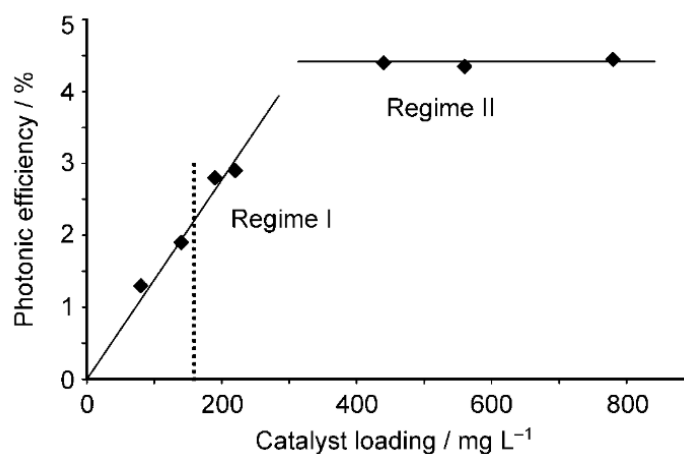


Figure 1.3. Photonic efficiency versus catalyst loading⁴⁶. Reproduced with permission from Ref 46.

Copyright (2010) Wiley-VCH Verlag GmbH & Co. KGaA

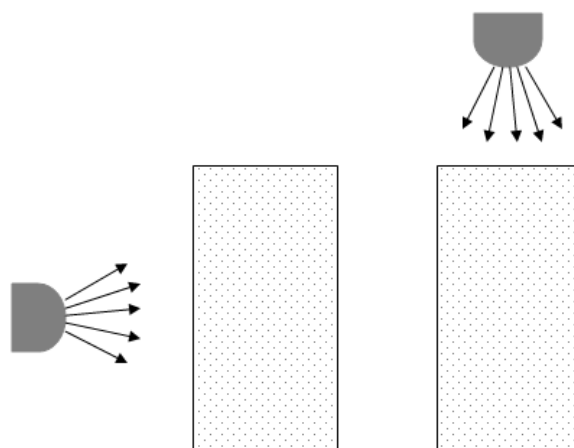


Figure 1.4. Schematic illustrations of conventional photocatalytic setups

As an exact measurement of the number of absorbed photons is usually difficult, it was suggested to calculate the photonic efficiency, which represents the number of converted molecules per number of incident photons within a defined wavelength range⁴¹. It was also recommended to apply the photonic efficiency defined as the ratio of the

photoreaction rate to the rate of incident photons at a specific wavelength range arriving at the internal surface of the irradiation window^{4,41}. These definitions represent a lower limit of the quantum yield of the process since not all the incident irradiation will be absorbed by the catalysts. The incident irradiation can be easily measured by radiometric or actinometric procedures¹⁷.

Some authors recommended to perform the photocatalytic experiments in setups with the illumination source outside the reactor as given in **Figure 1.4**⁴⁷⁻⁵² and measure the incident photon flux at the reactor window. However, all these setups have the disadvantage that only a fraction of the incoming light will be absorbed by the photocatalyst. A large fraction of the photons will be lost due to the light scattering by the photocatalyst inside the photoreactor and also due to the light reflection at the photoreactor window. Therefore, in the mentioned conventional reactors for heterogeneous systems, the amount of light loss due to the scattering and back reflections depends on optical properties of the photocatalyst and other parameters, varying between 13 % to 76 % of the incoming light⁵³.

Hence, the photonic efficiency not only depends on the absorption and the scattering coefficients of the photocatalyst, but is also strongly affected by the absorption coefficients of the substrates, light sources, and reactor geometries. For instance, in photocatalytic dye degradation, the substrates or semiconductor-substrate surface complexes may also absorb the light³⁷. Other experimental conditions such as pH and ionic strength also have a significant impact on the fraction of absorbed, reflected and scattered photon fluxes^{45,54,55}. This is mainly because aggregation of nano particles in aqueous suspensions is a function of ionic strength and pH of the aqueous environments and the agglomerates affect significantly the optical properties of the system⁵⁶. Therefore, the estimation of the amount of absorbed photons by the system requires the determination of the optical properties under the experimental conditions. The measured values of the two wavelength dependent parameters, k_λ and σ_λ , for six different commercially available titanium dioxide suspensions in water by Cabrera *et al.* are summarized in **Table 1.1** and **Table 1.2**⁵⁷.

1. Introduction and Objectives

Table 1.1. Absorption coefficient for different titanium dioxide samples⁵⁷. Reprinted with permission from Ref 57. Copyright (1996) American Chemical Society

λ [nm]	κ_{λ}^* [cm ² g ⁻¹]					
	ALDRICH	MERCK	FISHER	FLUKA	DEGUSSA	HOMBIKAT
275	4706	5462	5413	4706	12856	4602
285	4827	5653	5397	4796	13317	4621
295	4962	5627	5403	4938	12849	4588
305	5083	5717	5375	5001	12435	4543
315	5267	5938	5394	5065	11620	4376
325	5357	6029	5392	5132	9717	3995
335	5411	5895	5393	5172	7075	3170
345	4973	5372	5319	4710	4485	1930
355	3693	3902	4258	3560	2380	929
365	1153	1757	2272	2059	887	121
375	115	212	806	888	≅ 0	≅ 0
385	≅ 0	≅ 0	337	458	≅ 0	≅ 0
395	≅ 0	≅ 0	231	289	≅ 0	≅ 0
405	≅ 0	≅ 0	209	217	≅ 0	≅ 0

Table 1.2. Scattering coefficient for different titanium dioxide samples⁵⁷. Reprinted with permission from Ref 57. Copyright (1996) American Chemical Society

λ [nm]	σ_{λ}^* [cm ² g ⁻¹]					
	ALDRICH	MERCK	FISHER	FLUKA	DEGUSSA	HOMBIKAT
275	30057	22214	11227	11673	52567	20089
285	30130	22184	11437	11714	53020	20237
295	30329	22517	11653	11696	54259	20532
305	30547	22616	11923	11822	55353	20893
315	30610	22547	12109	11942	57520	21408
325	31116	22904	12350	12096	60683	21974
335	31917	24145	12674	12355	60577	22860
345	33386	25775	12936	13163	58653	24125
355	35699	28446	14543	14926	56979	25460
365	39154	31343	16771	16684	54208	26205
375	40654	33366	18444	17757	51305	26278
385	41433	34134	19135	18655	47999	26238
395	42245	34640	19459	19072	45071	26215
405	42773	35077	19654	19621	42343	26134

Therefore, a comparison of photonic efficiencies is only meaningful for reactions performed within the same photoreactor affording “relative photonic efficiencies”³⁸. Since the absorption of incident light depends not only on the properties of the photocatalyst, but also on the reactor geometry, the photonic efficiency gives a general

idea about the efficiency of the whole system, while only the quantum yield provides the actual activity of the photocatalyst particles¹⁷.

Considering that the photonic efficiency provides only the lower limit of the true quantum yield, Buriak *et al.* have suggested reporting the photonic efficiency with all related measurement conditions including the catalyst loading, the light source, the spectral distribution of the light source, the optical irradiance at the sample, and the substrate concentration⁵⁸. Moreover, statistics and error analysis should also be included providing an idea concerning the claimed materials improvements and the experimental error⁵⁸.

Serpone *et al.* presented an alternative method for the comparison of the activity of different photocatalysts named “Relative Photonic Efficiency (ξ_r)”⁵⁹. This method uses cross-reference experiments and correlates the activity of the photocatalyst for a given system with a standard process, a standard photocatalyst, and a standard actinometer⁵³. The efficiency of the given system is compared with the degradation of phenol as a standard secondary actinometer employing TiO₂ Degussa P25 as the standard photocatalyst^{59,60}. According to Rajeshwar *et al.* the comparison of photocatalyst performance for the test substrate with such a standard system solves some intrinsic problems regarding photon absorption, reactor geometry, and light source⁶¹. Therefore, this method is practical in case of reactors with complex geometries.

Following the definition of the relative photonic efficiency, when a standard quantum yield for a certain photocatalyst and a certain substrate (Φ_{standard}) is known, the quantum yield of the test system can be determined by the following equation:

$$\Phi = \Phi_{\text{standard}} \cdot \xi_r \quad (1.10)$$

where ξ_r is the relative photonic efficiency, Φ_{standard} is the quantum yield of a given photocatalyst (TiO₂ Degussa P25) and a standard organic substrate (phenol) under similar conditions, and Φ is the quantum yield of the test system⁵⁹. However, Ohtani *et al.* claimed that the composition of P25 was inhomogeneous and changed depending on the position of sampling from the same package⁶². Moreover, studies on photocatalytic properties of P25 and isolated pure anatase and rutile particles as a reference revealed that the photocatalytic activity of these materials changes considerably upon an isolation process including washing with water, ultrasonication and drying in air. These changes

1. Introduction and Objectives

can most probably be described through the aggregation of particles by inter-particle dehydration⁶².

In the early 1970s, Solonitsyn and Basov have applied the concept of black bodies for quantum yield measurements in gas-solid heterogeneous reactors^{63,64}. The concept of black bodies was presented for the first time by Gustav Kirchhoff in 1860⁶⁵:

“The supposition that bodies can be imagined which, for infinitely small thicknesses, completely absorb all incident rays, and neither reflect nor transmit any. I shall call such bodies perfectly black, or, more briefly, black bodies.”

A black body reactor is an idealized physical body with specific properties, which passes all the incoming light into the reactor without any loss of light through reflection. This reactor absorbs the entire incident light internally and the radiation energy will not be transmitted out from the reactor. Hence, the black body reactor is an ideal absorber for radiation from all incidence angles.

According to the conservation law of energy, assuming negligible emission of radiation, the energy balance between the number of incoming photons, and the fraction of the absorbed, reflected, and transmitted light can be presented as shown in the following equation⁶⁶:

$$n_{p,in} = n_{p,abs} + n_{p,refl} + n_{p,trans} \quad (1.11)$$

where $n_{p,in}$, $n_{p,abs}$, $n_{p,refl}$, and $n_{p,trans}$ are the number of incoming, absorbed, reflected, and transmitted photons (mol). Therefore, in order to absorb all the incoming light, the amount of reflected and transmitted light outside of the reactor should be zero. To overcome this problem the concept of a black body reactor (a cavity with a small hole as the light inlet) was used by Solonitsyn and Basov as a model. Therefore, in order to minimize the back reflection of the light outside of the reactor, the light inlet area of the light beam was chosen to be much smaller than the area of the inner cavity. Moreover, to make sure that the loss by transmitted light is also negligible, the optical density of the solid/liquid system needs to be high enough to ensure that no light is transmitted to the outside of the reactor.

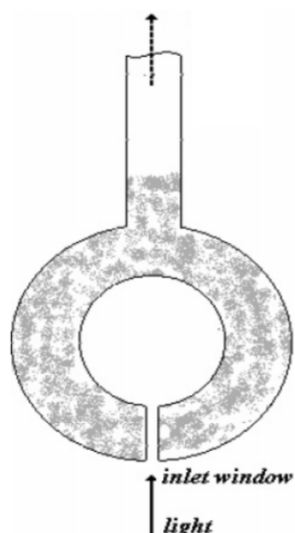


Figure 1.5. Schematic illustration of the black body reactor designed for gas-solid heterogeneous systems^{63,64}. Reprinted with permission from Ref 63. Copyright (2006) ACS

The schematic illustration of the black body reactor design for gas-solid heterogeneous systems is illustrated in **Figure 1.5**. In this reactor the light was passed through an inlet window with a diameter of 2 mm, while the inner and outer diameters of the sphere were approximately 25 mm and 28-30 mm, respectively. The distance between the reactor walls was filled with the photocatalyst particles. Since the light entrance diameter was much smaller than the area of the inner cavity, it was assumed that the back reflection through the light inlet is approximately zero. The reactor space filled with the photocatalyst powder had a high optical density to ensure that almost no light is transmitted through the reactor outer walls. Consequently, all the incoming light through the small light inlet, after reflection and scattering within the reactor and the inner cavity, will eventually be absorbed by the photocatalyst.

Emeline *et al.* have also reported an experimental application of the concept of a “black body” like reactor for quantum yield measurements in liquid-solid heterogeneous systems⁶³. **Figure 1.6** shows the schematic sketch and an actual photograph of this reactor. This reactor consisted of a glass beaker containing the reaction slurry and a cavity located in the center of the reaction slurry. The light was directed through an optical fiber into the cavity. The cross area of the optical fiber was small enough in comparison with the cavity area leading to negligible loss of light due to the back reflection. Furthermore, the loss by transmitted light through the reactor walls was also eliminated by increasing

1. Introduction and Objectives

the catalyst loading in the reaction slurry. A sufficiently high loading of the photocatalyst increases the optical density of the system resulting in a decrease in the absorption pathway. Therefore, at a suitable distance of the cavity from the reactor walls the transmitted light is approximately zero.

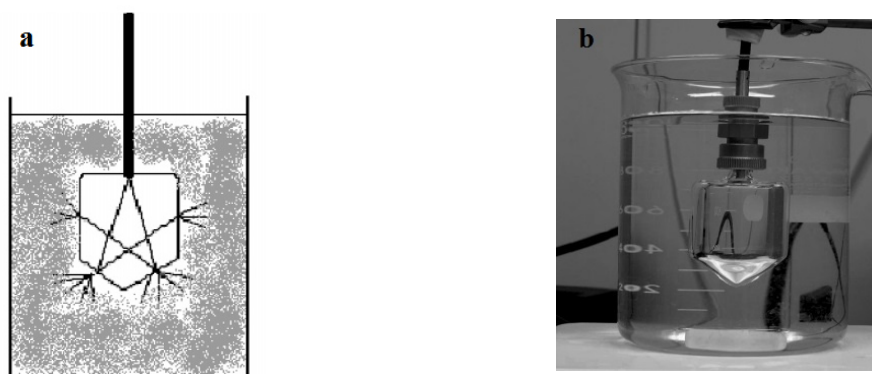


Figure 1.6. (a) Schematic sketch of the black body reactor for liquid-solid heterogeneous systems. (b) Photograph of the black body reactor in liquid-solid heterogeneous systems⁶³. Reprinted with permission from Ref 63. Copyright (2006) ACS

Emeline *et al.* have demonstrated that the experimentally measured quantum yield of a photocatalytic reaction in a non-uniformly irradiated heterogeneous system was constant and the reaction rate correlated linearly to the photon flux. They have also studied the effect of the shape of inner cavities of the black body photoreactor. Accordingly, the quantum yield seems to be independent from the light distribution in solution and thus on the irradiated surface area of the photocatalyst⁶³.

Independency of the measured quantum yield from the photon flux in a black body photoreactor can be applied for the design of photoreactors. Having the volume-averaged quantum yield of the photocatalytic reaction in a photoreactor, simplifies the development of the kinetic model through calculation of the local reaction rate according the following equation.

$$r_{local} = \Phi_{local} e_{\lambda}^a \quad (1.12)$$

in which Φ_{local} is the local quantum yield and e_{λ}^a is the local volumetric rate of photon absorption (at each point inside the photoreactor). Since the quantum yield is constant and

it does not depend on the photon flux inside the photoreactor, the reaction rate at any position of the photoreactor can be calculated using the volume-averaged value of the quantum yield.

Furthermore, considering the constant quantum yield inside the black body photoreactor and its independency from the photon flux, the idea of applying a blackbody photoreactor as a standard method to compare the activity of different photocatalyst is promoted. Nevertheless, apart from the independency of the quantum yield from the photon flux, it should also be independent from the other parameters such as the concentration of the probe molecule, the reaction volume, the catalyst loading, and the photon flux density inside the photoreactor.

In the current study, a black body reactor was applied to investigate a photocatalytic process and to develop a method allowing the comparison of different photocatalysts. Herein, the photocatalytic reaction was performed in a black body reactor and the photocatalyst was excited by a monochromatic light source, resulting in the decomposition of the model compound dichloroacetic acid monitored through its respective peak in a chromatogram. Consequently, the reaction rate and the number of converted molecules were determined. In order to obtain the number of absorbed photons, actinometrical measurements were carried out.

In this research TiO_2 was chosen as a reference material since it is the most common photocatalyst reported in the literature and exhibits a high stability, low toxicity, and low cost. Among different bulk or nanocrystalline phases of TiO_2 , rutile (tetragonal), anatase (tetragonal), and brookite (orthorhombic) are most commonly known⁶⁷. In comparison with anatase and brookite, rutile is the thermodynamically most stable phase at ambient temperature⁶⁸. The anatase and brookite phases transform to the rutile phase at temperatures higher than 600 °C. TiO_2 has a large band gap value, and, depending on its crystal structure, the band gap value can vary from 3.0 to 3.2 eV^{69,70}. Anatase and brookite have a larger band gap energy (3.2 eV) than rutile (3.0 eV)⁷¹. Anatase is for most test reactions the photocatalytically most active phase of TiO_2 suggesting that in the anatase phase the charge carrier mobility is higher and that it also has a higher number of surface hydroxyl groups⁷². Moreover, anatase has a low dielectric constant, and a more negative position of the Fermi level in comparison with the rutile phase^{68,73}.

1. Introduction and Objectives

In order to determine the quantum yield of a light-induced reaction in a photocatalyst suspension, dichloroacetic acid (DCA) was chosen here as an organic probe compound. The photocatalytic conversion of this probe compound does not yield intermediates and products which could absorb the incoming light⁷⁴. DCA presents some additional advantages for laboratory studies due to its low vapor pressure and high water solubility⁷⁴. Another argument for the use of DCA as the probe compound is that its photocatalytic degradation according to



can be monitored not only by measuring the DCA concentration but also by following the concentration of the total organic carbon (TOC) content, as well as the evolved amounts of CO_2 , Cl^- , and H^+ (employing e.g. a pH-stat technique)⁷⁴⁻⁷⁷.

Although the focus of this work was mainly on photocatalytic reactions with TiO_2 used as the photocatalyst, in order to generalize a method for all kinds of catalysts and to introduce it as a standard measurement, the method should be able to be applied for different photocatalysts. Therefore, various titanium based materials such as SrTiO_3 , and BaTiO_3 and non-titanium based materials, namely, WO_3 and ZnO , as well as different commercial TiO_2 powders including pure anatase, pure rutile, a mixture of anatase and rutile (P25) and pure brookite were investigated.

The objective of this study was to simplify the photocatalytic reactor design through the development of a straightforward method to measure quantum yields (Φ) of photocatalytic reactions in liquid-solid heterogeneous systems. A critical property of a suitable method for comparing data obtained under different experimental conditions is its independency from the experimental parameters. Therefore, the particular focus of this study was directed towards the effect of different parameters on the reaction rate such as the initial concentration of the model compound, the catalyst loading and the reaction volume.

Moreover, the kinetic behavior including both, reactant decay and product formation should also be considered in photocatalytic systems. Understanding the kinetics of the reactants' conversion should pave the way for a meaningful mechanistic proposal that integrates all observations⁷⁸.

Since light absorption is the first step in any photocatalytic process, the effect of the photon flux entering the reactor and of the types of the light inlet into the heterogeneous black body photoreactor were also studied. In a light induced reaction, following the absorption of light by the photocatalyst, electrons are excited from the valance band to the conduction band while holes remain in the valence band. A fraction of these generated charge carriers migrates to the surface of the photocatalyst particle where they participate in redox reactions, however, most of the electron-hole pairs recombine very fast limiting the photocatalytic efficiency⁷¹. The rate of this recombination process is assumed to be a function of the local volumetric rate of energy absorption¹⁸. Depending on the light distribution, the recombination rate and the quantum yield are different at different positions inside the photoreactor. Therefore, the effects of the light intensity and of the type of light inlets were also studied.

Having a simple method for the quantitative assessment of the performance of photocatalytic systems and for the respective quantum yield determination paves the way for a predictive photoreactor design. According to **Equation 1.9**, scattering is the most complicated term in solving the RTE in heterogeneous systems. Therefore, the independency of the determination method from the scattering properties of the system simplifies the photoreactor design.

Hence, the topics of this doctoral dissertation are presented in the following chapters. After giving a short introduction on the basic principles of photocatalytic reactor engineering in this chapter, the photoreactors which have so far been proposed and utilized for heterogeneous systems will be introduced in **Chapter 2** within a book chapter entitled “Reactors for Artificial Photosynthesis in Heterogeneous Systems” submitted to be published in *Artificial Photosynthesis*, World Scientific Series in Current Energy Issues: Solar Energy, Volume 6 Since the lack of a practical comparison method of the efficiency of different photocatalysts is one of the major obstacles for the development of photocatalytic reactors, the main objective of this thesis is to identify and design a standard approach for the comparison of the photocatalyst activities in heterogeneous systems. This topic is discussed in detail in **Chapter 3**, in an article entitled “A Method to Compare the Activities of Semiconductor Photocatalysts in Liquid-Solid Systems” published in *ChemPhotoChem* 2018, 2, 948 -951. In the proposed method, the reaction rate is found to be independent from parameters such as probe molecule concentration,

1. Introduction and Objectives

catalyst loading, and reaction volume. The dependency of the quantum yield on the photon flux and on the geometrical characteristics of the light inlet is discussed in **Chapter 4** in an article entitled “Determination of the Quantum Yield of Heterogeneous Photocatalytic Reactions Employing a Black Body Photoreactor” published in *Catalysis Today* 2019, doi:10.1016/j.cattod.2019.06.008. Furthermore, a detailed kinetic study and reaction rate evaluation of the photocatalytic dichloroacetic acid degradation in a black body reactor is presented in **Chapter 5** which includes the manuscript entitled “Reaction Rate Study of Photocatalytic Degradation of Dichloroacetic Acid in a Black Body Reactor” submitted for publication to *Catalysts*. Finally, a summarizing discussion of all results discussed will be presented in **Chapter 6**.

References

- (1) Tong, H.; Ouyang, S.; Bi, Y.; Umezawa, N.; Oshikiri, M.; Ye, J. Nano-Photocatalytic Materials: Possibilities and Challenges. *Adv. Mater.* **2012**, *24*, 229–251.
- (2) Pattanaik, P.; Sahoo, M. K. TiO₂ Photocatalysis : Progress from Fundamentals to Modification Technology. *Desalin. Water Treat.* **2014**, *52*, 6567–6590.
- (3) Huang, X.; Qu, Y.; Cid, C. A.; Finke, C.; Hoffmann, M. R.; Lim, K.; Jiang, S. C. Electrochemical Disinfection of Toilet Wastewater Using Wastewater Electrolysis Cell. *Water Res.* **2016**, *92*, 164–172.
- (4) Braslavsky, S. E.; Braun, A. M.; Cassano, A. E.; Emeline, A. V; Litter, M. I.; Palmisano, L.; Parmon, V. N.; Serpone, N. Glossary of Terms Used in Photocatalysis and Radiation Catalysis (IUPAC Recommendations 2011). *Pure Appl. Chem.* **2011**, *83*, 931–1014.
- (5) Mills, A.; Le Hunte, S. An Overview of Semiconductor Photocatalysis. *J. Photochem. Photobiol. A Chem.* **1997**, *108*, 1–35.
- (6) Hoffmann, M. R.; Martin, S. T.; Choi, W.; Bahnemann, D. W. Environmental Applications of Semiconductor Photocatalysis. *Chem. Rev.* **1995**, *95*, 69–96.
- (7) Li, J.; Wu, N. Semiconductor-Based Photocatalysts and Photoelectrochemical Cells for Solar Fuel Generation: A Review. *Catal. Sci. Technol.* **2015**, *5*, 1360–1384.
- (8) Fujishima, A.; Honda, K. Electrochemical Photolysis of Water at a Semiconductor Electrode. *Nature* **1972**, *238*, 37–38.
- (9) Linsebigler, A. L.; Lu, G.; Yates, J. T. Photocatalysis on TiO₂ Surfaces: Principles, Mechanisms, and Selected Results. *Chem. Rev.* **1995**, *95*, 735–758.
- (10) Shihong, X.; Daolun, F.; Wenfeng, S. Preparations and Photocatalytic Properties of Visible-Light-Active Zinc Ferrite-Doped TiO₂ Photocatalyst. *J. Phys. Chem. C* **2009**, *113*, 2463–2467.
- (11) Wang, R.; Hashimoto, K.; Fujishima, A.; Chikuni, M.; Kojima, E.; Kitamura, A.; Shimohigoshi, M.; Watanabe, T. Light-Induced Amphiphilic Surfaces. *Nature* **1997**, *388*, 431–432.
- (12) Lee, K. M.; Lai, C. W.; Ngai, K. S.; Juan, J. C. Recent Developments of Zinc Oxide Based Photocatalyst in Water Treatment Technology: A Review. *Water Res.* **2016**, *88*, 428–448.
- (13) Kudo, A.; Miseki, Y. Heterogeneous Photocatalyst Materials for Water Splitting. *Chem. Soc. Rev.* **2009**, *38*, 253–278.
- (14) Maeda, K.; Domen, K. Nano-Particulate Photocatalysts for Overall Water Splitting under Visible Light. *J. Phys. Chem. C* **2007**, *18*, 301–315.
- (15) Xiang, Q.; Yu, J.; Jaroniec, M. Synergetic Effect of MoS₂ and Graphene as

1. Introduction and Objectives

- Cocatalysts for Enhanced Photocatalytic H₂ Production Activity of TiO₂ Nanoparticles. *Am. Chem. Soc.* **2012**, *134*, 6575–6578.
- (16) Laidler, K. J. A Glossary of Terms Used in Chemical Kinetics, Including Reaction Dynamics (IUPAC Recommendation 1996). *Pure Appl. Chem* **1996**, *68*, 149–192.
- (17) Marugán, J.; Grieken, R. Van; Cassano, A. E.; Alfano, O. M. Photocatalytic Reactor Design. In *Photocatalysis: Fundamentals and Perspectives*; Schneider, J., Bahnemann, D., Ye, J., Li Puma, G., Dionysiou, D. D., Eds.; The Royal Society of Chemistry, 2016; pp 367–387.
- (18) Cassano, A. E.; Martin, C. A.; Brandi, R. J.; Alfano, O. M. Photoreactor Analysis and Design: Fundamentals and Applications. *Ind. Eng. Chem. Res.* **1996**, *34*, 2155–2201.
- (19) Martin, C. A.; Baltanas, M. A.; Cassano, A. E. Photocatalytic Reactors I. Optical Behavior of Titanium Oxide Particulate Suspensions. *J. Photochem. Photobiol. A Chem.* **1993**, *76*, 199–208.
- (20) Alfano, O. M.; Cassano, A. E.; Marugan, J.; Grieken, R. van. Fundamentals of Radiation Transport in Absorbing Scattering Media. In *Photocatalysis Fundamentals and perspectives*; Schneider, J., Bahnemann, D., Ye, J., Puma, G. L., Dionysiou, D. D., Eds.; The Royal Society of Chemistry, 2016; pp 351–366.
- (21) Alvarado-Rolon, O.; Natividad, R.; Romero, R.; Hurtado, L.; Ramírez-Serrano, A. Modelling and Simulation of the Radiant Field in an Annular Heterogeneous Photoreactor Using a Four-Flux Model. *Int. J. Photoenergy* **2018**, *2018*, 1–16.
- (22) Mendive, C. B.; Hansmann, D.; Bredow, T.; Bahnemann, D. New Insights into the Mechanism of TiO₂ Photocatalysis: Thermal Processes beyond the Electron-Hole Creation. *J. Phys. Chem. C* **2011**, *115*, 19676–19685.
- (23) *ISO 22197-1: 2007, Fine Ceramics (Advanced Ceramics, Advanced Technical Ceramics) — Test Method for Air-Purification Performance of Semiconducting Photocatalytic Materials — Part 1: Removal of Nitric Oxide*; Geneva, 2007.
- (24) *ISO 27448: 2009, Fine Ceramics (Advanced Ceramics, Advanced Technical Ceramics) — Test Method for Self-Cleaning Performance of Semiconducting Photocatalytic Materials — Measurement of Water Contact Angle*; Geneva, 2009.
- (25) *ISO 27447: 2009, Fine Ceramics (Advanced Ceramics, Advanced Technical Ceramics) — Test Method for Antibacterial Activity of Semiconducting Photocatalytic Materials*; Geneva, 2009.
- (26) *ISO 10678:2010, Fine Ceramics (Advanced Ceramics, Advanced Technical Ceramics) — Determination of Photocatalytic Activity of Surfaces in an Aqueous Medium by Degradation of Methylene Blue*; Geneva, 2010.
- (27) *ISO 10676. 2010, Fine Ceramics (Advanced Ceramics, Advanced Technical Ceramics) — Test Method for Water Purification Performance of Semiconducting Photocatalytic Materials by Measurement of Forming Ability of Active Oxygen*; Geneva, 2010.

- (28) *ISO 22197-2: 2011, Fine Ceramics (Advanced Ceramics, Advanced Technical Ceramics) — Test Method for Air-Purification Performance of Semiconducting Photocatalytic Materials — Part 2: Removal of Acetaldehyde*; Geneva, 2011.
- (29) *ISO 22197-3: 2011, Fine Ceramics (Advanced Ceramics, Advanced Technical Ceramics) — Test Method for Air-Purification Performance of Semiconducting Photocatalytic Materials — Part 3: Removal of Toluene*; Geneva, 2011.
- (30) Mills, A.; Hill, C.; Robertson, P. K. J. Overview of the Current ISO Tests for Photocatalytic Materials. *J. Photochem. Photobiol. A Chem.* **2012**, *237*, 7–23.
- (31) *CEN/TS 16599: 2014, Photocatalysis - Irradiation Conditions for Testing Photocatalytic Properties of Semiconducting Materials and Measurement of These Conditions*; 2014.
- (32) Keane, D. A.; Hamilton, N.; Gibson, L. T.; Pillai, S. C.; Holmes, J. D.; Morris, M. A. Photocatalytic Air-Purification: A Low-Cost, Real-Time Gas Detection Method. *Anal. Methods* **2017**, *9*, 170–175.
- (33) Chen, Z.; Jaramillo, T. F.; Deutsch, T. G.; Shwarsstein, A. K.; Forman, A. J.; Gaillard, N.; Garland, R.; Takanabe, K.; Heske, C.; Sunkara, M.; McFarland, E. W.; Domen, K.; Miller, E. L.; Turner, J. A.; Dinh, H. N. Accelerating Materials Development for Photoelectrochemical Hydrogen Production: Standards for Methods, Definitions, and Reporting Protocols. *J. Mater. Res.* **2010**, *25*, 3–16.
- (34) Qureshi, M.; Takanabe, K. Insights on Measuring and Reporting Heterogeneous Photocatalysis: Efficiency Definitions and Setup Examples. *Chem. Mater.* **2017**, *29*, 158–167.
- (35) Chen, Z.; Dinh, H. N.; Miller, E. *Photoelectrochemical Water Splitting Standards , Experimental Methods , and Protocols*; SpringerBriefs in Energy. Springer: New York, 2013.
- (36) Cabrera, M. I.; Alfano, O. M.; Cassano, A. E. Novel Reactor for Photocatalytic Kinetic Studies. *Ind. Eng. Chem. Res.* **1994**, *33*, 3031–3042.
- (37) Kisch, H.; Bahnemann, D. Best Practice in Photocatalysis: Comparing Rates or Apparent Quantum Yields? *J. Phys. Chem. Lett.* **2015**, *6*, 1907–1910.
- (38) Kisch, H. Semiconductor Photocatalysis — Mechanistic and Synthetic Aspects. *Angew. Chemie Int. Ed.* **2013**, *52*, 812–847.
- (39) Serpone, N.; Salinaro, A.; Emeline, A.; Ryabchuk, V. Turnovers and Photocatalysis. *J. Photochem. Photobiol. A Chem.* **2000**, *130*, 83–94.
- (40) Boudart, M. Turnover Rates in Heterogeneous Catalysis. *Chem. Rev.* **1995**, *95*, 661–666.
- (41) Serpone, N.; Emeline, A. V. Suggested Terms and Definitions in Photocatalysis and Radiocatalysis. *Int. J. Photoenergy* **2002**, *4*, 91–131.
- (42) Serpone, N.; Terzian, R.; Lawless, D.; Kennepohl, P.; Sauvé, G. On the Usage of Turnover Numbers and Quantum Yields in Heterogeneous Photocatalysis. *J. Photochem. Photobiol. A Chem.* **1993**, *73*, 11–16.

1. Introduction and Objectives

- (43) Laidler, K. J. Homogeneous Catalysis. In *Chemical Kinetics*; Harper Collins Publishers: New York, 1987; pp 377–426.
- (44) Maschmeyer, T.; Che, M. Catalytic Aspects of Light-Induced Hydrogen Generation in Water with TiO₂ and Other Photocatalysts: A Simple and Practical Way towards a Normalization? *Angew. Chemie - Int. Ed.* **2010**, *49*, 1536–1539.
- (45) Kisch, H. On the Problem of Comparing Rates or Apparent Quantum Yields in Heterogeneous Photocatalysis. *Angew. Chemie - Int. Ed.* **2010**, *49*, 9588–9589.
- (46) Maschmeyer, T.; Che, M. Intrinsic Catalytic Activity versus Effective Light Usage - A Reply to Professor Kisch's Comments. *Angew. Chemie - Int. Ed.* **2010**, *49*, 9590–9591.
- (47) Liou, P.-Y.; Chen, S.-C.; Wu, J. C. S.; Liu, D.; Mackintosh, S.; Maroto-Valer, M.; Linforth, R. Photocatalytic CO₂ Reduction Using an Internally Illuminated Monolith Photoreactor. *Energy Environ. Sci.* **2011**, *4*, 1487.
- (48) Jing, D.; Liu, H.; Zhang, X.; Zhao, L.; Guo, L. Photocatalytic Hydrogen Production under Direct Solar Light in a CPC Based Solar Reactor: Reactor Design and Preliminary Results. *Energy Convers. Manag.* **2009**, *50*, 2919–2926.
- (49) Ruban, P.; Sellappa, K. Development and Performance of Bench-Scale Reactor for the Photocatalytic Generation of Hydrogen. *Energy* **2014**, *73*, 926–932.
- (50) Lee, W. H.; Liao, C. H.; Tsai, M. F.; Huang, C. W.; Wu, J. C. S. A Novel Twin Reactor for CO₂ Photoreduction to Mimic Artificial Photosynthesis. *Appl. Catal. B Environ.* **2013**, *132–133*, 445–451.
- (51) Curcó, D.; Malato, S.; Blanco, J.; Giménez, J.; Marco, P. Photocatalytic Degradation of Phenol: Comparison between Pilot-Plant-Scale and Laboratory Results. *Sol. Energy* **1996**, *56*, 387–400.
- (52) Tanveer, M.; Tezcanli Guyer, G. Solar Assisted Photo Degradation of Wastewater by Compound Parabolic Collectors: Review of Design and Operational Parameters. *Renew. Sustain. Energy Rev.* **2013**, *24*, 534–543.
- (53) Serpone, N. Relative Photonic Efficiencies and Quantum Yields in Heterogeneous Photocatalysis. *J. Photochem. Photobiol. A Chem.* **1997**, *104*, 1–12.
- (54) Serpone, N.; Salinaro, A. Terminology, Relative Photonic Efficiencies and Quantum Yields in Heterogeneous Photocatalysis. Part I: Suggested Protocol. *Pure Appl. Chem.* **1999**, *71*, 303–320.
- (55) Minero, C.; Vione, D. A Quantitative Evaluation of the Photocatalytic Performance of TiO₂ Slurries. *Appl. Catal. B Environ.* **2006**, *67*, 257–269.
- (56) French, R. A.; Jacobson, A. R.; Kim, B.; Isley, S. L.; Penn, L.; Baveye, P. C. Influence of Ionic Strength, PH, and Cation Valence on Aggregation Kinetics of Titanium Dioxide Nanoparticles. *Environ. Sci. Technol.* **2009**, *43*, 1354–1359.
- (57) Cabrera, M. I.; Alfano, O. M.; Cassano, A. E. Absorption and Scattering Coefficients of Titanium Dioxide Particulate Suspensions in Water. *J. Phys. Chem.* **1996**, *100*, 20043–20050.

- (58) Buriak, J. M.; Kamat, P. V.; Schanze, K. S. Best Practices for Reporting on Heterogeneous Photocatalysis. *ACS Appl. Mater. Interfaces* **2014**, *6*, 11815–11816.
- (59) Serpone, N.; Sauvé, G.; Koch, R.; Tahiri, H.; Pichat, P.; Piccinini, P.; Pelizzetti, E.; Hidaka, H. Standardization Protocol of Process Efficiencies and Activation Parameters in Heterogeneous Photocatalysis: Relative Photonic Efficiencies. *J. Photochem. Photobiol. A Chem.* **1996**, *94*, 191–203.
- (60) Tahiri, H.; Serpone, N.; Le Van Mao, R. Application of Concept of Relative Photonic Efficiencies and Surface Characterization of a New Titania Photocatalyst Designed for Environmental Remediation. *J. Photochem. Photobiol. A Chem.* **1996**, *93*, 199–203.
- (61) Rajeshwar, K.; Thomas, A.; Janaky, C. Photocatalytic Activity of Inorganic Semiconductor Surfaces: Myths, Hype, and Reality. *J. Phys. Chem. Lett.* **2015**, *6*, 139–147.
- (62) Ohtani, B.; Prieto-Mahaney, O. O.; Li, D.; Abe, R. What Is Degussa (Evonic) P25? Crystalline Composition Analysis, Reconstruction from Isolated Pure Particles and Photocatalytic Activity Test. *J. Photochem. Photobiol. A Chem.* **2010**, *216*, 179–182.
- (63) Emeline, A. V.; Zhang, X.; Jin, M.; Murakami, T.; Fujishima, A. Application of a “Black Body” like Reactor for Measurements of Quantum Yields of Photochemical Reactions in Heterogeneous Systems. *J. Phys. Chem. B* **2006**, *110*, 7409–7413.
- (64) Emeline, A. V.; Kuzmin, G. N.; Purevdorj, D.; Ryabchuk, V. K.; Serpone, N. Spectral Dependencies of the Quantum Yield of Photochemical Processes on the Surface of Wide Band Gap Solids. 3. Gas/Solid Systems. *J. Phys. Chem. B* **2000**, *104*, 2989–2999.
- (65) Kirchhoff, G. On the Relation between the Radiating and Absorbing Powers of Different Bodies for Light and Heat. *London, Edinburgh, Dublin Philos. Mag. J. Sci.* **1860**, *20*, 1–21.
- (66) Wolfe, W. L. Transmission, Reflection, Emission, and Absorption. In *Introduction to Radiometry*; O’Shea, D. C., Ed.; SPIE Press, 1998.
- (67) Gupta, S. M.; Tripathi, M. A Review of TiO₂ Nanoparticles. *Chinese Sci. Bull.* **2011**, *56*, 1639–1657.
- (68) Carp, O.; Huisman, C. L.; Reller, A. Photoinduced Reactivity of Titanium Dioxide. *Prog. Solid State Chem.* **2004**, *32*, 33–177.
- (69) Kandiel, T. A.; Feldhoff, A.; Robben, L.; Dillert, R.; Bahnemann, D. W. Tailored Titanium Dioxide Nanomaterials: Anatase Nanoparticles and Brookite Nanorods as Highly Active Photocatalysts. *Chem. Mater.* **2010**, *22*, 2050–2060.
- (70) Wunderlich, W.; Oekermann, T.; Miao, L.; Hue, N. T.; Tanemura, S.; Tanemura, M. Electronic Properties of Nano-Porous TiO₂- and ZnO-Thin Films-Comparison of Simulations and Experiments. *J. Ceram. Process. Res.* **2004**, *5*, 343–354.
- (71) Kumar, S. G.; Devi, L. G. Review on Modified TiO₂ Photocatalysis under

1. Introduction and Objectives

- UV/Visible Light: Selected Results and Related Mechanisms on Interfacial Charge Carrier Transfer Dynamics. *J. Phys. Chem. A* **2011**, *115*, 13211–13241.
- (72) Fagan, R.; McCormack, D. E.; Dionysiou, D. D.; Pillai, S. C. A Review of Solar and Visible Light Active TiO₂ Photocatalysis for Treating Bacteria, Cyanotoxins and Contaminants of Emerging Concern. *Mater. Sci. Semicond. Process.* **2016**, *42*, 2–14.
- (73) Li, G.; Chen, L.; Graham, M. E.; Gray, K. A. A Comparison of Mixed Phase Titania Photocatalysts Prepared by Physical and Chemical Methods: The Importance of the Solid-Solid Interface. *J. Mol. Catal. A Chem.* **2007**, *275*, 30–35.
- (74) Ballari, M. M. D. L.; Alfano, O. O.; Cassano, A. E. Photocatalytic Degradation of Dichloroacetic Acid. A Kinetic Study with a Mechanistically Based Reaction Model. *Ind. Eng. Chem. Res.* **2009**, *48*, 1847–1858.
- (75) Zalazar, C. S.; Romero, R. L.; Martín, C. A.; Cassano, A. E. Photocatalytic Intrinsic Reaction Kinetics I: Mineralization of Dichloroacetic Acid. *Chem. Eng. Sci.* **2005**, *60*, 5240–5254.
- (76) Chemseddine, A.; Boehm, H. P. A Study of the Primary Step in the Photochemical Degradation of Acetic Acid and Chloroacetic Acids on a TiO₂ Photocatalyst. *J. Mol. Catal.* **1990**, *60*, 295–311.
- (77) Lindner, M.; Theurich, J.; Bahnemann, D. W. Photocatalytic Degradation of Organic Compounds: Accelerating the Process Efficiency. *Water Sci. Technol.* **1997**, *35*, 79–86.
- (78) Hoque, M. A.; Guzman, M. I. Photocatalytic Activity: Experimental Features to Report in Heterogeneous Photocatalysis. *Materials (Basel)*. **2018**, *11*, 10.

2. Reactors for Artificial Photosynthesis in Heterogeneous Systems

2.1. Foreword

This chapter includes the book chapter *Reactors for Artificial Photosynthesis in Heterogeneous Systems* by Lena Megatiff, Arsou Arimi, Ralf Dillert, and Detlef W. Bahnemann submitted for publication in *Artificial Photosynthesis*, World Scientific Series in Current Energy Issues: Solar Energy, Volume 6. Herein, an overview of the photoreactors in artificial photosynthesis and the recent developments made in this field has been provided. It has been shown that although significant progress has been made in development of new photocatalytic materials, designing an efficient solar photoreactor still remains a crucial challenge. Construction of a suitable solar photoreactor with the ability to harvest the light appropriately will drastically improve the overall performance of artificial photosynthesis processes.

2.2. Introduction

The conventional fossil fuels being coal, petroleum and natural gases are the main resources of the world's energy supply. However, the accelerated growth of energy demands resulting from rapid development of industry and global population, has posed serious constraints during recent years. The global energy consumption has been predicted to increase in the next decades and the energy demand will raise 2.3 % per year on average¹. Excessive consumption of fossil fuels and the pollution caused by them could irreparably harm the environment. According to the Environmental Protection Agency, the total amounts of U.S. greenhouse gas emissions have increased by 3.5 % from 1990 to 2015, while decreasing from 2014 to 2015 by 2.3 %. The decrease from 2014 to 2015 was due to the reduction of CO₂ emissions from fossil fuel combustion. The greenhouse gases insulate the planet, and could lead to potential catastrophic changes of the climate². It is predicted that the average global temperature will increase by 6 °C by the end of this century³. Currently the hydrocarbon based sources of energy provide more than 86 % of the energy demand in the world and the remaining 14 % are comprised by alternative energy sources⁴. Due to the growing concern of quick exhaustion of fossil fuels which are non-renewable resources, mankind has focused on alternative sources such as wind and biomass, as well as tidal, nuclear, and solar energy during the past

2. Reactors for Artificial Photosynthesis in Heterogeneous Systems

several decades. Among these so-called “green energy resources”, solar energy is the most abundant renewable energy source and that makes the artificial photosynthesis one of the potential methods to solve the energy problems. Solar CO₂ reduction and H₂ production could play a great role in addressing the climate change problem caused by fossil fuel combustion, coupled with the exhaustion of fossil fuel reservoirs.

In previous chapters, an overview of artificial photosynthesis has been presented. Artificial photosynthesis, mimicking the photosynthesis process in nature, can be summarized as a production of energy from sunlight, water and CO₂. Photolysis of water into molecular oxygen and H⁺ by sunlight is one of the main processes in photosynthesis. The generated H⁺ can be used for the reduction of CO₂ yielding organic compounds and the released oxygen can be utilized for burning fuels. The production of hydrogen and carbon neutral fuels through water splitting and CO₂ reduction are the most studied reactions in artificial photosynthesis⁵. Molecular hydrogen and molecular oxygen can also react yielding water in a fuel cell, providing electrical energy with a higher efficiency than conventional electrical generators⁶. Synthesis of various organic molecules and polymers is another way to harvest and store solar light and hydrogen in form of chemical bonds⁷. Organic compounds are able to produce energy by releasing the stored hydrogen. Photoreforming of organic species is also an efficient artificial photosynthetic process. In this process, photo-generated electrons and holes which act as strong reductants and oxidants, participate in hydrogen production and oxidation reactions of the organic species, respectively⁸.

Artificial photosynthesis seems to be able to move the world towards a green and sustainable energy path. Therefore, over the past few decades, the development of new photocatalysts suitable for water splitting and CO₂ reduction has made tremendous progresses. The potential of these approaches are unquestionably large but they are still not applicable in industrial scale due to their low efficiencies. Not only a highly efficient photocatalyst is required to increase the efficiency, but also the irradiation source, penetration depth, and reactor geometry can strongly influence the process yield⁹. Despite a wide range of research over several decades on artificial photosynthesis, it is still limited to lab scale studies and only a few scientific papers have discussed the design of photoreactors for hydrogen production or CO₂ reduction¹⁰. An ideal photoreactor is supposed to be highly efficient in utilizing the incident light for photocatalytic reactions.

2. Reactors for Artificial Photosynthesis in Heterogeneous Systems

This factor gets even more important in large scale and industrial applications, as a wide range of technical challenges and cost related issues also appear¹¹.

For an optimal photoreactor design, various parameters in particular light harvesting, reaction path, charge carrier recombination, the reactive surface area of a photocatalyst, flow behavior and heat-mass transfer have to be investigated and optimized¹². In order to have a predictable large scale photoreactor design, several challenges such as breakages, washouts, and dead zones should also be taken into account; considering that at larger scales, these problems become more severe as the inhomogeneity in the hydrodynamics increases¹³. In this chapter, reactors for artificial photosynthesis in liquid-solid (semiconductor) heterogeneous systems will be discussed.

2.3. Photoreactors for Heterogeneous Reactions

Artificial photosynthesis can be performed through photoelectrochemical (PEC), photovoltaic electrolysis (PV-E) and photocatalytic methods. According to Sayama *et al*¹⁴, PV-assisted electrolysis is the most efficient system compared to the other two methods. However, it is also the most complex method, while the photocatalytic system is considered to be the simplest one. Therefore, this chapter focuses on heterogeneous photocatalytic systems for water splitting and carbon dioxide reduction in artificial photosynthesis.

The design of a reactor in which photocatalytic reactions take place plays a crucial role in photocatalytic processes. Reactors for photocatalytic applications are basically conventional catalytic reactors which are modified in terms of mass transfer and photon transfer and which are considered for industrial integration¹⁵. In a photocatalytic reactor, the number of active sites on the photocatalyst surface, and the appropriate wavelength of the emitted photons are also factors which need to be considered¹⁶. Furthermore, the efficient and homogenous light distribution inside the reactor is a vital aspect in photoreactor design which is not taken into account when designing and optimizing conventional reactors (thermal or thermal-catalytic). Therefore, irradiation sources and their features such as the photonic output power, spectral distribution, shape, dimension, operating and maintenance requirements are of great importance. Moreover, the reactor geometry should be designed based on the source of irradiation and its entrance path into the reactor, whether through mirrors, reflectors, or windows. The mode of operation,

2. Reactors for Artificial Photosynthesis in Heterogeneous Systems

construction materials, and cleaning procedures of these devices should also be considered¹⁷. Photocatalytic reactors for CO₂ reduction and H₂ production can be classified based on their design characteristics including: mode of operation (batch, semi-batch or continuous), state of the photocatalyst (slurry or immobilized), and type of illumination (artificial UV and/or visible light source or solar light)¹⁶.

2.4. Reactors based on Mode of Operation

2.4.1. Batch Reactors

The most popular photoreactors for hydrogen production and CO₂ reduction are batch type reactors. Generally, batch reactors are operated for homogeneous liquid systems and heterogeneous liquid-solid systems in which isothermal conditions are required. In batch reactors, due to the suitable mixing ability, uniform chemical and thermal profiles can be achieved leading to a high degree of conversion. Batch photoreactors, are simple reactors which are only suitable for laboratory set-ups and small-scale or short-term productions^{18,19}. In batch reactors, first all the reactants are inserted. Then the process will start and proceed for a certain period of time. After a given time the educts have been reacted, therefore the process is finished and the whole mixture of catalyst, solvent and products are completely removed from the reactor. **Figure 2.1** shows the scheme of a typical batch type photoreactor.

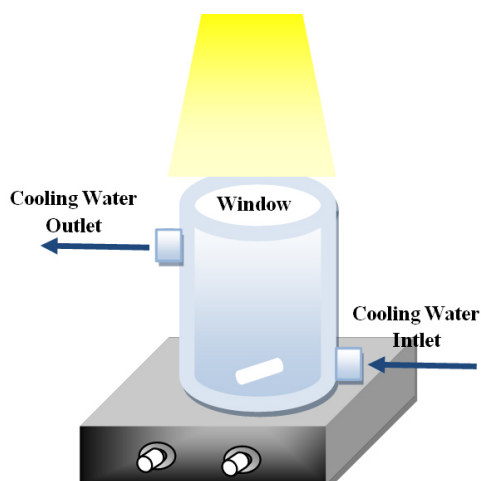


Figure 2.1. Schematic of a typical lab-scale batch-type photoreactor

2. Reactors for Artificial Photosynthesis in Heterogeneous Systems

In such a reactor, a magnetic stirrer is usually used to mix the reaction slurry. For keeping the temperature constant, water is circulated around the tank. In this case, the light is emitted from an artificial source through the quartz window of the reactor.

In case of introducing the reactants gradually to the reactor or discharging the product progressively, the reactor is operated in a semi-batch mode. This type of operation enables the temperature control by a gradual addition or removal of one of the reaction components.

2.4.2. Continuous Reactors

Continuous reactors could be divided into two categories; namely, plug flow reactors and mixed flow reactors. In the following, these types of reactors are explained in details.

2.4.2.1. Plug Flow Reactors

In a plug flow reactor shown in **Figure 2.2**, the fluid is continuously added to the reactor and moves with a uniform velocity along the reactor. Therefore, the concentrations of the reactants and products are functions of distance and will change by further movement through the reactor. Due to the ideal mixing in the radial dimension, a uniform concentration is obtained at the cross section of the reactor¹⁹. The continuous operation and production of products inside this type of reactor makes it a good candidate for large scale applications. Owing to an appropriate heat transfer, it can be applied for both homogeneous and heterogeneous reactions at high temperatures. Although, in most cases, the photochemical reactors do not reach high temperatures, it is important to consider the temperature dependence of the reaction kinetics¹⁷.



Figure 2.2. Schematic of a typical lab-scale plug flow photoreactor

2. Reactors for Artificial Photosynthesis in Heterogeneous Systems

2.4.2.2. Continuous Stirred-Tank Reactor (CSTR)

This type of reactor is the most common one in industrial processing. The CSTR reactor is a mixed flow reactor in which uniform composition and temperatures throughout the reactor and the outlet stream are achieved. Hence, the concentration and temperature gradients are zero inside the reactor and a uniform reaction rate prevails at whole reactor tank. This reactor is usually operated at steady state conditions for heterogeneous systems in which the mixing process is the crucial aspect of improving mass and heat transfer^{19,20}.

2.5. Reactors based on State of the Photocatalyst

Besides the mode of operation, photocatalytic reactors can also be categorized based on the state of the photocatalyst.

2.5.1. Slurry Reactors

In slurry reactors, the catalyst particles are dispersed in liquid phase with a proper mixing system resulting in a uniform mixture¹⁶. The most popular photocatalytic reactors for heterogeneous systems are slurry photoreactors²¹. In this type of reactor, the quantum efficiency of the catalyst, the absorption properties of the catalyst and the reactants and the light intensity determine the reaction rate²². In a slurry system, the entire external illumination surface is used for the reaction. It also has the benefit of high catalyst loading and simple structure design²².

Due to their large available surface area, slurry systems were found to have higher photocatalytic efficiencies compared to immobilized photocatalytic reactors²³. In addition to the high surface area to reactor volume ratio in slurry photoreactors, good mixing and uniform particle distribution, low pressure drop through the reactor, low probability of fouling effect and suitable mass transfer in the photoreactor can be mentioned as other advantages of slurry photoreactors. However, the major drawback of these types of reactors is the additional treatment step required to separate the photocatalyst from the suspension which is rather time and energy consuming. Another limitation of slurry photoreactors is that the suspended particles in the photoreactor strongly affect the light scattering and the adsorption capacity inside the reactor^{16,24}.

2.5.2. Immobilized Reactors

The immobilized-catalyst reactor design features a catalyst fixed on a support or coated on the reactor wall through a physical or chemical process. Photocatalytic reactors with an immobilized photocatalyst have the advantage that no extra catalyst regeneration and separation processes are required. Therefore, they can be continuously operated. However, limited mass transfer, low ratios of surface area to volume, considerable pressure drop throughout the reactor and the problems regarding the catalyst wash out can negatively affect the performance¹⁶.

2.6. Reactors Based on the Light Source

Conversion of light to chemical energy can be performed through different methods including CO₂ reduction, water splitting, reformation or production of organic compounds. All these processes aim to imitate natural photosynthesis to generate energy. In case of applying artificial light, energy production can be accomplished by conversion of fossil fuels energy through thermodynamic processes to mechanical energy, followed by conversion to electricity by dynamo-electric processes²⁵. The produced electrical energy can be utilized by an artificial light source to be converted to photonic energy. The electrical energy can also be obtained from mechanical energy of wind or tide or directly from solar energy by energy conversion in a photovoltaic system. However, considering the current performance of photocatalytically active semiconductors and the resulting low efficiency of the available photocatalytic water splitting or CO₂ reduction processes, conversion of electrical energy into photonic energy by applying artificial light sources are not economically feasible. Therefore, due to the abundance of sunlight, employing direct solar energy could formulate photocatalytic fuel production as an efficient and economical method. In case of reformation of organic compounds, the conversion of electricity to photonic energy process could be reasonable.

2.6.1. Solar Irradiation

Solar energy is the preferable energy provider for artificial photosynthesis, considering the fact that sunlight is not only environmentally friendly but also economically beneficial. The sun delivers a power of 1.365 kW m⁻² at the top of the earth's atmosphere²⁶. Solar energy must be effectively collected, converted and stored as an alternative fuel in order to solve the issue of energy shortage. This energy can be

2. Reactors for Artificial Photosynthesis in Heterogeneous Systems

harvested and utilized in different forms such as electrical energy, thermal energy and chemical energy. Moreover, this clean energy can be applied in terms of water or wastewater treatment²⁷.

According to ASTM G173-03 reference spectra for global tilt irradiation²⁸, the total number of photons as a function of wavelength has been calculated and is shown in **Figure 2.3**. The tilt irradiation contains a direct solar spectral radiation, sky diffused and diffused reflected from the ground on south facing surface tilted 37° from horizontal. In real applications, the efficiency value is very low. Therefore, the number of practicable photons for different solar to hydrogen conversion efficiencies (η) is also shown in **Figure 2.3**. It is worth considering that most photocatalysts are only able to absorb UV light ($\lambda < 400$ nm) which is 5 % of the sunlight and the visible part of the sunlight cannot be utilized²⁹.

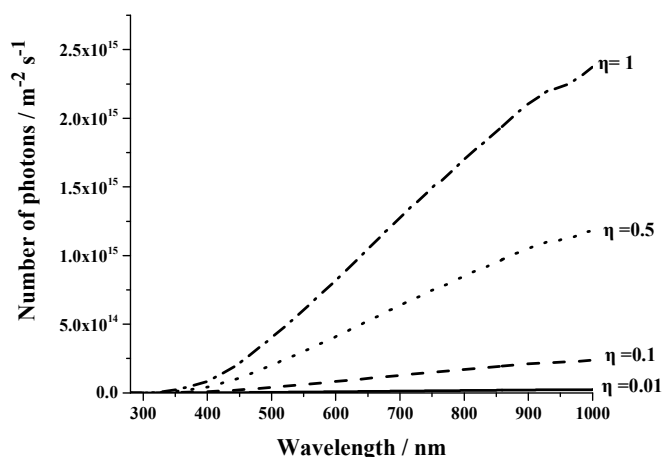


Figure 2.3. Photon number of ASTM G173-03 as a function of the wavelength

2.6.1.1. Solar Photocatalytic Reactors

To achieve a successful industrial scale photoreactor, efficiency and economic possibilities of artificial photosynthetic processes need to be considered. In most of the studies artificial light sources are applied for CO₂ reduction and H₂ production^{30–32}. Utilizing artificial illumination for generating electron hole pairs increases the unit energy cost dramatically and makes the term “renewable energy” not reasonable. Therefore,

2. Reactors for Artificial Photosynthesis in Heterogeneous Systems

artificial-light based photosynthetic methods are not economically beneficial in terms of energy shortage. Due to high expenses of artificial light, it is important to assess solar radiation as a light source and develop systems that are able to reduce CO₂ and produce H₂ upon solar irradiation. By applying solar light, the energy required for artificial illumination is omitted. However, utilizing sun irradiation requires collectors and facilities for improving solar usage and concentrating the solar irradiation which could still be costly. Hence, improving the efficiency of energy generation from the solar irradiation needs to be advanced to reach an acceptable energy unit cost. Solar reactors can be categorized in two different systems regarding their ability to collect the solar irradiation; these two categories are concentrating and non-concentrating systems.

Non-concentrating systems are simple, static and non-tracking solar collectors which utilize the direct and diffused solar energy with low efficiency. In this type of collectors, the solar energy collector and the absorber are the same and the system directly absorbs incident light on the surface³³. Therefore, the non-concentrating systems are usually large and require a huge area.

Despite the simplicity and low cost of the non-concentrating systems, they typically have a laminar flow regime, resulting in mass transfer limitations³⁴. To improve the efficiency of photoreactors and to address the optical problems of non-concentrating solar collector systems, a light concentrating system with increased UV reflectivity can be developed³⁵. Since the diffused UV light is only half of the incident UV light and the other half reaching the earth is direct radiation, by developing the light concentrating system, the direct rays of UV light can be employed. Therefore, providing high reflectivity in the UV spectrum, for example, by applying aluminum mirrors, leads to a more effective utilization of the UV range of the solar spectrum.

In concentrating systems, reflective surfaces are used to concentrate the solar irradiation with the help of a tracking system to collect the direct radiation. Light concentrating systems are able to harvest and concentrate the solar light by reflection through a smaller surface area in comparison with non-concentrating systems. This enables the designer to build a reactor which can be operated at high pressure and flow rates without considerable effects on the overall costs²⁴.

2. Reactors for Artificial Photosynthesis in Heterogeneous Systems

However, due to the reflective surfaces in concentrating systems, optical losses are larger than in non-concentrating systems. Another disadvantage of concentrating systems is their inability to operate under cloudy conditions; while non-concentrating systems could utilize the scattered diffused solar UV light in the environment which reaches up to 50 % of the total available UV light. Moreover, the efficiency of the photocatalytic processes in concentrating systems is lower than that of non-concentrating systems due to the higher UV energy flux density²⁴.

2.6.1.2. Examples of Solar Reactors

In this section, some examples of the solar photoreactors for CO₂ reduction and hydrogen production are presented.

2.6.1.2.1. Compound Parabolic Concentrator

Compound parabolic concentrators (CPC) provide two connected parabolic mirrors added up to a reflective surface with an absorber tube in the focus, granting the most proficient light-harvesting optics for the systems (shown in **Figure 2.4**). In a CPC structure, adjusting the perpendicular position of the collector aperture plane to the incident sun rays, results in maximum reflection and concentration of sun light on the absorber tube²⁴.

In CPC systems absorber tubes with different configurations can be utilized such as tabular, flat, fin and inverted vee (shown in **Figure 2.5**)³⁶. Due to the geometry of fin or tubular absorbers, all sides are illuminated. Therefore, compared to other kinds of absorbers, fewer amounts of the absorber materials are required which in turn results in less material costs. Moreover, due to the enhancement in transient response, the conductive losses to the back are decreased. The small back losses for these configurations can recompense their higher optical losses³⁷.

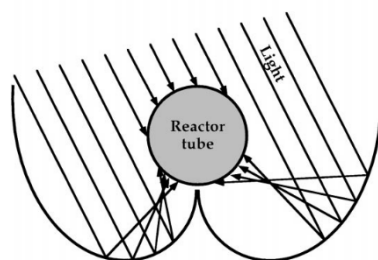


Figure 2.4. Geometric profile of a compound parabolic collecting reactor²⁴. Reprinted from Ref 24 Copyright (2000), with permission from Elsevier

2. Reactors for Artificial Photosynthesis in Heterogeneous Systems

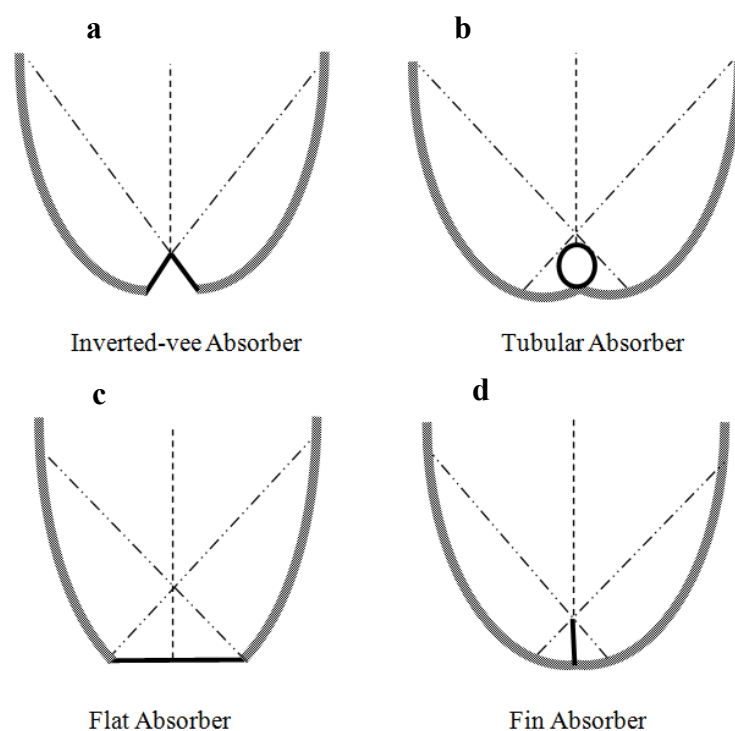


Figure 2.5. CPC configurations with different absorbers: a) Inverted-vee, b) Tubular, c) Flat, and d) Fin

Beside the simplicity, user friendliness and low capital costs, the CPC concentrator is able to gather almost all the UV light (direct and diffused) arriving at the collector from any direction and reflect it to the tubular reactor³⁸. Hence, nearly every point in the tubular reactor is illuminated and almost one sun photoreactor (concentration ratio=1) is provided³⁴. This collector is the most efficient one among other collectors³⁹. Moreover, the superior performance of the system is also due to the turbulent regime inside the reactor which overcomes the mass transfer limitations and provides a sufficient mixing. CPC designs have also some disadvantages such as troubles in handling, big aperture due to the strong raise of height and a low optical efficiency resulting from the loss of a considerable fraction of the incoming radiation due to multiple reflections³⁶. These collectors are commonly investigated at pilot plant scales⁴⁰⁻⁴⁴.

Jing *et al.* have developed a reactor with a CPC design for photocatalytic hydrogen production by direct solar light which is shown in **Figure 2.6**⁴⁵. Since the suspension of the catalyst particles affects the light absorption, for the capture of maximum sunlight energy, the CPC reactor was coupled with an inner-circulated reactor and the aperture of

2. Reactors for Artificial Photosynthesis in Heterogeneous Systems

the CPC was placed perpendicular to the incident light. The set up consisted of a constant stirring tank, a re-circulation pump and a solar collector which was composed of four CPC modules placed in series and oriented at an angle from the horizontal equal to the local latitude for optimal solar photon collection over the course of the entire year. The plant was designed for an operation in a batch mode⁴⁰. It should be noted that in heterogeneous systems, it is of high importance to keep the slurry uniform. Non-uniform slurry leads to non-uniform residence times which results in lower efficiencies. Moreover, a uniform slurry harvests the incident light more efficiently and avoids a loss of incoming light without intercepting with the particles in the slurry⁴⁵. Therefore, an appropriate mixing system is necessary to prevent the photocatalyst particles from sedimentation and to provide turbulent flow inside the reactor³⁴. The maximum hydrogen production rate of the system under optimum conditions with a CdS photocatalyst was reported to be 1.88 L h⁻¹. The apparent energy conversion efficiency was obtained to be 0.47 % by having the formation rate of hydrogen, the Gibbs free energy of formed hydrogen, intensity of incident radiation and the radiation area by following equation:⁴⁰

$$\eta_c = \frac{\Delta G_{H_2}^0 R_{H_2}}{w_s A} \times 100 \% \quad (2.1)$$



Figure 2.6. Direct solar photocatalytic hydrogen production reactor⁴⁵. Reprinted from Ref 45 Copyright (2010), with permission from Elsevier

A CPC was also designed and studied by Wei *et al.* for solar photocatalytic hydrogen production⁴⁴. They have investigated the important parameters influencing the CPC performance such as the reactor direction, the acceptance angle and the absorber tube

2. Reactors for Artificial Photosynthesis in Heterogeneous Systems

diameter. The pilot scale unit consisted of four rows (**Figure 2.7**). Each row had 19 single axis tracking truncated CPCs with a concentration ratio of 4.22 which were oriented in a specific angle. The unit had four different receiving angles with inclinations being 25°, 35°, 45° and 55° due to the different positions of the sun during the year. Furthermore, in order to decrease the costs, usually the system was running under a natural circulation mode, with the buoyancy effect from the tower (shown in **Figure 2.7.b**). In this study NiSCd_xZn_{1-x}S was applied as a photocatalyst. According to the reported results the average value of produced hydrogen for the horizontal row with an angle of 25° in a typical summer day with the sun shining from 10:00 to 16:00 was 7.14 L h⁻¹ and the conversion efficiency defined based on the received optical spectral energy was 0.087 %⁴⁴.

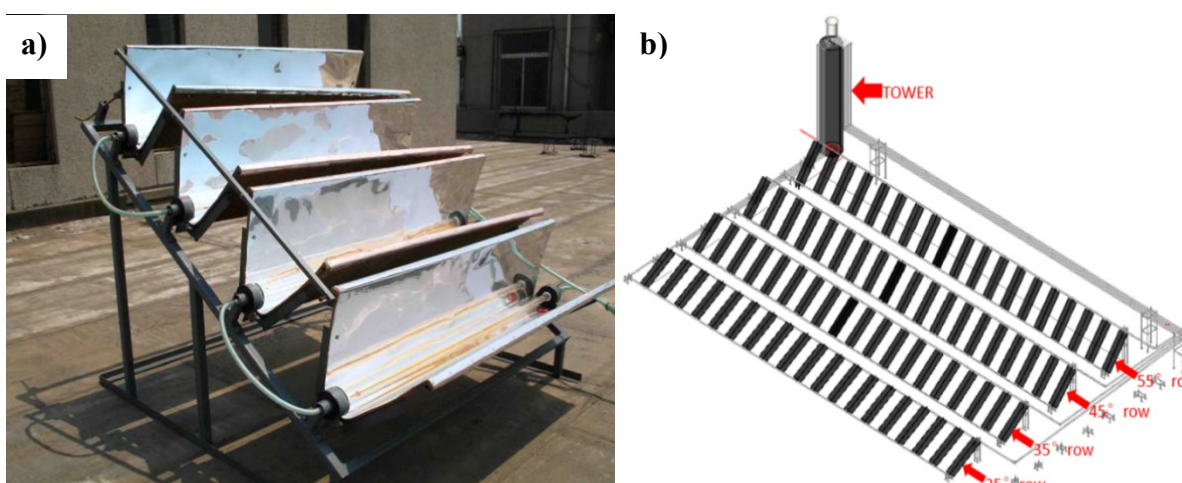


Figure 2.7. a) The outdoor photoreactor with un truncated CPCs for photocatalytic hydrogen production, b) The outdoor layout of the designed system⁴⁴. Reprinted from Ref 44 Copyright (2017), with permission from Elsevier

2.6.1.2.2. A Solar Concentrator for Carbon Dioxide Reduction

With the concept of energy production, continuous circular photoreactors were developed for photocatalytic CO₂ reduction by Nguyen *et al.*⁴⁶. The photocatalyst applied in the proposed photoreactor was metal doped TiO₂ sensitized with a ruthenium dye (Ru^{II}(2,2'-bipyridyl-4,4'-dicarboxylate)₂-(NCS)₂ (N3 dye). In this study, a continuous circular photoreactor was designed as a pyrex glass reactor with a quartz window through which

2. Reactors for Artificial Photosynthesis in Heterogeneous Systems

the light irradiation could penetrate along the fibers in order to improve the light distribution. The optical fibers were coated with the named catalyst. The full absorption of visible light by N3-dye facilitated the photocatalytic reaction on the surface of the catalyst. The reactor was placed under natural sunlight. For an effective harvesting of the natural solar light, a solar concentrator was applied as shown in **Figure 2.8**. The reflection dish of the solar concentrator tracked the daily movement of the sun. The photocatalytic reaction could be carried out by sending out the collected sunlight through an optical cable and focusing it at the photoreactor window. To keep the reaction temperature in a constant state, a heating tape connected to a temperature controller was applied. The production rate of methane over N3-dye-Cu (0.5 wt%) – Fe (0.5 wt%) / TiO₂ catalyst coated on optical fiber measured under the sunlight was about 0.617 $\mu\text{mol g}^{-1} \text{h}^{-1}$.



Figure 2.8. The solar concentrator employed by Nguyen et al.⁴⁶. Reprinted from Ref 46 Copyright (2008), with permission from Elsevier

2.6.1.2.3. Single Bed Colloidal Suspension Reactor

Single bed colloidal suspension reactors are massive continuous bags (baggies) filled with a photocatalytic suspension. These reactors are basically simple plastic bags with a transparent polyethylene (HDPE) film covered on the top. This layer transmits the solar radiation to the reactor slurry and provides a proper sealing to gather the gas products (**Figure 2.9**). The main advantage of these reactors is their low technology and low cost. However, due to their horizontal direction rather than being aimed towards the sun, the amount of produced hydrogen varies a lot during winter and summer. In these

2. Reactors for Artificial Photosynthesis in Heterogeneous Systems

photoreactors, the optical density of the photocatalytic slurry and the reactor depth are of high importance in absorption and utilization of incident solar photons. At a sufficiently high concentration of the particles, most of incoming photons will be absorbed in the upper layers of the bed, preventing the loss of photons due to the light transmission out of the reactor and its penetration to the bottom of the bed⁴⁷.

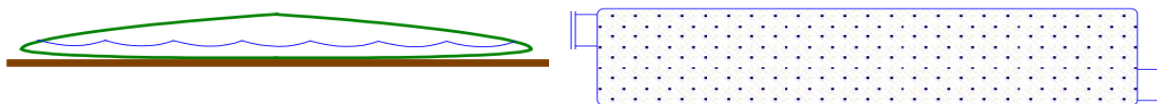


Figure 2.9. End and top views of the baggie configuration⁴⁷

2.6.1.2.4. Other Solar Reactors

Some of solar wastewater treatment systems are potential options for application in artificial photosynthesis. These two processes have a similar procedure from some points of view. For example in both cases the desired redox reactions are achieved under the contribution of the photocatalysts and solar light in reactors with desired mixing to overcome the mass transfer limitations. Nevertheless, there are some differences between solar photocatalytic water treatment and artificial photosynthesis reactors. The first obvious distinction is the necessity of the presence of molecular oxygen in photocatalytic water detoxification processes, while photocatalytic hydrogen production or CO₂ reduction should be performed in anaerobic conditions. Moreover, these two kinds of reactors are also different in separation procedures. In water treatment processes, the photocatalyst needs to be regenerated by one of post processing methods such as filtration or sedimentation. However, for example in case of hydrogen production, the separation of catalyst is not of high importance since water is the raw material in this process⁴⁴.

A proper sealing could be one of the most important modifications in wastewater treatment that should be considered and applied in practical systems in order to modify them to be utilized for artificial photosynthesis. For that matter, air-tight photoreactors are required to prevent the reaction of oxygen with reactants and also to avoid losses of gas compounds. In the following part, some types of wastewater photoreactors which have a potential to be applied in artificial photosynthesis will be introduced.

2. Reactors for Artificial Photosynthesis in Heterogeneous Systems

Parabolic Trough Reactors (PTR)

A parabolic trough reactor is a concentrating solar unit which consists of a tubular reactor and a reflector with parabolic profile and can be utilized for heterogeneous artificial photosynthesis. This reactor needs a sun-tracking system in order to ensure the maximum light capturing. Therefore the aperture is always perpendicular to the sun³⁶. In parabolic trough reactors, only direct radiation can be focused into the reactor²⁴. The concentrated solar light in this reactor is in the range of 5 to 50 times larger than non-concentrating systems⁴⁸. The parabolic trough collector was applied for water treatment in large scale in USA for the first time⁴⁹. The same facility was also developed by Plataforma Solar de Almeria (PSA) research centre in Spain³⁵. This kind of reactor is able to collect the direct sun radiations efficiently. Furthermore, gathering a large amount of solar energy in a small volume of the reactor provides a considerable amount of thermal energy at the same time³⁴.

Thin film fixed bed configuration

The thin-film fixed-bed reactor (TFFBR) was developed from a rectangular glass plate coated with a thin UV transmissive glazing. This reactor gets illuminated from the top⁵⁰. The most important advantages of this type of reactor are the high optical efficiency, the ability of employing direct and diffused portion of the solar light, their simplicity, and utilizing the entire solar UV irradiation⁵¹. Furthermore, no extra separation processes are required for these reactors and their sealed system makes them a good candidate for H₂ production or CO₂ reduction, as all the gas will be kept inside¹⁶. Generally, TFFBRs function under a laminar flow regime, since increasing the flow rate provides a thicker liquid film resulting in the solar light penetration limitation for colored wastewater. This limitation is responsible for UV-A absorption. However, in artificial photosynthesis this issue cannot pose any limitations, since in most cases the liquid film is colorless. Therefore, the flow rate and the film thickness should be adjusted to the mass transfer in the liquid film and to the absorption of the liquid phase⁵². Moreover, increasing the fluid flow rate decreases the residence time inside the reactor which in turn leads to lower efficiencies⁵³.

Double skin sheet reactor (DSSR)

Double skin sheet reactor (DSSR) comprises a flat transparent box framework constructed from poly methyl methacrylate (PMMA) and is applicable for heterogeneous artificial photosynthesis. The slurry of dispersed photocatalyst is circulated by pump throughout the reactor channels. After the process period is completed the slurry can be taken out. In this reactor the direct and diffused radiation of solar light can be utilized⁵⁴. This reactor has a simple structure and its almost sealed structure prevents the liquid vaporization and loss of evolved gases.

2.6.1.3. Economic Analysis in Solar Photoreactors

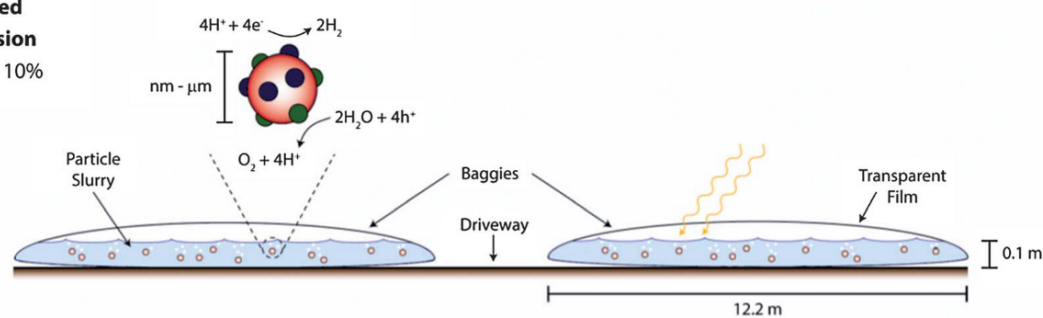
In 2013, a technical and economical study was carried out for solar hydrogen production considering different types of photoreactors (**Figure 2.10**)⁵⁵. The first type of system consisted of the semiconductor (slurry) in a plastic bag that allowed light penetration while holding the aqueous electrolyte. The plastic bags were made of high density polyethylene (HDPE) with 90 % optical transmission and they were impermeable to hydrogen. The low cost of these bags made their large sized application possible (323 m long and 12.2 m wide). The second considered reactor type was similar to the first one, but included also a porous membrane running through the entire length of the bags to separate the produced O₂ and H₂. This system could be operated in a safer mode compared to the prior one, as the gas separation processes were not required anymore. The third type of reactor was a plastic frame which contained an electrolyte and two electrodes with several photoactive layers in between in order to enhance the solar light usage and to provide the requisite voltage to split water⁵⁵. This system was placed on fixed supports inclined 35° with respect to the horizontal plane. The last reactor type (**Figure 2.10.d**) was basically a linear photoelectrochemical (PEC) cell receiver coupled with a parabolic cylinder reflector in order to concentrate the solar light on a PEC cell. This system was able to collect the sunlight by tracking the sun trajectory. The concentrator array had 6 m width and 3 m height.

Additionally, cost calculations for hydrogen production have been done according to the U.S. Department of Energy H₂A model for 10 tons per day production scale and 300 psi at the plant gate. All capital, auxiliaries and operation costs were also considered. Among the four studied reactor types, the lowest cost calculated for energy production belongs to

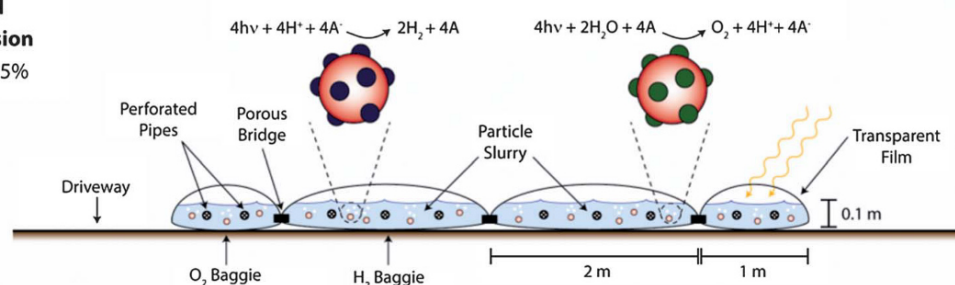
2. Reactors for Artificial Photosynthesis in Heterogeneous Systems

the single bed slurry system which was 1.60\$ per kg H₂. However, safety and efficiency of this system still count as negative factors. On the other hand, the solar concentrator and tracking components were able to capture more solar radiation leading to a higher efficiency. However, applying parabolic cylinder arrays to focus the sunlight drives the cost in this system.

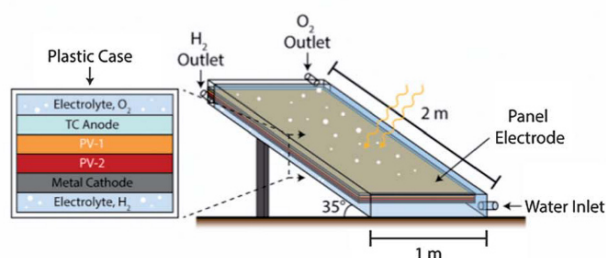
Type 1: Single Bed
Particle Suspension
STH Efficiency 10%



Type 2: Dual Bed
Particle Suspension
STH Efficiency 5%



Type 3: Fixed
Panel Array
STH Efficiency 10%



Type 4: Tracking
Concentrator Array
STH Efficiency 15%

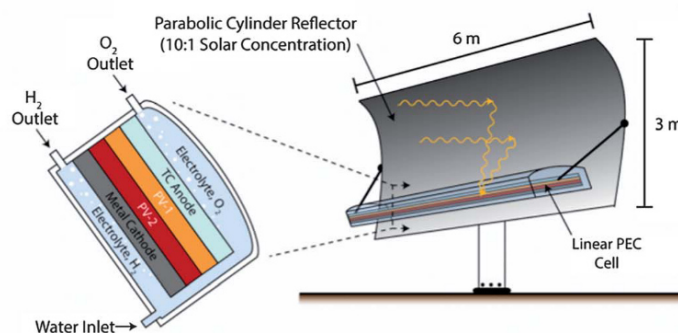


Figure 2.10. Schematic of the four reactor types including a) single bed slurry, b) dual bed slurry, c) fixed bed, d) tracking concentrator array⁵⁵. Reproduced by permission of The Royal Society of Chemistry

2. Reactors for Artificial Photosynthesis in Heterogeneous Systems

Based on a comparative techno-economic analysis of renewable hydrogen production using solar energy for a system with even more than 20 % efficiency, solar hydrogen production is not economical in comparison to fossil-fuel¹⁴. The available energy provided by electricity powered through nuclear plants as well as fossil fuel energy is rather preferred in the market, compared to the high-cost fuel produced from solar energy. In order to make the energy produced by CO₂ reduction and hydrogen production, cost competitive with thermochemical processes, a number of complications such as mass transfer limitations, low catalyst efficiencies, and feedstock costs need to be overcome¹⁴.

Some economical design aspects for a solar hydrogen production system have been studied by Rodriguez *et al.*⁵⁶. According to this study, since the catalytic components have relatively low costs, the most significant cost-effective factor in solar hydrogen production system was found to be the light absorbing component to which more than 95 % of the total cost can be allocated. However, applying a light concentrator would save the costs of the huge area required to absorb the solar light. Therefore, to make solar hydrogen production commercially viable, they suggested decreasing the capital cost of the solar concentrator. If this capital cost value could reach to less than the cost savings from the required area for a given fuel production with a highly efficient material, then a cost effective system will be achieved.

2.6.2. Artificial light Sources

As previously mentioned, the energy generation through artificial photosynthesis is still limited to lab scale. Therefore, the required light and radiation field for photocatalyst activation is usually provided by artificial lamps. Most of the studies in this field are limited to investigations on different types of photoreactor designs operated with artificial light sources. Different artificial light sources such as solar simulator³¹, xenon lamp⁵⁷, mercury lamp³⁰, halogen lamp³², and LED lamps are used for photocatalytic energy production. In this section different lab scale photoreactors used for artificial photosynthesis are presented.

2.6.2.1. Slurry Photoreactors with Artificial Light Sources

Generally, the simple geometry and facile operation of slurry photoreactors leads to their extensive application in bench scale experiments. Typically, the shape of these reactors

2. Reactors for Artificial Photosynthesis in Heterogeneous Systems

provides a symmetric irradiation field inside the reactor making them more attractive for lab scale studies.

Huang *et al.* have discussed photocatalytic hydrogen production from aqueous ammonium sulfite solutions with CdS based photocatalysts in a batch reactor. They also have determined the rates of hydrogen generation as a function of parameters such as reaction temperature, concentration of ammonium sulfite, depth of photolyte, photocatalyst loading and window materials¹¹. One example for overall system set-up of batch-type photoreactor is reported by Chen *et al.*⁵⁸. As shown in **Figure 2.11**, Xe lamp ($\lambda > 400$ nm) projected visible light onto the Pyrex reactor side surface and the UV source in the center of the reactor provided the UV irradiation. This system was evacuated with high-purity argon gas and the gas content was checked by a GC (Gas Chromatography)⁵⁸.

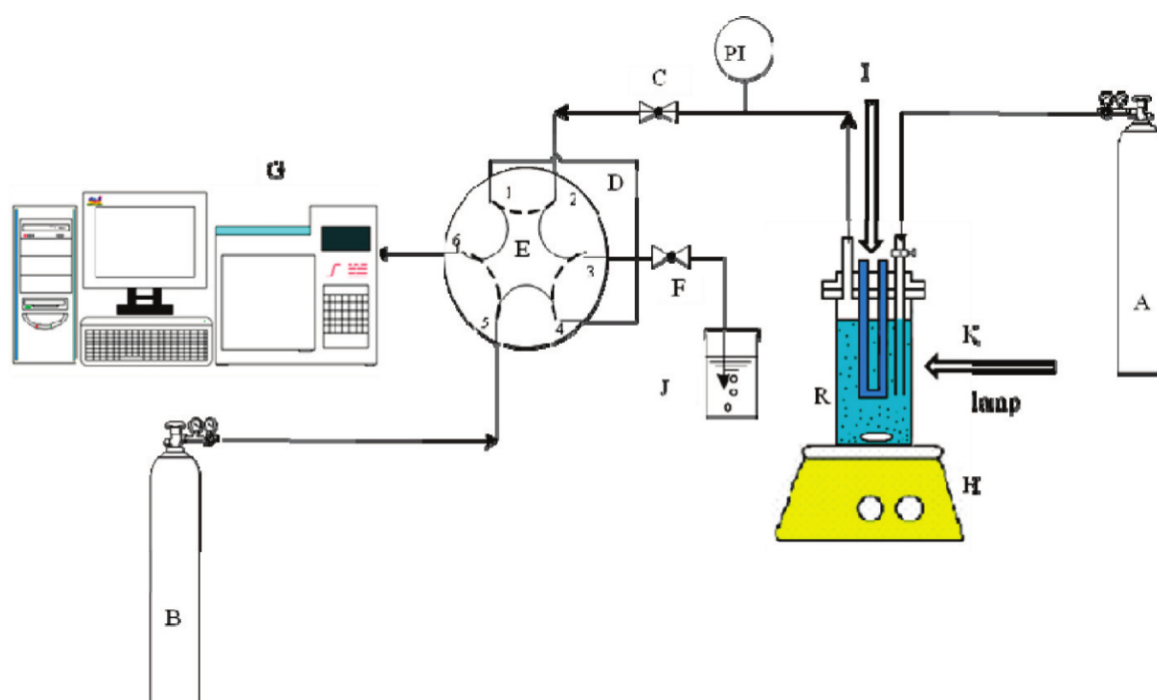


Figure 2.11. Schematics of batch-type photoreactor overall system set-up⁵⁸. Reprinted with permission from Ref 58 Copyright (2011) American Chemical Society

Due to the high expenses, applying magnetic stirring within a photoreactor is impractical in large-scale usages. Hence, a design with facile mixing of the flow within the photoreactor which provides a completely sealed reactor is desired.

2. Reactors for Artificial Photosynthesis in Heterogeneous Systems

Inoue *et al.* have discussed photocatalytic reduction of CO₂ from aqueous solutions and formation of organic compounds in a slurry reactor irradiated with Xe lamp in the end of 1970s⁵⁹. Afterwards, slurry photoreactors were used for reduction of CO₂ in a wide range of research cases⁶⁰. The most common photocatalyst reported in the literature is TiO₂ which benefits from its high stability, low toxicity and low cost. However, it can absorb only 5% of sunlight²⁹. An ideal photocatalytic process should be able to utilize the abundant available solar energy in an efficient way. Over the last decades, a large number of visible-light photocatalysts have been developed. In order to exploit the photocatalysts responsive to visible-light irradiation the modification of TiO₂ or development of a new material can be suggested⁶¹. Lee *et al.* have applied a slurry batch photoreactor for utilizing visible light irradiation by developing light-harvesting complexes (LHCII) attached to the surface of Rh-doped TiO₂ (TiO₂:Rh)⁶². The LHCII is the light absorber in the plants which makes the photosynthesis process to convert CO₂ to sugars possible. Attaching this complex to Rh-doped TiO₂ enhanced the yields of acetaldehyde and methyl formate ten and four times, respectively.

In order to mimic the natural photosynthesis process, a twin slurry photoreactor containing two separated reaction chambers for H₂ production and O₂ evolution was demonstrated by Lee *et al.*⁶³. In this reactor, as illustrated in **Figure 2.12** the undesired reaction of water formation was prevented by placing a membrane between the two compartments and isolating the produced O₂. Hence, the generated hydrogen was facilitated to CO₂ reduction. For the water splitting combined with CO₂ photoreduction reaction, two systems were compared. In the first system, Pt/CuAlGaO₄ was applied as a photocatalyst for both H₂ production and CO₂ reduction. The dual photocatalyst system using Pt/SrTiO₃:Rh for H₂ evolution and Pt/CuAlGaO₄ for CO₂ reduction were also applied. The results showed that the quantum efficiency of CO₂ reduction in dual system was two times larger than the single system.

2. Reactors for Artificial Photosynthesis in Heterogeneous Systems

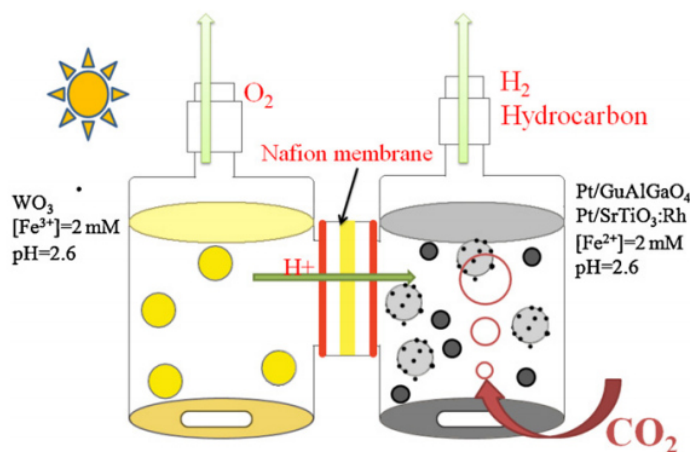


Figure 2.12. Schematic diagram of the twin reactor system⁶³. Reprinted from Ref 63 Copyright (2013), with permission from Elsevier

Skillen *et al.* have designed and investigated a fluidized photoreactor for the production of H₂ under UV–Visible and natural solar illumination over two photocatalysts, Pt-C₃N₄ and NaTaO₃.La⁶⁴. As can be seen in **Figure 2.13**, inside this tubular reactor a propeller was placed at the bottom to provide suitable mixing of catalyst powder. According to this study, the rotational speed of the propeller affects the light penetration and the photocatalytic activity of the system by influencing the mass transfer between the catalyst and the solution. By starting the propeller, cavitations appear which result in fluidization of catalyst particles and increase of interaction between the catalyst surface and the reaction components. Increasing the propeller speed enhances the dispersion of particles in the solution and forces the aqueous reaction medium towards the wall of the unit. Therefore, the required depth penetration of photons to the catalyst surface decreases and maximum exposure of the aqueous medium to the 360° irradiation array is provided⁶⁴. The maximum hydrogen production rate reported in this system was 89 μmol h⁻¹ g⁻¹ over Pt-C₃N₄⁶⁴. Nevertheless, this design illustrated a limitation in practical applications resulted from the corrosion of the propeller. The propeller was constructed from stainless steel 316 which reacted with the sacrificial agent, oxalic acid, leading to the formation of Fe²⁺ ions on the propeller surface and consequently hydrogen evolution. The level of corrosion depends on the concentration of Fe²⁺ and carbon content in the steel⁶⁵. The amount of produced hydrogen was proportional to the level of corrosion. By increase of corrosion, the amount of produced hydrogen was also increased until Fe²⁺ ion made a temporary protective barrier and stopped the hydrogen production.

2. Reactors for Artificial Photosynthesis in Heterogeneous Systems

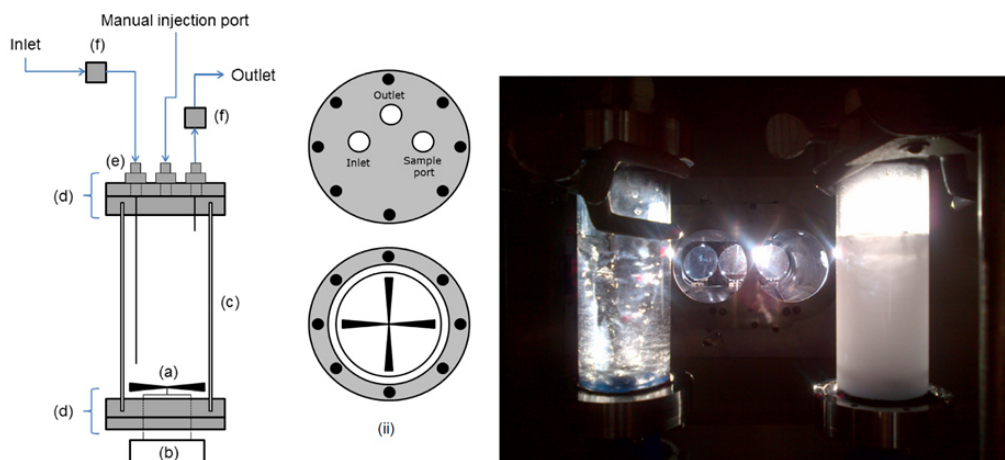


Figure 2.13. Fluidized photo reactor under UV–Visible irradiation⁶⁴. Reprinted from Ref 64

A number of slurry reactor designs reported in the literature are shown in **Figure 2.14** including the annular photoreactor⁶⁶, rotating reactor⁶⁷, spinning disc reactor⁶⁸, fluidized bed reactor⁶⁹ and falling film reactor⁷⁰.

2. Reactors for Artificial Photosynthesis in Heterogeneous Systems

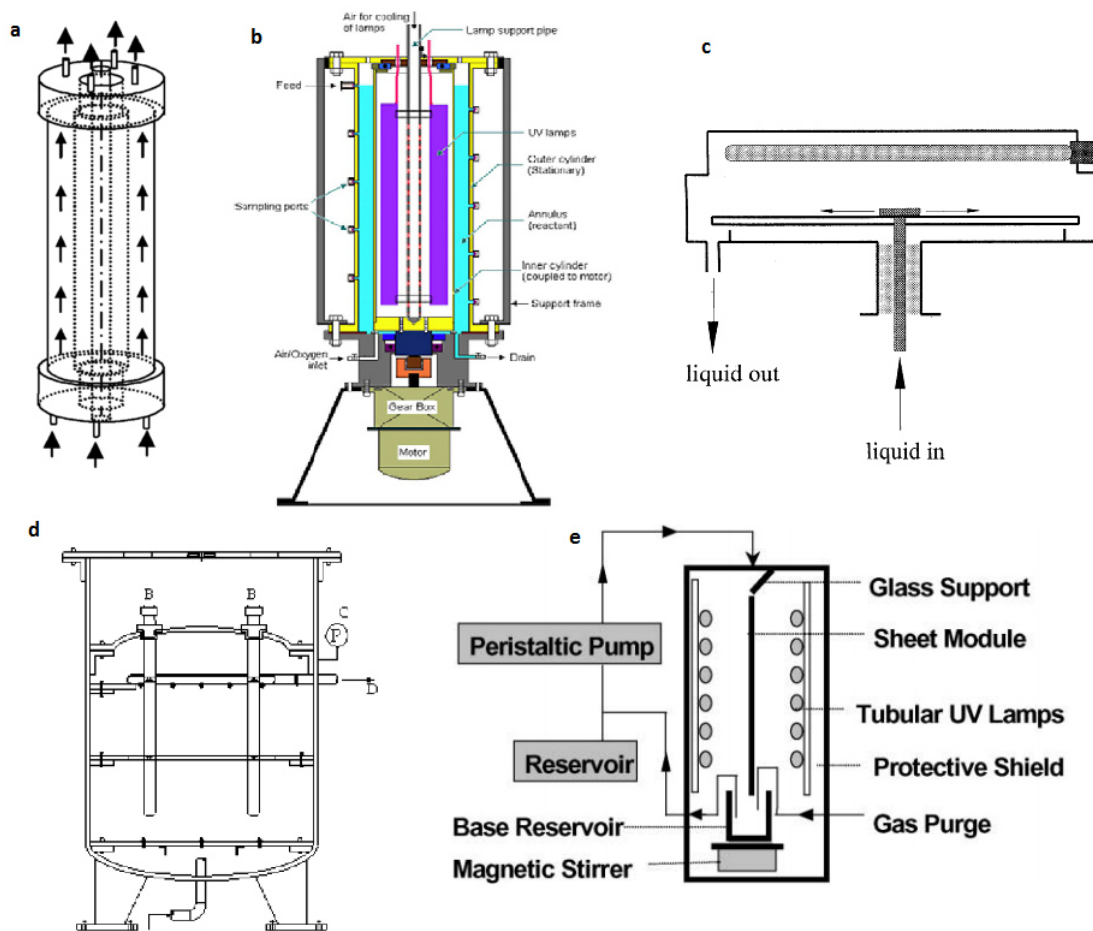


Figure 2.14. Different slurry reactor designs. (a) annular reactor⁶⁶ Reprinted from Ref 66 Copyright (2007), with permission from Elsevier, (b) rotating annular reactor⁶⁷ Reprinted from Ref 67 Copyright (2010), with permission from Elsevier, (c) spinning disc reactor⁶⁸ Reprinted from Ref 68 Copyright (2001), with permission from Elsevier, (d) fluidized bed reactor⁶⁹ Reprinted from Ref 69 Copyright (2004), with permission from Elsevier, (e) falling film reactor⁷⁰ Reprinted from Ref 70 Copyright (2002), with permission from Elsevier

2.6.2.2. Immobilized Photoreactor with Artificial Light Source

A continuous flow quartz-fixed-bed reactor was utilized for the photocatalytic reduction of CO_2 over $\text{Cu/CdS-TiO}_2/\text{SiO}_2$ catalyst upon UV light irradiation with a 125 W ultrahigh pressure mercury lamp, as shown in **Figure 2.15**⁷¹. The pressure of reaction system was kept at 1 atm, and the temperature was not higher than 473 K. Shi *et al.* have observed direct synthesis of acetone from CO_2 and CH_4 over this photocatalyst with 0.74% and 1.47% conversion for CO_2 and CH_4 , respectively.

2. Reactors for Artificial Photosynthesis in Heterogeneous Systems

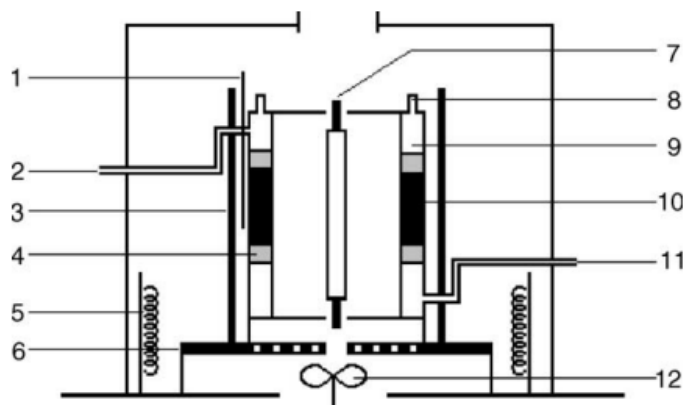


Figure 2.15. Schematic representative of photocatalytic reaction system: (1) thermocouple; (2) gas outlet; (3) aluminum foil; (4) sieve plate; (5) heater; (6) graphite plate; (7) mercury lamp; (8) catalyst inlet; (9) quartz reactor; (10) catalyst bed; (11) gas inlet; (12) fan⁷¹. Reprinted from Ref 71 Copyright (2004), with permission from Elsevier

Optical fiber photoreactors are another example of an immobilized design in which the light distribution inside the photoreactor can be controlled. The uniform annular tubes with tiny inner diameters of optical fibers enable them to guide and manipulate the photons accurately. In these kinds of photoreactors, crystalline semiconductors such as silicon or titania are deposited on the wall of the long and narrow optical fibers. In this way, the semiconductors can control the electron transfer by splitting the light to two beams because of a different refraction index between the semiconductor and the quartz core (**Figure 2.16**)^{72,73}. A fraction of the light gets absorbed by the semiconductor and excites it, while the other part of the light is reflected and transmitted along the fiber and gradually spreads and diminishes to the end of the fiber.

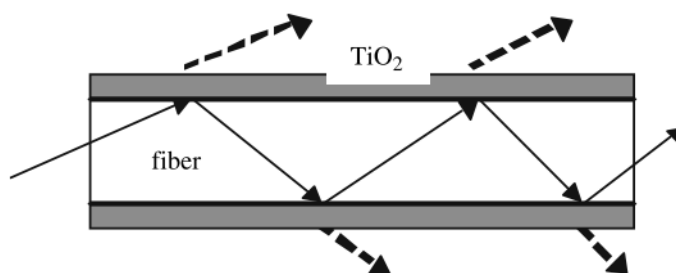


Figure 2.16. The schematic of light transmission and spread of a TiO₂ coated-optical fiber⁷². Reprinted from Ref 72 Copyright (2005), with permission from Elsevier

2. Reactors for Artificial Photosynthesis in Heterogeneous Systems

The photocatalytic reduction of CO₂ with H₂O was demonstrated by Wu *et al.* using a steady-state optical fiber photoreactor with Cu/TiO₂ catalyst. This photoreactor which had a diameter of 3.2 cm and was 16 cm long contained about 120 fibers with 16 cm long. A Hg lamp with a wavelength of 365 nm and adjustable light intensity between 1 and 16 W/cm² was utilized as an irradiation source for this reactor. Inside this reactor, the light distribution was nearly uniform and the maximum methanol yield was 0.46 mmole g_{cat}⁻¹ h⁻¹ upon UV irradiation⁷². This optical fiber photoreactor is illustrated in **Figure 2.17**.



Figure 2.17. A photo of optical fiber photoreactor⁷². Reprinted from Ref 72 Copyright (2005), with permission from Elsevier

They have also designed and assembled an optical fiber photoreactor for CO₂ reduction with water in which, 216 catalyst-coated fibers with 11cm length were used to distribute the light homogeneously over the catalysts surface⁷⁴. Schematics of optical fiber photoreactor and the photo reaction system are illustrated in **Figure 2.18**. A continuous stream of CO₂ was passed through the reactor under UV irradiation. The optical fibers were homogeneously coated with TiO₂, Cu/TiO₂ and Ag/TiO₂ films. The maximum obtained methanol production yield was about 4.12 μmole g_{cat}⁻¹ h⁻¹. Reduction of CO₂ with water under UVA light was also studied using Cu-Fe/TiO₂ as a catalyst on optical fibers⁷⁵. Methane and ethylene were reported as main products with similar quantum yields of 0.025 % and 0.024 %, respectively. According to this study, under a constant photon flux, implying higher number of optical fibers in a photoreactor leads to a higher

2. Reactors for Artificial Photosynthesis in Heterogeneous Systems

production rate of ethylene and consequently a higher quantum yield. This is mainly due to the increased amount of employed catalyst in the photoreactor and more efficient utilization of the incoming light. Moreover, applying optical fibers coated with the catalyst showed one order of magnitude higher yield in comparison with the glass plate counterpart. These results confirmed that the optical fiber photoreactor can utilize the light efficiently and the problem of non-uniform light distribution and dark spots in the reactor can be solved.

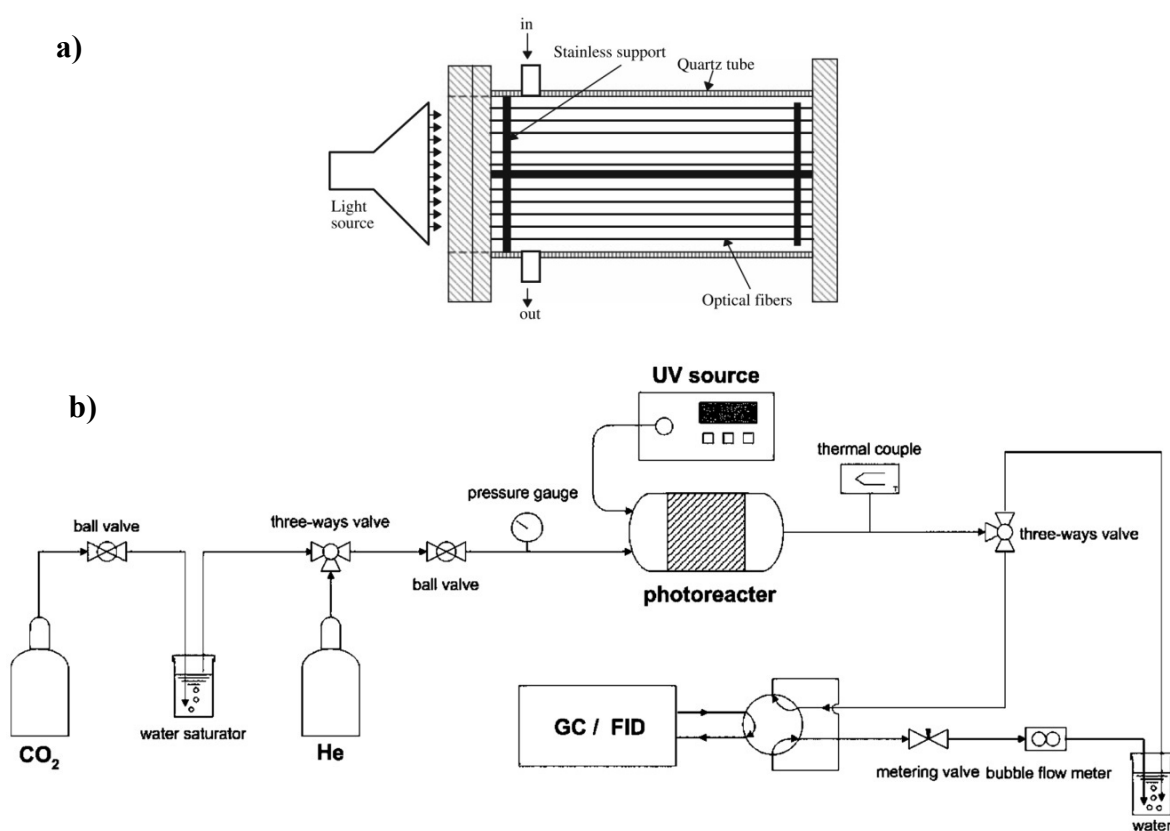


Figure 2.18. Schematics of a) optical-fiber, b) photo reaction system⁷⁴. Reprinted from Ref 74 Copyright (2008), with permission from Springer Nature

Besides the high efficient photon distribution to the accessible high surface area of the catalyst, optical fiber photoreactors have the advantage of higher processing capacities⁷⁶. Coating the photocatalyst on a large external area of optical fibers provides the ability of increasing the process capacity in a given reactor⁷⁵.

2. Reactors for Artificial Photosynthesis in Heterogeneous Systems

Despite the proper light distribution inside the reactor, the optical fiber reactor faces several challenges. The first drawback is the non-uniform deposition of the semiconductor on the optical fibers leading to detachment of deposition as a result of severe liquid flow. Moreover, mass transfer in this reactor is slow compared to the conventional reactors and the light propagation is short which can result in local deactivation of the catalyst⁷⁷.

To enhance the reaction yield of CO₂ reduction, the irradiated surface of the catalyst should be maximized. Applying monolith structures as distributors in optical fibers has attracted a lot of attention due to their three-dimensional structures containing multiple channels^{78–81}. Low pressure drop and excellent mass transfer for gas/liquid systems are counted as the advantages of these structures over optical fiber reactors. Joo *et al.* have coated a monolith surface with polyaniline nanofibers in order to convert glucose to glucolactone⁸². This reactor achieved a yield of 83 % with a residence time of 2.0 min.

A monolith photoreactor has also been presented by Liou *et al.* as shown in **Figure 2.19**, applying NiO/InTaO₄ as a photocatalyst dip coated on the SiO₂ sub-layer. In this configuration, CO₂ was reduced photocatalytically to methanol under visible-light irradiation in a steady-state operation mode. The maximum achieved methanol conversion rate was 0.16 mmol g_{cat}⁻¹ h⁻¹⁸³. The major advantage of this reactor compared to the commonly used ones was the lower loss of light leading to higher quantum efficiencies.

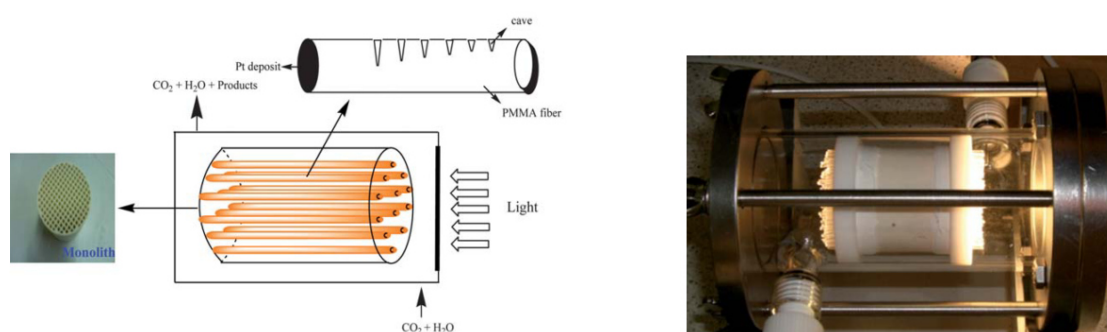


Figure 2.19. Schematics and photo of the monolith reactor and illumination fibers⁸³. Reproduced by permission of The Royal Society of Chemistry

2. Reactors for Artificial Photosynthesis in Heterogeneous Systems

Tahir and Amin have studied the performance of a montmorillonite (MMT)/TiO₂ coated monolith photoreactor for photocatalytic CO₂ reduction⁸¹. The main products were CO, CH₄, C₂H₄, C₂H₆, C₃H₆ and C₃H₈ and the highest reaction yield belonged to CH₄ production with 139 $\mu\text{mole g}_{\text{cat}}^{-1} \text{h}^{-1}$. As can be seen in **Figure 2.20**, the illuminated surface area in monolith photoreactor was larger than that of cell type photoreactor with dispersed catalyst leading to higher adsorption of gaseous species. Therefore, the light distribution was enhanced and utilized more efficiently compared to the cell type photoreactor which resulted in higher yield rates in monolith photoreactor. Due to this high ratio of surface area to reactor volume, even at high flow rates only a very low pressure drop was observed. Furthermore, in the monolith photoreactor the configuration can be easily modified⁷⁶.

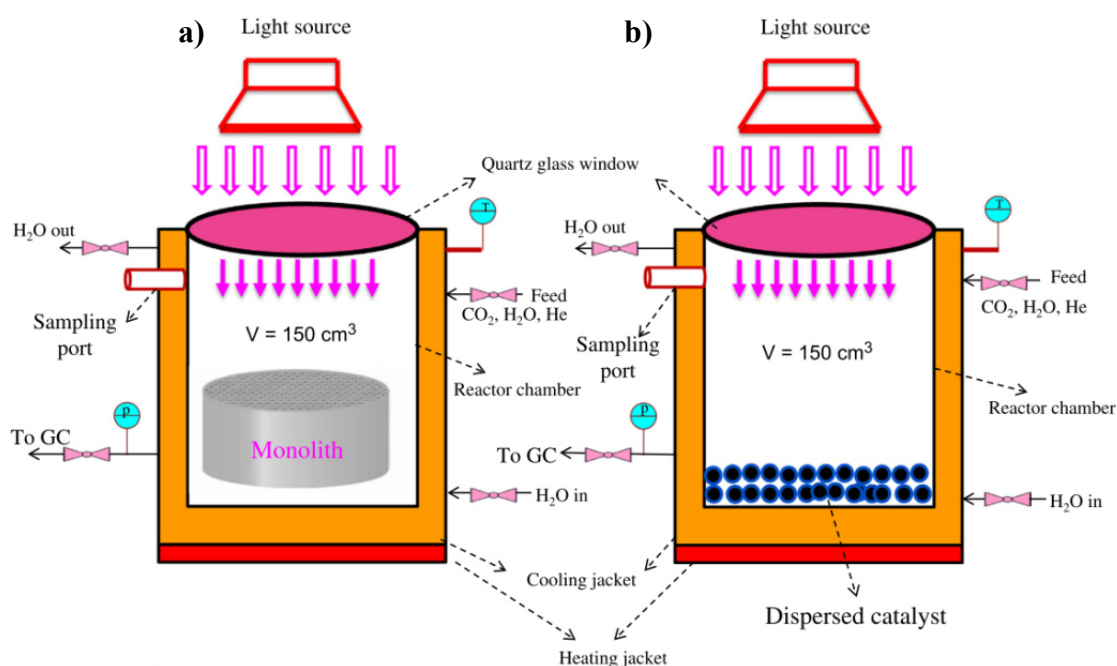


Figure 2.20. Schematic of experimental setup for photocatalytic CO₂ reduction with H₂O vapors: (a) monolith photoreactor and (b) cell type photoreactor⁸¹. Reprinted from Ref 81 Copyright (2013), with permission from Elsevier

To scale-up artificial photosynthetic photoreactors, immobilized batch-type photocatalytic systems have been modified to circulated reactors⁸⁴. A configuration of experimental setup is depicted in **Figure 2.21**, which is designed according to three main aspects: the

2. Reactors for Artificial Photosynthesis in Heterogeneous Systems

gas generation system, the photocatalytic reactor, and the sampling and analytic system. First of all, the system gets evacuated through hydrogen gas flow by the gas generation system. Afterwards, the diaphragm pump starts to circulate and inject the reaction gas which is a mixture of CO_2 with H_2 to the photocatalytic reactor section. In order to adjust the moisture content of the reaction gas, nitrogen or hydrogen are bubbled into deionized water and controlled by a hydrometer. The circulated reactors require to be designed in a way to ensure homogeneous distribution of gas flow inside the reactor and to shorten the reaction time¹². In the circulated system developed by Lo *et al.* (**Figure 2.22**), immobilized pyrex glass pellets with anatase titanium dioxide powder or zirconium oxide powder were packed⁸⁴. The whole system was placed under UV irradiation, and gas products were collected from a port in the photoreactor and analyzed by gas chromatography. According to the experimental results, TiO_2 with $\text{H}_2+\text{H}_2\text{O}$ and ZrO_2 with H_2 showed the highest yield for CO_2 photoreduction.

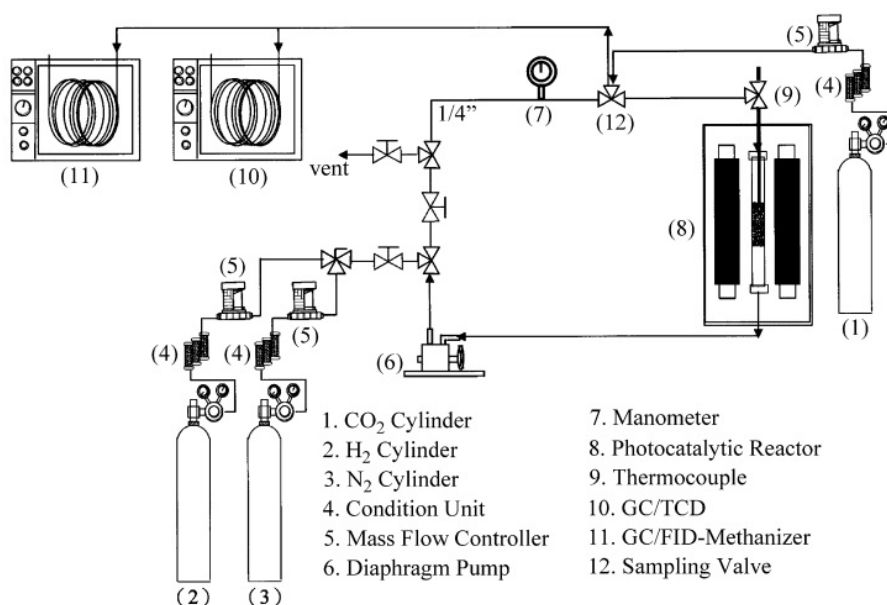


Figure 2.21. Schematic of circulated photocatalytic reaction system⁸⁴. Reprinted from Ref 84 Copyright (2007), with permission from Elsevier

2. Reactors for Artificial Photosynthesis in Heterogeneous Systems

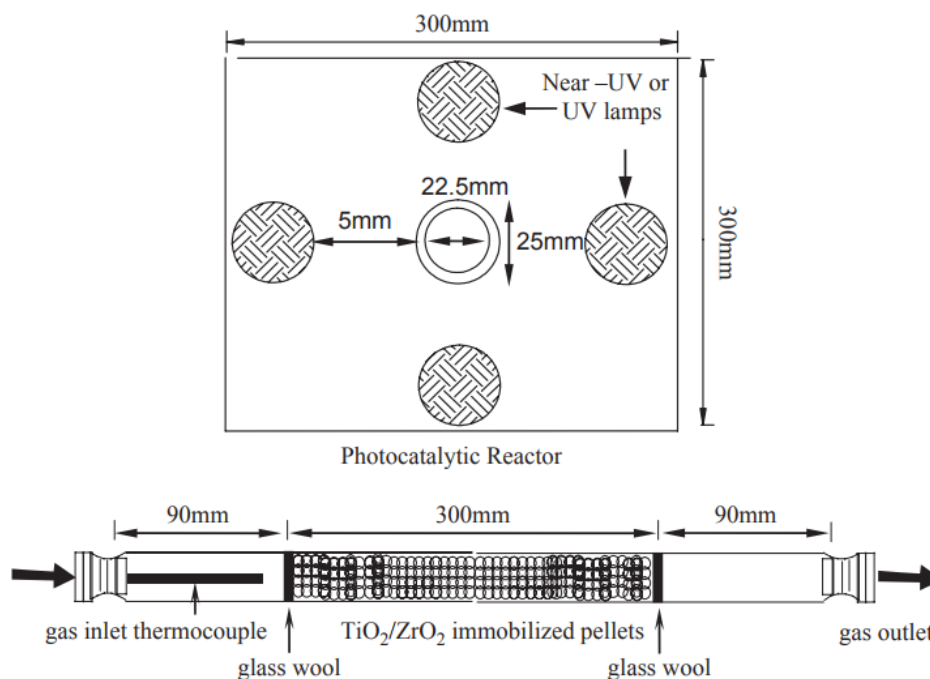


Figure 2.22. Schematic of a packed-bed photocatalytic reactor used in circulated system⁸⁴. Reprinted from Ref 84 Copyright (2007), with permission from Elsevier

Recently, Noji *et al.* have developed a nanoporous glass reactor with a considerable photoreduction of CO₂ to formic acid using a photosensitizer, methyl viologen (MV²⁺), and formate dehydrogenase (FDH)⁸⁵. In this design, porous glass plates (PGPs) have been chosen as the platform for the photoreaction to immobilize the ternary redox components. These are transparent plates in visible-NIR region which have penetrating nanopores. A photoreaction system which is tightly immobilized inside the nanopores, could reach to superior reaction efficiencies compared to a homogeneous solution system. The overall efficiency of this reactor was reported to be 14 times higher than that of the equivalent solution and the formic acid accumulation rate in 50 nm nanopores was found to be 83 times faster compared to an equivalent solution. Therefore, this reactor design was suggested as an efficient artificial photosynthesis system to convert CO₂ to fuel. Relevant examples of immobilized reactors are illustrated in **Table 2.1**.

2. Reactors for Artificial Photosynthesis in Heterogeneous Systems

Table 2.1. Summary of immobilized photoreactors in the literature

Reactor name	Catalyst	Support
Flat plate reactor ⁸⁶	Titanium dioxide	Borosilicate glass
Micro reactors ⁸⁷	Titanium dioxide	Silicon chips
Optical fiber reactor ⁸⁸	Titanium dioxide	Optical fiber
Carberry reactor ⁸⁹	Titanium dioxide	Sodium glass
Carbon foam-based ⁹⁰	Titanium dioxide	Carbon foam

2.7. Photocatalytic Reactor Design

One of the essential factors required to design a reactor is the knowledge of reaction kinetics. Since light absorption is the activation and first step in photocatalytic reactions, radiation distribution in the reactor needs to be well known in order to derive the local reaction rate and reaction kinetics. By having the knowledge of reaction rate, similar to the conventional reactors, designing photoreactors requires solving the conservation equations of momentum, energy and mass on the system. Moreover, in photoreactors the irradiative energy balance is of high importance⁹¹. Therefore, for designing a photoreactor, all associated radiation source specifications should be considered. These include the photon flux, the spectrum, the geometrical properties of the lamp, the distance from reaction system and the radiation entrance system into the reactor¹⁷. All these parameters affect the radiation field inside the reactor. Furthermore, in suspended solid heterogeneous systems, the light gets scattered due to the solid particles in slurry which act as a photocatalyst. Depending on the photocatalys, the amount of scattered light varies between 13 % to 76 % of the incoming light⁹². Not only the absorption coefficients of the photocatalyst, but also the absorption coefficients of the substrates, and reactor geometries can affect the amount of scattered light. Consequently, the irradiation field cannot be described by the well-known Lambert–Beer equation and it should be described with the complete radiative transfer equation⁹³.

Radiation field can be expressed as an amount of irradiative energy per unit wavelength, per solid angle, per unit normal area, and per unit time. Therefore the radiation intensity for a given wavelength is defined as **Equation 2.2**⁹⁴

$$I_{\lambda}(x, \Omega, t) = \frac{dE_{\lambda}}{dA \cos \theta d\Omega d\lambda dt} \quad (2.2)$$

2. Reactors for Artificial Photosynthesis in Heterogeneous Systems

where x is the position, Ω is direction, and t is time.

Considering photons coming from different directions to one point inside the photoreactor over the entire spherical space, the incident radiation can be written as **Equation 2.3**

$$G_{\lambda} = \int_{\lambda_1}^{\lambda_2} \int_{\theta_1}^{\theta_2} \int_{\varphi_1}^{\varphi_2} I_{\lambda}(x, \theta, \varphi, t) \sin \theta d\varphi d\theta \quad (2.3)$$

The energy due to the photon flux absorbed by each point in the reactor considering the direction, spatial, and spectral characterization can be calculated from the photon transport equation. Through this equation, the local volumetric rate of photon absorption (LVRPA) at any position of the system can be determined⁹¹. The LVREA is defined based on the radiation field inside the reactor which is not uniform due to the different light absorptions by present species, physical and geometrical characteristics of the irradiation source. This term is defined as **Equation 2.4**.

$$e_{\lambda}^a(x, t) = \int_{\lambda_1}^{\lambda_2} \int_{\varphi_1}^{\varphi_2} \int_{\theta_1}^{\theta_2} k_{\lambda}(x, t) I_{\lambda}(x, \theta, \varphi, t) \sin \theta d\theta d\varphi d\lambda \quad (2.4)$$

which is a function of position (x), time (t), wavelength (λ), direction (φ) and angle (θ).

The radiation transfer equation (RTE) is the balance between incident intensity and the rate of photon absorption, emission, in-scattered and out-scattered per unit time, unit volume, unit solid angle, and unit frequency interval (**Equation 2.5, Figure 2.23**)¹⁷.

$$\frac{1}{c} \frac{\partial I_{\Omega, \nu}}{\partial t} + \nabla \cdot (I_{\Omega, \nu} \Omega) = -W_{\Omega, \nu}^{absorption} + W_{\Omega, \nu}^{emission} + W_{\Omega, \nu}^{scattering-in} - W_{\Omega, \nu}^{scattering-out} \quad (2.5)$$

in which, $I_{\Omega, \nu}$ is the incident intensity with direction Ω and frequency ν . As the radiation field reaches the steady state almost instantaneously the first term on the left can be neglected. Depending on the system, some of the mentioned phenomena can be neglected as well. For example, scattering plays a significant role in heterogeneous solid-fluid or gas-liquid systems, however in homogenous systems it is approximately zero. Emission can also be negligible in the reactors. This is mainly because of the dependency of emission to temperature. Therefore, it is only important at high temperatures and as the photocatalytic reactions normally proceed at relatively low temperatures, this term can be assumed to be zero.

2. Reactors for Artificial Photosynthesis in Heterogeneous Systems

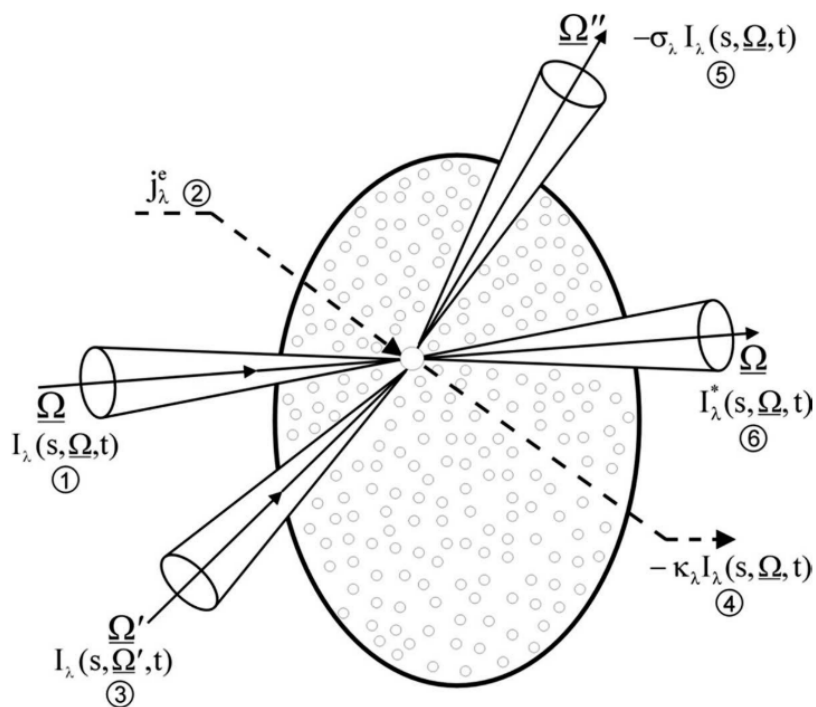


Figure 2.23. schematic representation of the absorption, emission and scattering phenomena in radiation transport for the wavelength λ . (1) incident intensity along s with direction Ω , (2) emission of radiation in the direction Ω , (3) intensity in a representative, arbitrary direction Ω' to be scattered in the direction Ω , (4) absorbed intensity in the direction Ω , (5) scattered intensity in a representative, arbitrary direction Ω'' out of the direction Ω , and (6) emerging intensity along s in the direction Ω , after losses by absorption and out-scattering and gains by emission and in-scattering^{17,95}. Reprinted with permission from Ref 95 Copyright (1995) American Chemical Society and from Ref 17 Copyright (1998), with permission from Elsevier

All the mentioned phenomena can be expressed by constitutive equations. Therefore, assuming to have an independent, multiple and elastic scattering⁹³, the radiation transfer equation can be written as **Equation 2.6**:

$$\frac{dI_\lambda(x, \Omega)}{dx} = -(k_\lambda + \sigma_\lambda)I_\lambda(x, \Omega) + j_\lambda^e(x, \Omega) + \frac{\sigma_\lambda}{4\pi} \int_0^{4\pi} I_\lambda(x, \hat{\Omega}) \mathbf{p}(\hat{\Omega} \rightarrow \Omega) d\hat{\Omega} \quad (2.6)$$

in which $I_\lambda(x, \Omega)$ is the spectral radiation intensity, λ , x and Ω represent the wavelength, position, and the solid angle, respectively. k_λ is the absorption coefficient, σ_λ is the scattering coefficient and j_λ^e is the spontaneous emission by a body. $\mathbf{p}(\hat{\Omega} \rightarrow \Omega)$ is the phase function describing the directional distribution of scattered radiation^{94,96}. According to the presented equation, scattering and absorption are of considerable importance in radiative energy balance. The first term on the right represents the fraction of the extinction of incident radiation that is absorbed and scattered in all directions and

2. Reactors for Artificial Photosynthesis in Heterogeneous Systems

frequencies by the matter per unit length along the path of the beam, per unit time, per unit volume, per unit solid angle of incidence and per unit frequency. The last term on the right expresses the received energy in scattering phenomenon from all directions (Ω') along the direction Ω . The incoming photons can be scattered inside the reactor in all directions according to the phase function. Generally the phase function can be given as the following expression(**Equation 2.7**)⁹⁷

$$p(\Omega) = \sum_{n=0}^N a_n P_n(\Omega), \quad a_0 = 1 \quad (2.7)$$

in which, $P_n(\Omega)$ presents the Legendre polynomials of order n and Ω and a_n expresses the corresponding expansion coefficients. Choosing a suitable phase function model to represent scattering inside the reactor is a big challenge in solving the radiative equation. Assuming to have an isotropic scattering, simplifies the phase function to a unit value. However, the complicated model functions are normally the main reason of complexity in solving the radiative equation. The scattering model frequently described is the linear anisotropic model (**Equation 2.8**):

$$p(\theta) = 1 + a_0 \cos(\theta) \quad (2.8)$$

with $a_0 = 1, 0, -1$ for forward, isotropic and backward scattering, respectively⁹⁸.

The complete radiative transfer equation should be solved considering the optical properties of the photocatalytic suspension and the boundaries conditions.

The obtained radiative transfer equation enables the calculation of the local value of the radiation absorption rate. In solar systems, the boundary conditions can be obtained by determining the radiation flux on the reactor window. This evaluation should be done considering the geometry and variations of the light during the day and throughout the year.

2.8. Conclusions

This chapter has provided an overview of photoreactors for artificial photosynthesis in liquid-solid heterogeneous systems. Photocatalytic technologies for artificial photosynthesis applications, employing either artificial or solar light, should be developed. Scaling up the designed solar hydrogen production and CO₂ reduction systems is of high importance. However, due to the low efficiency of these systems, the expenses of existing technologies do not allow the real application of artificial photosynthesis

2. Reactors for Artificial Photosynthesis in Heterogeneous Systems

based on semiconductor systems. Thus, essential advances in both solar-to-hydrogen conversion efficiency values and charges are required⁹⁹.

2.9. Acknowledgments

Financial Support from the Deutscher Akademischer Austauschdienst (DAAD) and the Global Research Laboratory program (2014K1A1A2041044), Korea government (MSIP) through NRF is gratefully acknowledged.

2.10. References

- (1) Kęsicki, F.; Walton, M. A.; Gould, T.; Cozzi, L.; Naceur, K. Ben; Hugues, P.; Park, R.; Wilkinson, D. *Water Energy Nexus*; Paris, 2016.
- (2) United States Environmental Protection Agency. *Inventory of U.S. Greenhouse Gas Emissions and Sinks: 1990-2015*; Washington, 2017.
- (3) Girod, B.; Wiek, A.; Mieg, H.; Hulme, M. The Evolution of the IPCC's Emissions Scenarios. *Environ. Sci. Policy* **2009**, *12*, 103–118.
- (4) Delucchi, M. A.; Jacobson, M. Z. Providing All Global Energy with Wind, Water, and Solar Power, Part II: Reliability, System and Transmission Costs, and Policies. *Energy Policy* **2011**, *39*, 1170–1190.
- (5) Zhang, B.; Sun, L. Artificial Photosynthesis: Opportunities and Challenges of Molecular Catalysts. *Chem. Soc. Rev.* **2019**, *48*, 2216–2264.
- (6) Eisenberg, R.; Nocera, D. G. Erratum: Preface: Overview of the Forum on Solar and Renewable Energy. *Inorg. Chem.* **2006**, *45*, 1880.
- (7) Shen, Y. Carbon Dioxide Bio-Fixation and Wastewater Treatment via Algae Photochemical Synthesis for Biofuels Production. *RSC Adv.* **2014**, *4*, 49672–49722.
- (8) Clarizia, L.; Russo, D.; Di Somma, I.; Andreozzi, R.; Marotta, R. Hydrogen Generation through Solar Photocatalytic Processes: A Review of the Configuration and the Properties of Effective Metal-Based Semiconductor Nanomaterials. *Energies* **2017**, *10*, 1624.
- (9) Oppenländer, T. *Photochemical Purification of Water and Air*; WILEY-VCH, 2003.
- (10) Xing, Z.; Zong, X.; Pan, J.; Wang, L. On the Engineering Part of Solar Hydrogen Production from Water Splitting: Photoreactor Design. *Chem. Eng. Sci.* **2013**, *104*, 125–146.
- (11) Huang, C.; Yao, W.; T-Raissi, A.; Muradov, N. Development of Efficient Photoreactors for Solar Hydrogen Production. *Sol. Energy* **2011**, *85*, 19–27.
- (12) Li, K.; An, X.; Park, K. H.; Khraisheh, M.; Tang, J. A Critical Review of CO₂ Photoconversion: Catalysts and Reactors. *Catal. Today* **2014**, *224*, 3–12.

2. Reactors for Artificial Photosynthesis in Heterogeneous Systems

- (13) Wang, X.; Ding, J.; Guo, W. Q.; Ren, N. Q. Scale-up and Optimization of Biohydrogen Production Reactor from Laboratory-Scale to Industrial-Scale on the Basis of Computational Fluid Dynamics Simulation. *Int. J. Hydrogen Energy* **2010**, *35*, 10960–10966.
- (14) Shaner, M. R.; Atwater, H. A.; Lewis, N. S.; McFarland, E. W. A Comparative Technoeconomic Analysis of Renewable Hydrogen Production Using Solar Energy. *Energy Environ. Sci.* **2016**, *9*, 2354–2371.
- (15) Leblebici, M. E.; Stefanidis, G. D.; Van Gerven, T. Comparison of Photocatalytic Space-Time Yields of 12 Reactor Designs for Wastewater Treatment. *Chem. Eng. Process. Process Intensif.* **2015**, *97*, 106–111.
- (16) De Lasa, H.; Serrano, B.; Salaiques, M. *Photocatalytic Reaction Engineering*; Springer US: New York, 2005.
- (17) Cassano, A. E.; Martin, C. A.; Brandi, R. J.; Alfano, O. M. Photoreactor Analysis and Design: Fundamentals and Applications. *Ind. Eng. Chem. Res.* **1995**, *34*, 2155–2201.
- (18) Levenspiel, O. *Chemical Reaction Engineering*, Third.; John Wiley & Sons: New York, 1999.
- (19) Froment, G. F.; Bischoff, K. B.; De Wilde, J. *Chemical Reactor Analysis and Design*; 2011.
- (20) Fogler, H. S. *Essentials of Chemical Reaction Engineering*, Third.; Pearson Education, 2014.
- (21) Pozzo, R. L.; Baltanás, M. a.; Cassano, a. E. Supported Titanium Oxide as Photocatalyst in Water Decontamination: State of the Art. *Catal. Today* **1997**, *39*, 219–231.
- (22) Fajrina, N.; Tahir, M. A Critical Review in Strategies to Improve Photocatalytic Water Splitting towards Hydrogen Production. *Int. J. Hydrogen Energy* **2019**, *44*, 540–577.
- (23) McCullagh, C.; Skillen, N.; Adams, M.; Robertson, P. K. J. Photocatalytic Reactors for Environmental Remediation: A Review. *J. Chem. Technol. Biotechnol.* **2011**, *86*, 1002–1017.
- (24) Alfano, O.; Bahnemann, D.; Cassano, A. Photocatalysis in Water Environments Using Artificial and Solar Light. *Catal. today* **2000**, *58*, 199–230.
- (25) McClure, J. . B.; Marsh, W. D. *Economics of Conversion of Fossil Fuels to Electricity*; New York, 1963.
- (26) Kopp, G.; Lean, J. L. A New, Lower Value of Total Solar Irradiance: Evidence and Climate Significance. *Geophys. Res. Lett.* **2011**, *38*, 1–7.
- (27) Hoffmann, M. R.; Martin, S. T.; Choi, W.; Bahnemann, D. W. Environmental Applications of Semiconductor Photocatalysis. *Chem. Rev.* **1995**, *95*, 69–96.
- (28) ASTM G173-03 (Reapproved 2008) Standard tables for reference solar spectral

2. Reactors for Artificial Photosynthesis in Heterogeneous Systems

- irradiance: direct normal and hemispherical on 37° Tilted Surface ASTM International, West Conshohocken, PA, 2008, www.astm.org.
- (29) Shihong, X.; Daolun, F.; Wenfeng, S. Preparations and Photocatalytic Properties of Visible-Light-Active Zinc Ferrite-Doped TiO₂ Photocatalyst. *J. Phys. Chem. C* **2009**, *113*, 2463–2467.
 - (30) Li, L.; Chen, R.; Liao, Q.; Zhu, X.; Wang, G.; Wang, D. High Surface Area Optofluidic Microreactor for Redox Mediated Photocatalytic Water Splitting. *Int. J. Hydrogen Energy* **2014**, *39*, 19270–19276.
 - (31) Shamim, R. O.; Dincer, I.; Naterer, G. F.; Zamfirescu, C. Experimental Investigation of a Solar Tower Based Photocatalytic Hydrogen Production System. *Int. J. Hydrogen Energy* **2014**, *39*, 5546–5556.
 - (32) Lo, C. C.; Huang, C. W.; Liao, C. H.; Wu, J. C. S. Novel Twin Reactor for Separate Evolution of Hydrogen and Oxygen in Photocatalytic Water Splitting. *Int. J. Hydrogen Energy* **2010**, *35*, 1523–1529.
 - (33) Real, D.; Johnston, R.; Lauer, J.; Schicho, A.; Hotz, N. Novel Non-Concentrating Solar Collector for Intermediate-Temperature Energy Capture. *Sol. Energy* **2014**, *108*, 421–431.
 - (34) Malato, S.; Blanco, J.; Vidal, A.; Richter, C. Photocatalysis with Solar Energy at a Pilot-Plant Scale: An Overview. *Appl. Catal. B Environ.* **2002**, *37*, 1–15.
 - (35) Blanco, J.; Malato, S.; Fernández, P.; Vidal, A.; Morales, A.; Trincado, P.; Oliveira, J. ; Minero, C.; Musci, M.; Casalle, C.; et al. Compound Parabolic Concentrator Technology Development to Commercial Solar Detoxification Applications. *Sol. Energy* **1999**, *67*, 317–330.
 - (36) Tanveer, M.; Tezcanli Guyer, G. Solar Assisted Photo Degradation of Wastewater by Compound Parabolic Collectors: Review of Design and Operational Parameters. *Renew. Sustain. Energy Rev.* **2013**, *24*, 534–543.
 - (37) Rabl, A.; Goodman, N. B.; Winston, R. Practical Design Considerations for CPC Solar Collectors. *Sol. Energy* **1979**, *22*, 373–381.
 - (38) Goswami, D. Y.; Sharma, S. K.; Mathur, G. D.; Jotshi, C. K. Techno-Economic Analysis of Solar Detoxification Systems. *J. Sol. Energy Eng.* **1997**, *119*, 108.
 - (39) Romero, M.; Blanco, J.; Sánchez, B.; Vidal, A.; Sixto Malato; Cardona, A. I.; Garcia, E. Solar Photocatalytic Degradation of Water and Air Pollutants: Challenges and Perspectives. *Sol. Energy* **1999**, *66*, 169–182.
 - (40) Jing, D.; Liu, H.; Zhang, X.; Zhao, L.; Guo, L. Photocatalytic Hydrogen Production under Direct Solar Light in a CPC Based Solar Reactor: Reactor Design and Preliminary Results. *Energy Convers. Manag.* **2009**, *50*, 2919–2926.
 - (41) Ruban, P.; Sellappa, K. Development and Performance of Bench-Scale Reactor for the Photocatalytic Generation of Hydrogen. *Energy* **2014**, *73*, 926–932.
 - (42) Yang, Y.; Wei, Q.; Hou, J.; Liu, H.; Zhao, L. Solar Concentrator with Uniform Irradiance for Particulate Photocatalytic Hydrogen Production System. *Int. J.*

2. Reactors for Artificial Photosynthesis in Heterogeneous Systems

Hydrogen Energy **2016**, *41*, 16040–16047.

- (43) Arzate Salgado, S. Y.; Ramírez Zamora, R. M.; Zanella, R.; Peral, J.; Malato, S.; Maldonado, M. I. Photocatalytic Hydrogen Production in a Solar Pilot Plant Using a Au/TiO₂ Photo Catalyst. *Int. J. Hydrogen Energy* **2016**, *41*, 11933–11940.
- (44) Wei, Q.; Yang, Y.; Hou, J.; Liu, H.; Cao, F.; Zhao, L. Direct Solar Photocatalytic Hydrogen Generation with CPC Photoreactors: System Development. *Sol. Energy* **2017**, *153*, 215–223.
- (45) Jing, D.; Guo, L.; Zhao, L.; Zhang, X.; Liu, H.; Li, M.; Shen, S.; Liu, G.; Hu, X.; Zhang, X.; et al. Efficient Solar Hydrogen Production by Photocatalytic Water Splitting: From Fundamental Study to Pilot Demonstration. *Int. J. Hydrogen Energy* **2010**, *35*, 7087–7097.
- (46) Nguyen, T. V.; Wu, J. C. S.; Chiou, C. H. Photoreduction of CO₂ over Ruthenium Dye-Sensitized TiO₂-Based Catalysts under Concentrated Natural Sunlight. *Catal. Commun.* **2008**, *9*, 2073–2076.
- (47) James, B. D.; Baum, G. N.; Perez, J.; Baum, K. N. *Technoeconomic Analysis of Photoelectrochemical (PEC) Hydrogen Production*; 2009.
- (48) Blanco Gálvez, J.; Malato Rodríguez, S. Solar Photochemistry Technology. In *Solar Energy Conversion and Photoenergy Systems*; Encyclopedia of Life Support Systems (EOLSS): Oxford, United Kingdom, 2009; Vol. II, pp 139–162.
- (49) Alpert, D. J.; Sprung, J. L.; Pacheco, J. E.; Prairie, M. R.; Reilly, H. E.; Milne, T. A.; Nimlos, M. R. Sandia National Laboratories' Work in Solar Detoxification of Hazardous Wastes. *Sol. Energy Mater.* **1991**, *24*, 594–607.
- (50) Bekbölet, M.; Lindner, M.; Weichgrebe, D.; Bahnemann, D. W. Photocatalytic Detoxification with the Thin-Film Fixed-Bed Reactor (TFFBR): Clean-up of Highly Polluted Landfill Effluents Using a Novel TiO₂-Photocatalyst. *Sol. Energy* **1996**, *56*, 455–469.
- (51) Goslich, R.; Dillert, R.; Bahnemann, D. Solar Water Treatment - Principles and Reactors. *Water Sci. Technol.* **1997**, *35*, 137–148.
- (52) Bousselmi, L.; Geissen, S.; Schroeder, H. Textile Wastewater Treatment and Reuse by Solar Catalysis : Results from a Pilot Plant in Tunisia. *Water Sci. Technol.* **2004**, *49*, 331–337.
- (53) Abdel-Maksoud, Y.; Imam, E.; Ramadan, A. TiO₂ Solar Photocatalytic Reactor Systems: Selection of Reactor Design for Scale-up and Commercialization—Analytical Review. *Catalysts* **2016**, *6*, 138.
- (54) Dillert, R.; Cassano, A. E.; Goslich, R.; Bahnemann, D. Large Scale Studies in Solar Catalytic Wastewater Treatment. *Catal. Today* **1999**, *54*, 267–282.
- (55) Pinaud, B. A.; Benck, J. D.; Seitz, L. C.; Forman, A. J.; Chen, Z.; Deutsch, T. G.; James, B. D.; Baum, K. N.; Baum, G. N.; Ardo, S.; et al. Technical and Economic Feasibility of Centralized Facilities for Solar Hydrogen Production via Photocatalysis and Photoelectrochemistry. *Energy Environ. Sci.* **2013**, *6*, 1983–

2. Reactors for Artificial Photosynthesis in Heterogeneous Systems

- 2002.
- (56) Rodriguez, C. A.; Modestino, M. A.; Psaltis, D.; Moser, C. Design and Cost Considerations for Practical Solar-Hydrogen Generators. *Energy Environ. Sci.* **2014**, *7*, 3828–3835.
- (57) Maeda, K. Photocatalytic Water Splitting Using Semiconductor Particles: History and Recent Developments. *J. Photochem. Photobiol. C Photochem. Rev.* **2011**, *12*, 237–268.
- (58) Chen, J. J.; Wu, J. C. S.; Wu, P. C.; Tsai, D. P. Plasmonic Photocatalyst for H₂ Evolution in Photocatalytic Water Splitting. *J. Phys. Chem. C* **2011**, *115*, 210–216.
- (59) Inoue, T.; Fujishima, A.; Konishi, S.; Honda, K. Photoelectrocatalytic Reduction of Carbon Dioxide in Aqueous Suspensions of Semiconductor Powders. *Nature* **1979**, *277*, 637–638.
- (60) Tahir, M.; Amin, N. S. Advances in Visible Light Responsive Titanium Oxide-Based Photocatalysts for CO₂ Conversion to Hydrocarbon Fuels. *Energy Convers. Manag.* **2013**, *76*, 194–214.
- (61) Tang, J.; Zou, Z.; Ye, J. Efficient Photocatalytic Decomposition of Organic Contaminants over CaBi₂O₄ under Visible-Light Irradiation. *Angew. Chemie - Int. Ed.* **2004**, *43*, 4463–4466.
- (62) Lee, C. W.; Antoniou Kourouniotti, R.; Wu, J. C. S.; Murchie, E.; Maroto-Valer, M.; Jensen, O. E.; Huang, C. W.; Ruban, A. Photocatalytic Conversion of CO₂ to Hydrocarbons by Light-Harvesting Complex Assisted Rh-Doped TiO₂ Photocatalyst. *J. CO₂ Util.* **2014**, *5*, 33–40.
- (63) Lee, W. H.; Liao, C. H.; Tsai, M. F.; Huang, C. W.; Wu, J. C. S. A Novel Twin Reactor for CO₂ Photoreduction to Mimic Artificial Photosynthesis. *Appl. Catal. B Environ.* **2013**, *132–133*, 445–451.
- (64) Skillen, N.; Adams, M.; McCullagh, C.; Ryu, S. Y.; Fina, F.; Hoffmann, M. R.; Irvine, J. T. S.; Robertson, P. K. J. The Application of a Novel Fluidised Photo Reactor under UV-Visible and Natural Solar Irradiation in the Photocatalytic Generation of Hydrogen. *Chem. Eng. J.* **2016**, *286*, 610–621.
- (65) Abdel Aal, M. S.; Wahdan, M. H.; Gomma, G. K. Influence of Fe²⁺ Ion on the Corrosion of Carbon Steel. *Mater. Chem. Phys.* **1995**, *39*, 290–297.
- (66) Imoberdorf, G. E.; Cassano, A. E.; Irazoqui, H. A.; Alfano, O. M. Optimal Design and Modeling of Annular Photocatalytic Wall Reactors. *Catal. Today* **2007**, *129* (1-2 SPEC. ISS.), 118–126.
- (67) Subramanian, M.; Kannan, A. Photocatalytic Degradation of Phenol in a Rotating Annular Reactor. *Chem. Eng. Sci.* **2010**, *65*, 2727–2740.
- (68) Yatmaz, H. C.; Wallis, C.; Howarth, C. R. The Spinning Disc Reactor - Studies on a Novel TiO₂ Photocatalytic Reactor. *Chemosphere* **2001**, *42*, 397–403.
- (69) Lee, D. K.; Kim, S. C.; Cho, I. C.; Kim, S. J.; Kim, S. W. Photocatalytic Oxidation of Microcystin-LR in a Fluidized Bed Reactor Having TiO₂-Coated Activated

2. Reactors for Artificial Photosynthesis in Heterogeneous Systems

- Carbon. *Sep. Purif. Technol.* **2004**, *34*, 59–66.
- (70) Shephard, G. S.; Stockenström, S.; De Villiers, D.; Engelbrecht, W. J.; Wessels, G. F. S. Degradation of Microcystin Toxins in a Falling Film Photocatalytic Reactor with Immobilized Titanium Dioxide Catalyst. *Water Res.* **2002**, *36*, 140–146.
- (71) Shi, D.; Feng, Y.; Zhong, S. Photocatalytic Conversion of CH₄ and CO₂ to Oxygenated Compounds over Cu/CdS-TiO₂/SiO₂ Catalyst. *Catal. Today* **2004**, *98*, 505–509.
- (72) Wu, J. C. S.; Lin, H. M.; Lai, C. L. Photo Reduction of CO₂ to Methanol Using Optical-Fiber Photoreactor. *Appl. Catal. A Gen.* **2005**, *296*, 194–200.
- (73) Sazio, P. J. A.; Amezcua-Correa, A.; Finlayson, C. E.; Hayes, J. R.; Scheidemantel, T. J.; Baril, N. F.; Jackson, B. R. Microstructured Optical Fibers as High-Pressure Microfluidic Reactors. *Science*. **2006**, *311*, 1583–1586.
- (74) Wu, J. C. S.; Wu, T. H.; Chu, T.; Huang, H.; Tsai, D. Application of Optical-Fiber Photoreactor for CO₂ Photocatalytic Reduction. *Top. Catal.* **2008**, *47*, 131–136.
- (75) Nguyen, T.; Wu, J. C. S. Photoreduction of CO₂ in an Optical-Fiber Photoreactor: Effects of Metals Addition and Catalyst Carrier. *Appl. Catal. A Gen.* **2008**, *335*, 112–120.
- (76) Ola, O.; Maroto-Valer, M. M. Review of Material Design and Reactor Engineering on TiO₂ Photocatalysis for CO₂ Reduction. *J. Photochem. Photobiol. C Photochem. Rev.* **2015**, *24*, 16–42.
- (77) Du, P.; Carneiro, J. T.; Moulijn, J. A.; Mul, G. A Novel Photocatalytic Monolith Reactor for Multiphase Heterogeneous Photocatalysis. *Appl. Catal. A Gen.* **2008**, *334*, 119–128.
- (78) Nakata, K.; Fujishima, A. TiO₂ Photocatalysis: Design and Applications. *J. Photochem. Photobiol. C Photochem. Rev.* **2012**, *13*, 169–189.
- (79) Lin, H.; Valsaraj, K. T. An Optical Fiber Monolith Reactor for Photocatalytic Wastewater Treatment. *J. Appl. Electrochem.* **2005**, *35*, 699–708.
- (80) Tahir, M.; Amin, N. S. Photocatalytic CO₂ Reduction and Kinetic Study over In/TiO₂ Nanoparticles Supported Microchannel Monolith Photoreactor. *Appl. Catal. A Gen.* **2013**, *467*, 483–496.
- (81) Tahir, M.; Amin, N. S. Photocatalytic CO₂ Reduction with H₂O Vapors Using Montmorillonite/TiO₂ Supported Microchannel Monolith Photoreactor. *Chem. Eng. J.* **2013**, *230*, 314–327.
- (82) Joo, H.; Lee, J. H. Polyaniline Nanofiber Coated Monolith Reactor for Enzymatic Bioconversion. *J. Mol. Catal. B Enzym.* **2010**, *67*, 179–183.
- (83) Liou, P.-Y.; Chen, S.-C.; Wu, J. C. S.; Liu, D.; Mackintosh, S.; Maroto-Valer, M.; Linforth, R. Photocatalytic CO₂ Reduction Using an Internally Illuminated Monolith Photoreactor. *Energy Environ. Sci.* **2011**, *4*, 1487.
- (84) Lo, C. C.; Hung, C. H.; Yuan, C. S.; Wu, J. F. Photoreduction of Carbon Dioxide

2. Reactors for Artificial Photosynthesis in Heterogeneous Systems

- with H₂ and H₂O over TiO₂ and ZrO₂ in a Circulated Photocatalytic Reactor. *Sol. Energy Mater. Sol. Cells* **2007**, *91*, 1765–1774.
- (85) Noji, T.; Jin, T.; Nango, M.; Kamiya, N.; Amai, Y. CO₂ Photoreduction by Formate Dehydrogenase and a Ru-Complex in a Nanoporous Glass Reactor. *ACS Appl. Mater. Interfaces* **2017**, *9*, 3260–3265.
- (86) Vezzoli, M.; Martens, W. N.; Bell, J. M. Investigation of Phenol Degradation: True Reaction Kinetics on Fixed Film Titanium Dioxide Photocatalyst. *Appl. Catal. A Gen.* **2011**, *404*, 155–163.
- (87) Visan, A.; Rafieian, D.; Ogieglo, W.; Lammertink, R. G. H. Modeling Intrinsic Kinetics in Immobilized Photocatalytic Microreactors. *Appl. Catal. B Environ.* **2014**, *150–151*, 93–100.
- (88) Danion, A.; Disdier, J.; Guillard, C.; Païssé, O.; Jaffrezic-Renault, N. Photocatalytic Degradation of Imidazolinone Fungicide in TiO₂-Coated Optical Fiber Reactor. *Appl. Catal. B Environ.* **2006**, *62*, 274–281.
- (89) Černigoj, U.; Štangar, U. L.; Trebše, P. Evaluation of a Novel Carberry Type Photoreactor for the Degradation of Organic Pollutants in Water. *J. Photochem. Photobiol. A Chem.* **2007**, *188*, 169–176.
- (90) Hajiesmaili, S.; Josset, S.; Bégin, D.; Pham-Huu, C.; Keller, N.; Keller, V. 3D Solid Carbon Foam-Based Photocatalytic Materials for Vapor Phase Flow-through Structured Photoreactors. *Appl. Catal. A Gen.* **2010**, *382*, 122–130.
- (91) Marugán, J.; Grieken, R. Van. Photocatalytic Reactor Design. In *Photocatalysis: Fundamentals and Perspectives*; Schneider, J., Bahnemann, D., Ye, J., Puma, G. L., Dionysiou, D. D., Eds.; The Royal Society of Chemistry, 2016; pp 367–387.
- (92) Serpone, N. Relative Photonic Efficiencies and Quantum Yields in Heterogeneous Photocatalysis. *J. Photochem. Photobiol. A Chem.* **1997**, *104*, 1–12.
- (93) Cassano, A. E.; Alfano, O. M. Reaction Engineering of Suspended Solid Heterogeneous Photocatalytic Reactors. *Catal. Today* **2000**, *58*, 167–197.
- (94) Alfano, O. M.; Cassano, A. E.; Marugan, J.; Grieken, R. van. Fundamentals of Radiation Transport in Absorbing Scattering Media. In *Photocatalysis Fundamentals and perspectives*; The Royal Society of Chemistry, 2016; pp 351–366.
- (95) Martin, C. A.; Baltanas, M. A.; Cassano, A. E. Photocatalytic Reactors I. Optical Behavior of Titanium. *J. Photochem. Photobiol. A Chem.* **1993**, *76*, 199–208.
- (96) Alvarado-Rolon, O.; Natividad, R.; Romero, R.; Hurtado, L.; Ramírez-Serrano, A. Modelling and Simulation of the Radiant Field in an Annular Heterogeneous Photoreactor Using a Four-Flux Model. *Int. J. Photoenergy* **2018**, *2018*, 1–16.
- (97) Satuf, M. L.; Brandi, R. J.; Cassano, A. E.; Alfano, O. M. Experimental Method to Evaluate the Optical Properties of Aqueous Titanium Dioxide Suspensions. *Ind. Eng. Chem. Res.* **2005**, *44*, 6643–6649.
- (98) Pareek, V.; Cox, S.; Adesina, A. Light Intensity Distribution in Photocatalytic

2. Reactors for Artificial Photosynthesis in Heterogeneous Systems

Reactors. *Third Int. Conf. CFD Miner. Process Ind.* **2003**, No. December, 229–234.

- (99) Hisatomi, T.; Domen, K. Introductory Lecture: Sunlight-Driven Water Splitting and Carbon Dioxide Reduction by Heterogeneous Semiconductor Systems as Key Processes in Artificial Photosynthesis. *Faraday Discuss.* **2017**, *198*, 11–35.

2. Reactors for Artificial Photosynthesis in Heterogeneous Systems

3. A Method to Compare the Activities of Semiconductor Photocatalysts in Liquid-Solid Systems

3.1. Foreword

Scattering is the main reason for the majority of the complexities associated with the analysis and design of suitable photoreactors for heterogeneous photocatalysis. This phenomenon is also responsible for the difficulties of the usual methods used to investigate the photocatalytic activity of semiconductors. Therefore, solving this obstacle in the photoreactor design requires the knowledge and thus the determination of absolute values of the quantum yield of photocatalytic processes employing semiconductor particles. As outlined in **Chapter 1**, in a black body reactor it can be assumed that all the incoming light is absorbed by the photocatalyst particles and that the fractions of reflected and transmitted light are insignificant due to the reactor geometry and the high optical density of the heterogeneous system. Therefore, considering the properties of a black body photoreactor, the scattering phenomenon in such a reactor can be neglected. Consequently, the regarding problems of scattering in photoreactors for the calculations related to the volume-averaged quantum yield can be solved as shown in this chapter.

This chapter contains the article *A Method to compare the activities of semiconductor photocatalysts in liquid-solid systems* by Lena Megatiff, Ralf Dillert, and Detlef W. Bahnemann, published in ChemPhotoChem 2018, 2, 948 -951. Herein, a standard method for the comparison of the intrinsic photocatalytic activity of various materials in liquid-solid heterogeneous systems has been developed. The experimental application of the concept of a “black body” like reactor provides a simple method to measure the reaction rate as well as the respective quantum yield of photocatalytic reactions in heterogeneous liquid-solid systems without dealing with difficulties of the quantification of the amount of absorbed photons. Hence, the developed method presented in this paper plays a significant role in simplifying the photoreactor design through the calculation of the local reaction rate inside the photoreactor using the volume-averaged value of the quantum yield.

3. A Method to Compare the Activities of Semiconductor Photocatalysts in Liquid-Solid Systems

3.2. Abstract

A method to determine the activity of semiconducting photocatalysts in liquid–solid systems is suggested employing a black body photoreactor. The reaction rates, defined as the converted amount of the probe molecule per unit time (dn/dt), in the presence of nine different photocatalysts, were found to be constant and not affected by the initial concentration of the probe compound dichloroacetic acid (C_0), the mass concentration of the photocatalyst (γ), and the suspension volume (when C_0 and γ are larger than 5 mM and 1 g L⁻¹, respectively). The method presented here thus seems to be generally applicable to obtain experimental data allowing the comparison of the photocatalytic activities of different semiconductors.

3.3. Keywords

Photocatalysis, semiconductors, kinetics, black body photoreactor, liquid-solid system.

3.4. Manuscript

Semiconductor photocatalysis is considered to be one of the most effective techniques to harvest solar light for environmental remediation and to produce solar fuels¹⁻⁵. Consequently, synthesis of new semiconductors designed for photocatalytic applications has attracted considerable attention⁶⁻⁹. Despite the progress in the development of photocatalysts, a standard method to compare the photocatalytic activities of different photocatalysts in liquid-solid heterogeneous systems has still not been established. Recently, Kisch and Bahnemann recommended in a very general way to compare the activities of photocatalysts in solid/liquid systems by measuring the reaction rates of a probe compound with the same type of photoreactor under identical irradiation conditions¹⁰. Although, the necessity of reaction rate measurements at an optimal catalyst concentration was mentioned, no discussion about the reaction rate unit, the suspension volume, and the effect of the initial concentration of the probe molecule was provided.

The kinetics of a photocatalytic reaction is in most cases given by a rate law having the mathematical form.

$$dc/dt = kKc/(1+Kc) \quad (3.1)$$

3. A Method to Compare the Activities of Semiconductor Photocatalysts in Liquid-Solid Systems

where c is the molar concentration of the probe compound. The kinetic parameters k and K are the maximum reaction rate accessible under the given experimental conditions and a physical parameter which is usually attributed to be the adsorption constant, respectively^{11,12}. In nearly all cases the comparative evaluation of the activities of photocatalysts is performed under experimental conditions where $Kc \ll 1$ holds. Consequently, the change of concentration of the probe molecule during irradiation follows an apparent first-order rate law, $dc/dt = kKc = k_{app}c$. The analysis of published results reveals that the apparent first-order rate constant k_{app} is usually not independent from the concentration of the probe molecule thus indicating complex interactions between the photocatalyst surface and the probe molecule¹³⁻¹⁵. Therefore, the reaction rate dc/dt determined under the condition of apparent first-order kinetics seems not to be suitable as a measure to compare the activities of different photocatalysts.

It was also not discussed in the paper of Kisch and Bahnemann that in the usual experimental procedure, in which the suspensions are irradiated through a window in the outer wall of the photoreactor from an external light source, the measured reaction rates also depend on the scattering properties of the photocatalyst¹⁶⁻²⁰. The portion of photons that is not absorbed by the semiconductor but is scattered out of the reactor may be different for the photocatalysts to be compared. Measurements in which light losses occur due to the optical properties of the photocatalysts, which are cumbersome to quantify experimentally, permit only very limited statements concerning their activities.

To ensure the comparability of the results of different laboratories, a method to determine photocatalytic activities in liquid-solid systems with a given probe compound at defined wavelength and photon flux should fulfill at least five conditions. (i) The reaction rates should not be affected by the scattering of photons out of the photoreactor. Additionally, the rates should be independent of (ii) the geometry of the photoreactor, (iii) the suspension volume, (iv) the concentration of the probe compound, and (v) the mass concentration of the photocatalyst. It can be shown that the conditions (i), (ii), and (iii) are fulfilled within the limits of experimental error when a black body photoreactor is employed as introduced by Emeline *et al.*²¹. In a black body reactor, the fractions of reflected and transmitted light are approximately zero due to the reactor geometry and the high optical density of the heterogeneous system. For this type of photoreactor, it can be assumed that all photons of suitable wavelengths emitted by the light source and entering the suspension are absorbed by the photocatalyst. Therefore, the reaction rate defined on

3. A Method to Compare the Activities of Semiconductor Photocatalysts in Liquid-Solid Systems

an amount basis (dn/dt) can be easily measured and compared for different systems. From the rate law of a photocatalytic reaction given above (**Equation 3.1**) it is readily deduced that the rate at a given mass concentration of the photocatalyst becomes independent from the concentration of the probe molecule provided that this concentration is sufficiently large ($Kc \gg 1$)²². The determination of reaction rates under this condition of apparent zero order kinetics therefore provides values ($dn/dt = Vdc/dt = Vk$) being constant over a wide range of concentrations of the probe compound, thus fulfilling condition (iv). Moreover, at sufficiently high photocatalyst concentration, the number of photons absorbed by the photocatalyst per unit time remains constant resulting in a reaction rate being independent from the mass concentration of the photocatalyst, thus fulfilling condition (v)^{10,23,24}.

In this study the effect of the initial concentration c_0 of the probe molecule, the mass concentration γ of the heterogeneous photocatalyst, and the suspension volume V on the rate of the photocatalytic degradation of dichloroacetic acid (DCA) have been investigated. The rates were measured employing a black body photoreactor in which the light entrance is surrounded by a sufficient amount of suspension in all three spatial directions to guarantee the complete absorption of the entering photons. The reaction rates dc/dt obtained from the slopes of the concentration vs. time plots of the experimental runs have been used to calculate the rates on an amount basis ($dn/dt = Vdc/dt$). The thus calculated rates are presented in **Figure 3.1**.

As can be seen from **Figure 3.1a**, the reacted amount of the probe compound per unit time is constant and the reaction rate is not affected by the initial concentration c_0 of the probe molecule when $c_0 \geq 2$ mM. The average rate was calculated to be $1.91 \pm 0.15 \mu\text{mol min}^{-1}$. **Figure 3.1b** and **3.1c** reveal that the rates dn/dt are neither affected by increasing the catalyst concentration γ nor by changing the suspension volume V . Average reaction rates of $1.89 \pm 0.10 \mu\text{mol min}^{-1}$ and $2.12 \pm 0.15 \mu\text{mol min}^{-1}$ were calculated. The average value for the reaction rate of all experimental runs performed with UV 100 in this study ($N = 12$) was calculated to be $1.98 \pm 0.18 \mu\text{mol min}^{-1}$.

3. A Method to Compare the Activities of Semiconductor Photocatalysts in Liquid-Solid Systems

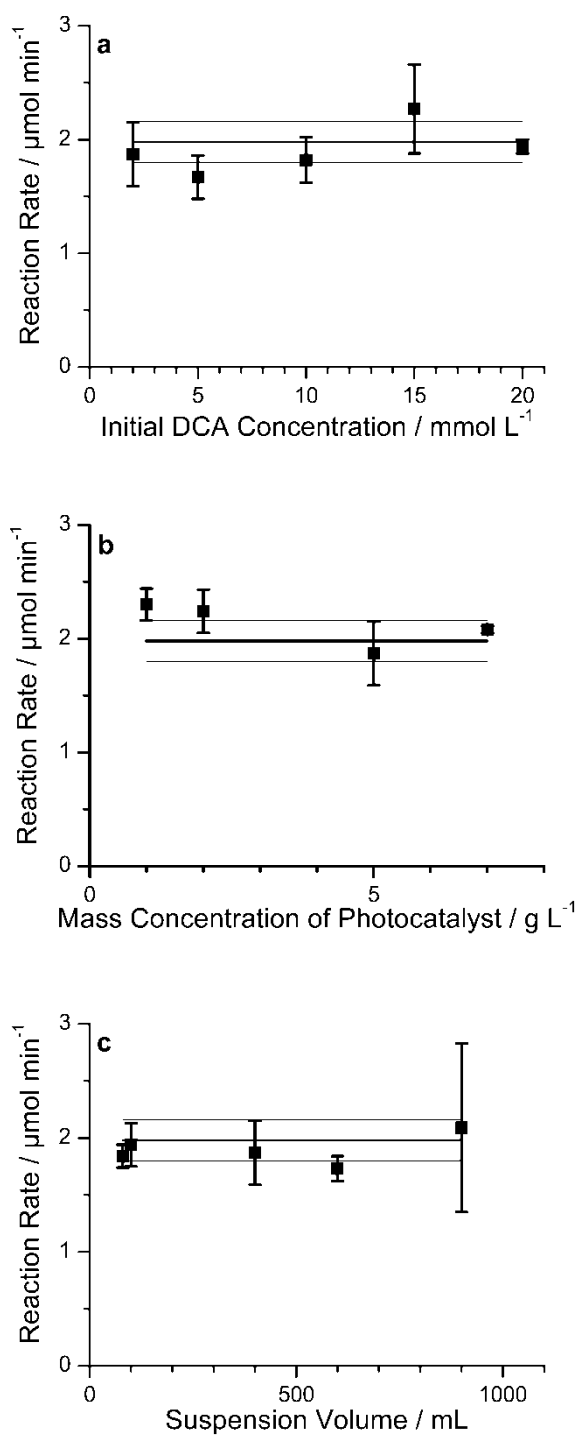


Figure 3.1. Reaction rates dn/dt as a function of a) the initial concentration of DCA, b) the mass concentration of the Sachtleben Hombikat UV100 photocatalyst, and c) the suspension volume. The lines in a, b and c present the average value \pm standard deviation of all experimental runs ($N = 12$) performed in this study. Experimental conditions: a) $2 \text{ mM} \leq c_0 \leq 20 \text{ mM}$, $\gamma = 5 \text{ g L}^{-1}$, $V = 400 \text{ mL}$; b) $c_0 = 10 \text{ mM}$, $1 \text{ g L}^{-1} \leq \gamma \leq 7 \text{ g L}^{-1}$, $V = 400 \text{ mL}$; c) $c_0 = 10 \text{ mM}$, $\gamma = 5 \text{ g L}^{-1}$, $80 \text{ mL} \leq V \leq 900 \text{ mL}$.

3. A Method to Compare the Activities of Semiconductor Photocatalysts in Liquid-Solid Systems

To test whether the observed reaction rate independence from the initial concentration of the probe compound, the catalyst concentration, and the suspension volume also applies to other photocatalysts, a limited number of experimental runs was performed employing pure rutile, an anatase-rutile mixture (Evonik TiO₂ Aeroxide P25), a commercially available surface-modified anatase (KRONOClean 7000), pure brookite, SrTiO₃ and BaTiO₃ nanopowders as well as bulk WO₃ and ZnO as photocatalysts. The obtained reaction rates dn/dt are given in **Figure 3.2**.

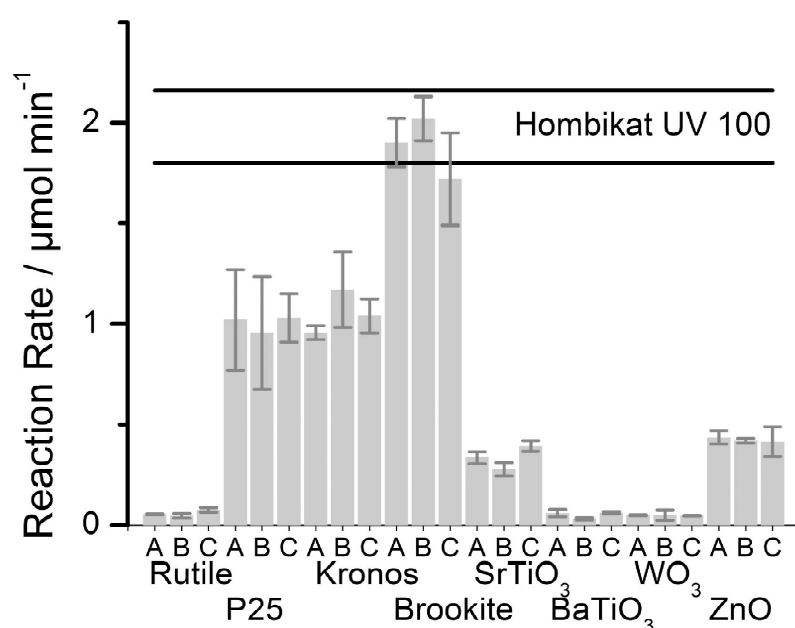


Figure 3.2. Reaction rates dn/dt of the photocatalytic degradation of DCA in the presence of rutile, Evonik TiO₂ Aeroxide P25, KRONOClean 7000, brookite, SrTiO₃, BaTiO₃, WO₃, and ZnO. The upper and lower values of the reaction rate obtained in the presence of Hombikat UV 100 are given for comparison.

Experimental conditions: A) $c_0 = 5 \text{ mM}$, $\gamma = 5 \text{ g L}^{-1}$, $V = 400 \text{ mL}$; B) $c_0 = 10 \text{ mM}$, $\gamma = 5 \text{ g L}^{-1}$, $V = 400 \text{ mL}$;
C) $c_0 = 10 \text{ mM}$, $\gamma = 7 \text{ g L}^{-1}$, $V = 600 \text{ mL}$.

The difference in the activities of Hombikat UV 100 and Aeroxide P25 found here is consistent with published results obtained with DCA as the probe compound^{25,26}. In agreement with published results, the data presented in **Figure 3.2** demonstrate the known low photocatalytic activity of rutile TiO₂ and the high activity of brookite TiO₂^{27,28}. Also, the low reaction rates obtained in the presence of SrTiO₃, BaTiO₃, WO₃, and ZnO compared to Aeroxide P25 are consistent with published results. The alkaline earth

3. A Method to Compare the Activities of Semiconductor Photocatalysts in Liquid-Solid Systems

titanates SrTiO₃ and BaTiO₃ are known to have only a fairly weak activity in photocatalytic oxidation reactions of organic compounds in aqueous suspensions²⁹⁻³¹. The semiconductors WO₃ and ZnO have also long been known to have a significantly lower photocatalytic activity than TiO₂³². Reported photocatalytic reaction rates of different probe compounds in the presence of bulk ZnO revealed a 30 % to 50 % lower activity of bulk ZnO in comparison to Aeroxide P25^{33,34}.

According to the data presented in the **Figures 3.1** and **3.2** the reaction rates dn/dt for a photocatalyst under consideration were found to be constant within the limits of the experimental error and not affected by the initial concentration of the probe compound, *i.e.*, dichloroacetic acid, the mass concentration of the photocatalyst, and the suspension volume as long as the photoreactor meets the requirements for a black body reactor and the concentration of the probe compound is sufficiently high to ensure that the reaction kinetics are of zero order.

The method presented here for determining photocatalytic degradation rates in a black body reactor seems to be generally applicable to obtain experimental data allowing the interlaboratory comparison of the photocatalytic activities of different semiconductors. By employing a black body reactor, it becomes technically very simple to measure reaction rates with the same type of photoreactor under identical irradiation conditions as requested by Kisch and Bahnemann³. It is only necessary to ensure that the position of the light entrance is surrounded by a sufficient amount of suspension in all three spatial directions (as far as technically feasible) to guarantee the complete absorption of the entering photons along the optical path to fulfil the requirement for a black body reactor. Applying a black body reactor ensures that the measured reaction rates are not diminished by the scattering of photons out of the photoreactor.

3.5. Experimental Procedure

Anatase TiO₂ (Hombikat UV 100, Sachtleben Chemie, now Venator Materials PLC), anatase-rutile mixture (Aeroxide® TiO₂ P25, Evonik Industries), a commercial surface modified anatase (KRONOClean 7000, Kronos), rutile (E3-231-034-007, Sachtleben Chemie), brookite, strontium titanate, barium titanate, tungsten(VI) oxide, and zinc oxide (Sigma–Aldrich) were used as the photocatalysts. All other chemicals purchased from reputable suppliers (Sigma–Aldrich, Merck, Fluka, Roth) were of analytical grade and

3. A Method to Compare the Activities of Semiconductor Photocatalysts in Liquid-Solid Systems

used as received. Ultrapure water ($\geq 18.2 \text{ M}\Omega \text{ cm}$) was applied in all experimental runs. The suspensions were prepared by dissolving dichloroacetic acid and potassium nitrate in water resulting in solutions with 10 mM potassium nitrate and varying concentrations of the probe compound (2 mM to 20 mM). After adding the desired amount of the chosen photocatalyst, the resulting suspension was stirred in the dark and the pH was adjusted at pH 3 by addition of potassium hydroxide. The experimental determination of the activities of the photocatalysts in liquid-solid heterogeneous systems was performed in a glass bottle filled with the magnetically stirred suspension. The suspension was irradiated with a monochromatic light source (Omicron Laserage Laserprodukte GmbH, $\lambda_{\text{max}} = 365 \text{ nm}$ with full width at half maximum = 10 nm as determined with a B&W Tek SpectraRad® Xpress, photon flux = $12 \mu\text{mol min}^{-1}$ as determined by ferrioxalate actinometry) equipped with a suitable wave guide within a glass tube outer diameter = 11 mm, inner diameter = 9 mm). The exit of the wave guide was placed in the center of the reactor. In all experimental runs, the suspension was stirred for 2 h in the dark in order to establish the adsorption equilibrium. Subsequently, the light source was switched on and the suspension was irradiated for 3 h. Samples were taken at 30 min intervals and centrifuged for 5 min at 13000 rpm. The supernatant solutions were filtered through syringe filters with 0.2 μm pore size and diluted 20 times. Quantitative analysis of dichloroacetic acid was performed by high performance ion chromatography (HPIC) employing a DIONEX ICS-1000 instrument equipped with an anion exchange column (Ion Pac AS9-HC 2 \times 250 mm) in combination with a guard column (Ion Pac AG9-HC 2 \times 50 mm). The aqueous mobile phase contained 8 mM Na_2CO_3 and 1.5 mM NaHCO_3 . The flow rate of the mobile phase was set to 0.3 mL min^{-1} , and the applied column temperature was 35 $^\circ\text{C}$.

3.6. Acknowledgements

L. M. gratefully acknowledges a scholarship of the Deutscher Akademischer Austauschdienst (DAAD). Financial Support from the Global Research Laboratory program (2014K1A1A2041044), Korea government (MSIP) through NRF is gratefully acknowledged.

3.7. References

- (1) Li, J.; Wu, N. Semiconductor-based photocatalysts and photoelectrochemical cells

3. A Method to Compare the Activities of Semiconductor Photocatalysts in Liquid-Solid Systems

- for solar fuel generation: a review. *Catal. Sci. Technol.* **2015**, *5*, 1360–1384.
- (2) Nakata, K.; Fujishima, A. TiO₂ photocatalysis: Design and applications. *J. Photochem. Photobiol. C: Photochem. Rev.* **2012**, *13*, 169–189.
 - (3) Fujishima, A.; Zhang, X.; Tryk, D. Heterogeneous photocatalysis: From water photolysis to applications in environmental cleanup. *Int. J. Hydrogen Energy* **2007**, *32*, 2664–2672.
 - (4) Mills, A.; Le Hunte, S. An overview of semiconductor photocatalysis. *J. Photochem. Photobiol. A: Chem.* **1997**, *108*, 1–35.
 - (5) Hoffmann, M. R.; Martin, S. T.; Choi, W.; Bahnemann, D. W. Environmental Applications of Semiconductor Photocatalysis. *Chem. Rev.* **1995**, *95*, 69–96.
 - (6) Nursam, N. M.; Wang, X.; Caruso, R. A. High-Throughput Synthesis and Screening of Titania-Based Photocatalysts. *ACS Comb. Sci.* **2015**, *17*, 548–569.
 - (7) Bagheri, S.; Mohd Hir, Z. A.; Yousefi, A. T.; Abdul Hamid, S. B. Progress on mesoporous titanium dioxide: Synthesis, modification and applications. *Microporous Mesoporous Mater.* **2015**, *218*, 206–222.
 - (8) Marschall, R. Semiconductor Composites: Strategies for Enhancing Charge Carrier Separation to Improve Photocatalytic Activity. *Adv. Funct. Mater.* **2014**, *24*, 2421–2440.
 - (9) Tong, H.; Ouyang, S.; Bi, Y.; Umezawa, N.; Oshikiri, M.; Ye, J. Nano-photocatalytic materials: possibilities and challenges. *Adv. Mater.* **2012**, *24*, 229–251.
 - (10) Kisch, H.; Bahnemann, D. Best Practice in Photocatalysis: Comparing Rates or Apparent Quantum Yields? *J. Phys. Chem. Lett.* **2015**, *6*, 1907–1910.
 - (11) Herrmann, J.-M. Heterogeneous photocatalysis: state of the art and present applications In honor of Pr. R.L. Burwell Jr. (1912–2003), Former Head of Ipatieff Laboratories, Northwestern University, Evanston (Ill). *Top. Catal.* **2005**, *34*, 49–65.
 - (12) Herrmann, J.-M. Photocatalysis fundamentals revisited to avoid several misconceptions. *Appl. Catal. B: Environ.* **2010**, *99*, 461–468.
 - (13) Wei, T. Y.; Wan, C. C. Heterogeneous photocatalytic oxidation of phenol with titanium dioxide powders. *Ind. Eng. Chem. Res.* **1991**, *30*, 1293–1300.
 - (14) Hatipoğlu, A.; San, N.; Çınar, Z. An experimental and theoretical investigation of the photocatalytic degradation of meta-cresol in TiO₂ suspensions: a model for the product distribution. *J. Photochem. Photobiol. A: Chem.* **2004**, *165*, 119–129.
 - (15) Atitar, M. F.; Bouziani, A.; Dillert, R.; El Azzouzi, M.; Bahnemann, D. W. Photocatalytic degradation of the herbicide imazapyr: do the initial degradation rates correlate with the adsorption kinetics and isotherms? *Catal. Sci. Technol.* **2018**, *8*, 985–995.

3. A Method to Compare the Activities of Semiconductor Photocatalysts in Liquid-Solid Systems

- (16) Martín, C. A.; Baltanás, M. A.; Cassano, A. E. Photocatalytic reactors I. Optical behavior of titanium oxide particulate suspensions. *J. Photochem. Photobiol. A: Chem.* **1993**, *76*, 199–208.
- (17) Cabrera, M. I.; Alfano, O. M.; Cassano, A. E. Absorption and Scattering Coefficients of Titanium Dioxide Particulate Suspensions in Water. *J. Phys. Chem.* **1996**, *100*, 20043–20050.
- (18) Brandi, R. J.; Alfano, O. M.; Cassano, A. E. Evaluation of Radiation Absorption in Slurry Photocatalytic Reactors. 1. Assessment of Methods in Use and New Proposal. *Environ. Sci. Technol.* **2000**, *34*, 2623–2630.
- (19) Brandi, R. J.; Citroni, M. A.; Alfano, O. M.; Cassano, A. E. Absolute quantum yields in photocatalytic slurry reactors. *Chem. Eng. Sci.* **2003**, *58*, 979–985.
- (20) Satuf, M. L.; Brandi, R. J.; Cassano, A. E.; Alfano, O. M. Experimental Method to Evaluate the Optical Properties of Aqueous Titanium Dioxide Suspensions. *Ind. Eng. Chem. Res.* **2005**, *44*, 6643–6649.
- (21) Emeline, A. V.; Zhang, X.; Jin, M.; Murakami, T.; Fujishima, A. Application of a "black body" like reactor for measurements of quantum yields of photochemical reactions in heterogeneous systems. *J. Phys. Chem. B* **2006**, *110*, 7409–7413.
- (22) Kisch, H. *Semiconductor Photocatalysis: Principles and applications*; Wiley-VCH: Weinheim, Germany, 2015.
- (23) Kisch, H. On the problem of comparing rates or apparent quantum yields in heterogeneous photocatalysis. *Angew. Chem. Int. Ed. Engl.* **2010**, *49*, 9588–9589.
- (24) Kisch, H. On the Problem of Comparing Rates or Apparent Quantum Yields in Heterogeneous Photocatalysis. *Angew. Chem.* **2010**, *122*, 9782–9783.
- (25) Lindner, M.; Theurich, J.; Bahnemann, D. W. Photocatalytic degradation of organic compounds: Accelerating the process efficiency. *Water Sci. Technol.* **1997**, *35*, 79–86.
- (26) Lindner, M.; Bahnemann, D. W.; Hirthe, B.; Griebler, W.-D. Solar Water Detoxification: Novel TiO₂ Powders as Highly Active Photocatalysts. *Environ. Sci. Technol.* **1997**, *119*, 120–125.
- (27) Kandiel, T. A.; Feldhoff, A.; Robben, L.; Dillert, R.; Bahnemann, D. W. Tailored Titanium Dioxide Nanomaterials: Anatase Nanoparticles and Brookite Nanorods as Highly Active Photocatalysts. *Chem. Mater.* **2010**, *22*, 2050–2060.
- (28) Kandiel, T. A.; Robben, L.; Alkaim, A.; Bahnemann, D. Brookite versus anatase TiO₂ photocatalysts: phase transformations and photocatalytic activities. *Photochem. Photobiol. Sci.* **2013**, *12*, 602–609.
- (29) Suri, R. P. S.; Liu, J.; Hand, D. W.; Crittenden, J. C.; Perram, D. L.; Mullins, M. E. Heterogeneous photocatalytic oxidation of hazardous organic contaminants in water. *Water Environ. Res.* **1993**, *65*, 665–673.
- (30) Ahuja, S.; Kutty, T.R.N. Nanoparticles of SrTiO₃ prepared by gel to crystallite

3. A Method to Compare the Activities of Semiconductor Photocatalysts in Liquid-Solid Systems

conversion and their photocatalytic activity in the mineralization of phenol. *J. Photochem. Photobiol. A: Chem.* **1996**, *97*, 99–107

- (31) Otsuka-Yao-Matsuo, S.; Omata, T.; Ueno, S.; Kita, M. Photobleaching of Methylene Blue Aqueous Solution Sensitized by Composite Powders of Titanium Oxide with SrTiO₃, BaTiO₃, and CaTiO₃. *Mater. Trans.* **2003**, *44*, 2124–2129.
- (32) Noda, H.; Oikawa, K.; Ohya-Nishiguchi, H.; Kamada, H. Efficient Hydroxyl Radical Production and Their Reactivity with Ethanol in the Presence of Photoexcited Semiconductors. *Bull. Chem. Soc. Jpn.* **1994**, *67*, 2031–2037.
- (33) Hariharan, C. Photocatalytic degradation of organic contaminants in water by ZnO nanoparticles: Revisited. *Appl. Catal. A: Gen.* **2006**, *304*, 55–61.
- (34) Mrowetz, M.; Selli, E. Photocatalytic degradation of formic and benzoic acids and hydrogen peroxide evolution in TiO₂ and ZnO water suspensions. *J. Photochem. Photobiol. A: Chem.* **2006**, *180*, 15–22.

3. A Method to Compare the Activities of Semiconductor Photocatalysts in Liquid-Solid Systems

4. Determination of the Quantum Yield of a Heterogeneous Photocatalytic Reaction Employing a Black Body Photoreactor

4.1. Foreword

This chapter includes the article *Determination of the Quantum Yield of a Heterogeneous Photocatalytic Reaction Employing a Black Body Photoreactor* by Lena Megatiff, Ralf Dillert, and Detlef W. Bahnemann, published in *Catalysis Today* 2019, doi:10.1016/j.cattod.2019.06.008. After introducing the concept of the black body reactor and its advantages for comparing the activities of various photocatalysts in liquid-solid heterogeneous systems, the effects of photon flux and photon flux density on the reaction rate and on the respective quantum yield are investigated herein. The appropriate design and scale-up of a photocatalytic reactor inevitably requires the knowledge of the quantum yield. Thus, the absorption of the radiant energy needs to be known. However, not all the absorbed photons lead to a photocatalytic reaction. The photo generated electron-hole pairs are likely to recombine and therefore will not be able to diffuse to the surface of the semiconductor particle. Therefore, the determination of photon flux and photon flux density is of great importance for designing a photoreactor, since both, the recombination rate of the electron-hole pairs and the photocatalytic reaction rate are strongly dependent on these two parameters. According to the Langmuir-Hinshelwood type rate law, the dependency of the photocatalytic reaction rate on the photon flux can be concluded from the following equation:

$$R = k_r I^n \frac{K(I)C}{1+K(I)C} \quad (4.a)$$

where k_r is the rate constant, $K(I)$ is considered to be a light-intensity dependant factor, and C is the concentration. Furthermore, the photon flux can also affect the recombination rate of the electron-hole pairs. This can be concluded from the following correlations:

4. Determination of the Quantum Yield of a Heterogeneous Photocatalytic Reaction Employing a Black Body Photoreactor

$$\langle x \rangle(t) = \frac{\langle x \rangle_0}{1 + \langle x \rangle_0 k_r t} \quad (4.b)$$

$$\langle x \rangle(t) = \langle x \rangle_0 \exp(-k_r t) \quad (4.c)$$

in which $\langle x \rangle(t)$ is the average number of electron-hole pairs at time t , $\langle x \rangle_0$ at time $t = 0$ and k_r is the recombination rate constant. Accordingly, the recombination of the electron-hole pairs follows the second order kinetics at high occupancy of the semiconductor particles (**Equation 4.b**), while at low occupancy it obeys the first order kinetics (**Equation 4.c**). Since the number of generated electron-hole pairs is proportional to the number of absorbed photons, it can be concluded that the charge carrier recombination depends on the photon flux. Hence, determining the experimental conditions in which the quantum yield is independent from the photon flux is an important factor that simplifies the process of designing an efficient photoreactor.

4.2. Abstract

Quantum yields of the photocatalytic DCA degradation in aqueous titanium dioxide suspensions (Hombikat UV100, Aeroxide P25) were determined employing a black body like photoreactor. The amounts of photons absorbed by the photocatalysts per unit time were determined by chemical actinometry varying the photon flux and the photon flux density. The photocatalytic DCA degradation experiments were performed under zero order conditions regarding the concentration of the probe compound. The obtained results suggest that the quantum yield of the photocatalytic DCA degradation depends on the photon flux density. Only the low flux density resulting from a large surface area of the light inlet seems to allow the determination of a quantum yield as a photocatalyst-inherent property.

4.3. Keywords

Black body photoreactor, dichloroacetic acid, heterogeneous photocatalysis, quantum yield, titanium dioxide.

4. Determination of the Quantum Yield of a Heterogeneous Photocatalytic Reaction Employing a Black Body Photoreactor

4.4. Introduction

Semiconductor photocatalysis is considered as one of the potent methods to utilize the solar energy for fuel production and environmental remediation. As photocatalytic reactions are light induced processes which need active materials to absorb the light, synthesis of new photocatalysts has generated a great interest in the last decades.¹⁻⁸ In order to compare the activity of different photocatalysts, in addition to the reaction rate, the number of absorbed photons should be measured to obtain the quantum yield.⁹⁻¹³ However, determining the absorbed photons in heterogeneous systems involves some difficulties. This is mainly because of scattering and reflection of the light by solid particles of the photocatalyst which results in a loss of photons.¹⁴

In light-induced chemical reactions, the photons inevitably enter the fluid phase through a window. At the two interfaces of the window some photons are reflected. The portion of photons transmitted through the window enters the fluid phase where the photons then hit the photocatalyst particles and are absorbed or scattered by them. Losses by photon transmittance through the suspension can be completely avoided by an appropriate reactor geometry and by choosing a sufficiently high catalyst concentration along the optical path of sufficient length.

For photoreactors having positive irradiation geometry, reflection at the interfaces of the window and scattering out of the suspension results in significant losses of photons which are therefore not available for the desired chemical reaction (**Figure 4.1a**). The photon losses by reflection and scattering can be reduced by using a photoreactor with negative irradiation geometry. The reason is that some of the reflected photons may enter the fluid phase elsewhere inside the photoreactor (**Figure 4.1b**). Ideally, as technically realized by the black body like photoreactor introduced by Emeline *et al.*,¹⁵ these photon losses are nearly zero (**Figure 4.1c**). All photons entering the suspension are absorbed by the photocatalyst particles, thus exciting electrons from the valence band into the conduction band. The conduction band electrons and valence band holes either recombine or they migrate to the particle surfaces where they can react with suitable electron acceptors and donors.

4. Determination of the Quantum Yield of a Heterogeneous Photocatalytic Reaction Employing a Black Body Photoreactor

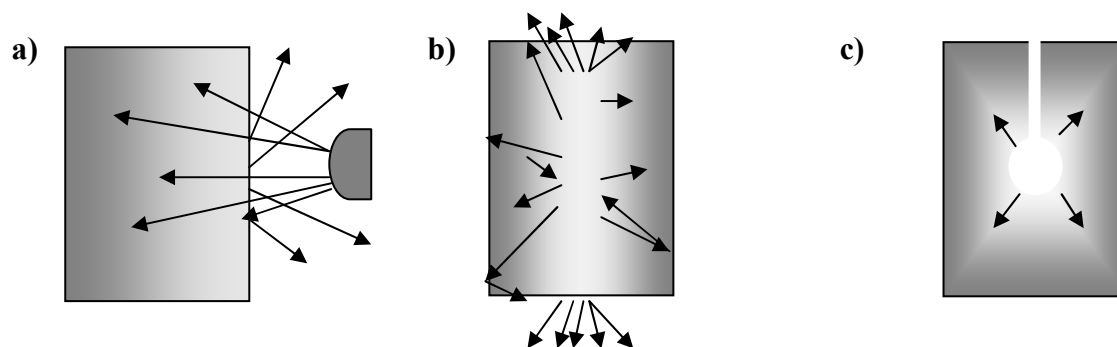


Figure 4.1. Reactor configurations according to the location of the light source: a) positive irradiation geometry, b) and c) negative irradiation geometry where c) describes the concept of a black body reactor.

Employing the photoreactors depicted in **Figure 4.1a** and **4.1b** for heterogeneous photocatalytic reactions results in the absorption of only a fraction of the incoming photons by the photocatalyst. The other fraction is lost due to scattering and reflection. This undesired loss of photons can vary between 13 % to 76 % of the incoming light.¹⁴ To address the problems related with the photoreactors depicted in **Figure 4.1a** and **4.1b**, it was proposed to calculate the photonic efficiency and to use the amount of incident photons instead of the amount of photons absorbed by the photocatalyst.^{9,16} Hence, the assumption of equal absorbed photons of light for different photocatalysts will not be accurate due to the strong dependency of the scattered and absorbed light fractions on the surface properties of the window materials and the photocatalyst particles. Generally, the number of photons absorbed by the photocatalyst are not the same in different systems. This is mainly because of the variations in light sources, reactor geometries, absorption coefficients of the photocatalyst and substrates. Also overall experimental conditions are significantly influencing the fraction of back reflected and absorbed photon flux.¹⁰⁻¹² In 2006, Emeline *et al.* proposed a simple and practical way towards quantum yield measurements for photochemical reactions in heterogeneous systems¹⁵. By applying a black body reactor it can be assumed that the amount of reflected and transmitted light is negligible. Therefore, all the light will be absorbed by the photocatalyst. Considering this property of the black body reactor, comparison of the photocatalytic activity of various semiconductors is feasible under zero order kinetic conditions of reaction regarding the photocatalyst and model compound concentration.¹⁷ However, the quantum yield of the photocatalytic reactions depends also on the light intensity. Moreover, type and size of the light inlet in a black body reactor affect the ratio of back reflection or the light

4. Determination of the Quantum Yield of a Heterogeneous Photocatalytic Reaction Employing a Black Body Photoreactor

distribution inside the reactor. Since the local volumetric rate of photon absorption depends on the light distribution inside the reactor, geometrical characteristics of the light inlet can affect the amount of absorbed photons and consequently the quantum yield.¹⁸

In the present work, an experimental evaluation of the quantum yield applying various photon fluxes and light inlet types in a heterogeneous black body photoreactor was performed. Dichloroacetic acid (DCA) was applied as the probe compound. By measuring the absorbed photon flux *via* actinometry and the amount of degraded DCA, the quantum yield was calculated.

4.5. Materials

Aeroxide[®] TiO₂ P25 and TiO₂ Hombikat UV 100 were provided by Evonik Industries and Huntsman, respectively. Dichloroacetic acid (DCA), iron(III)chloride, 1,10-phenanthroline, sodium acetate, sulfuric acid and iron(II)sulfate were purchased from Sigma–Aldrich. Potassium hydroxide (KOH) and potassium nitrate were purchased from Fluka and Merck respectively. Potassium oxalate was provided from Carl Roth. All chemicals were of analytical grade and used without further purification. All experiments were carried out employing ultrapure water (≥ 18.2 M Ω cm).

4.6. Experimental Procedure

The photocatalytic degradation of dichloroacetic acid was carried out using Hombikat UV100 and P25 under monochromatic UV light. In all experimental runs, the initial pH and the initial ionic strength of the suspensions were adjusted by adding potassium hydroxide and potassium nitrate (pH 3, 10 mM KNO₃).

The experimental determination of the quantum yields was performed in a glass flask filled with the magnetically stirred photocatalyst suspension (400 ml, 10 mM DCA, 5 g L⁻¹ photocatalyst). The suspension was irradiated with a monochromatic light source (Omicron Laserage Laserprodukte GmbH, $\lambda_{\text{max}} = 365$ nm with full width at half maximum = 10 nm as determined with a B&W Tek SpectraRad[®] Xpress) equipped with a suitable wave guide within a glass tube. The exit of the wave guide was placed in the center of the reactor to ensure that the position of the light entrance is surrounded by a sufficient amount of suspension in all three spatial directions to guarantee the complete absorption of the entering photons along the optical path. Three different types of light

4. Determination of the Quantum Yield of a Heterogeneous Photocatalytic Reaction Employing a Black Body Photoreactor

inlet with different sizes were studied (**Figure 4.2**). The light inlet type 1 was a glass tube with an inner diameter of 9 mm and an outer diameter of 11 mm closed by a semicircle. Light inlet type 2 consisted of a glass tube with an inner diameter of 9 mm and an outer diameter of 11 mm and a hollow sphere at the end having an outer diameter of 16 mm. The light inlet type 3 was a glass tube with the same diameters as the other types but a closed sphere at the end with an outer diameter of 19 mm.

In all experimental runs, the suspension was stirred for 2 h in the dark in order to establish the adsorption equilibrium. Subsequently, the light source was switched on and the suspension was irradiated for 3 h. The DCA concentration was measured by high performance ionic chromatography (HPIC) utilizing a DIONEX ICS-1000 instrument with an Ion Pac AS9-HC anion exchange column and Ion Pac AG9-HC guard column. A mixture of Na_2CO_3 and NaHCO_3 , with a flow rate of 0.3 mL min^{-1} was used as the mobile phase. More details of the experimental procedure have already been published.¹⁷

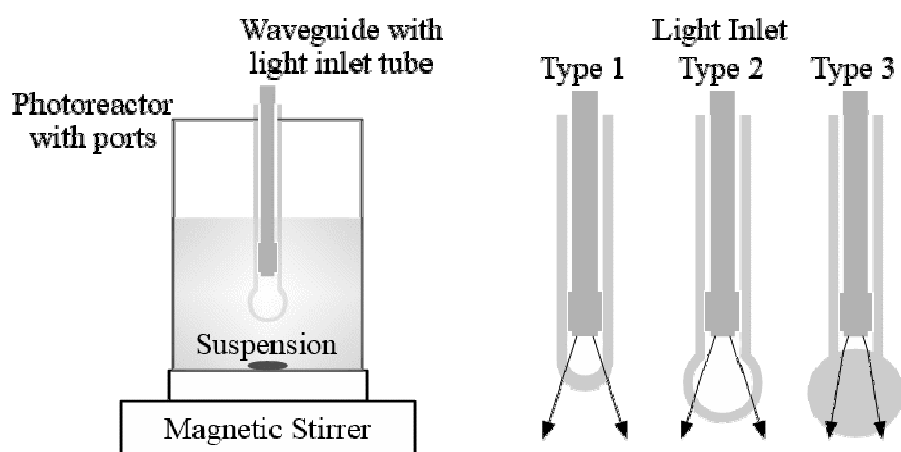


Figure 4.2. Schemes of the experimental set-up and the three types of light inlet. Note the lens effect of light inlet type 3.

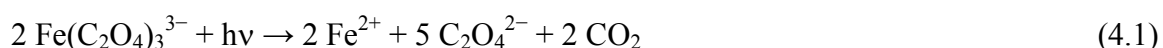
The determination of the incident photon flux was performed using ferrioxalate $[\text{Fe}(\text{C}_2\text{O}_4)_3]^{3-}$ as an actinometer.¹⁹ Potassium ferrioxalate was prepared by mixing a solution of 1.5 M $\text{K}_2\text{C}_2\text{O}_4$ with a solution of 1.5 M FeCl_3 in the ratio of 3 to 1. The mixed solution was recrystallized 3 times. After each step, the crystals were washed with water. The obtained $\text{K}_3\text{Fe}(\text{C}_2\text{O}_4)_3 \cdot 3\text{H}_2\text{O}$ crystals were placed in a dark bottle and dried overnight in 45°C in the oven. It should be mentioned that all the procedure was done in a dark room under red light. The photolysis experiments were done by preparing 30 mM

4. Determination of the Quantum Yield of a Heterogeneous Photocatalytic Reaction Employing a Black Body Photoreactor

ferrioxalate solution in 0.1 N H₂SO₄. The solution was placed in the glass flask used as the black body reactor and illuminated for 60 min. Samples were taken in 5 minutes' time intervals. For analysis, the samples were mixed with a buffer solution with the ratio of 2 to 1 and 2 mL 0.1 wt % 1,10-phenanthroline in a 20 mL volumetric flasks and made up to 20 mL by adding water. Exactly after 60 min for each sample, the concentration of the complex of ferrous iron and 1,10-phenanthroline was measured with a UV-visible spectrophotometer at 510 nm. In order to interpret the obtained results, a standard curve was prepared. For this purpose, a solution of ferrous iron in 0.1 N H₂SO₄ was mixed with a buffer solution and 0.1 wt % 1,10-phenanthroline and left for 60 min so that the complex of ferrous iron and 1,10-phenanthroline could fully develop.

4.7. Results

The photocatalytic decomposition rate of dichloroacetic acid (DCA) in aqueous suspensions containing Hombikat UV100 and P25 was examined employing a black body photoreactor and varying the flux of UV photons (0.01 μmol s⁻¹ – 0.2 μmol s⁻¹) and the photon flux density. The photon flux density was varied by means of three light inlets of different geometry. The photon fluxes were measured employing ferrioxalate actinometry which is one of the classical tools for the determination of the photon flux in photochemical reactions recommended by IUPAC.²⁰ The number of photons absorbed by the iron complex can easily be calculated by measuring the rate of the light-induced reduction of Fe³⁺ (**Equation 4.1**) for which the quantum yield is known.



The concentration of Fe(II) is measured through monitoring the colored complex of this ion with 1,10-phenanthroline at 510 nm wavelength by means of a UV-vis spectrophotometer.

4. Determination of the Quantum Yield of a Heterogeneous Photocatalytic Reaction Employing a Black Body Photoreactor

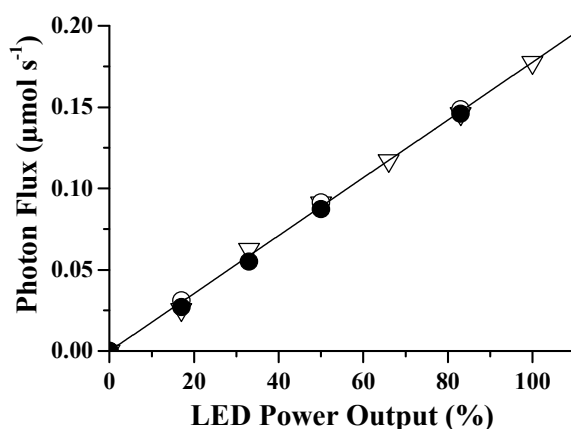


Figure 4.3. Photon fluxes determined inside the photoreactor by actinometry varying the output of the UV LED lamp and the light inlet type 1 (▽), type 2 (○), and type 3 (●).

As shown in **Figure 4.3**, the photon fluxes emitted by the monochromatic UV LED source with various light intensities and light inlet types were measured. The light inlet type 1 was a closed tube with an outer diameter of 11 mm while light inlet type 2 was a tube with a hollow sphere with a diameter of 16 mm at the end. Light inlet type 3 has a closed sphere with a diameter of 19 mm. For the same photon flux, the photon flux density for geometric reasons (neglecting the possible scattering of photons at phase interfaces) is about 50 % lower in type 3 than in type 1.

As becomes obvious from **Figure 4.3**, the photon flux increases linearly by increasing the energy output of the UV LED. According to the obtained data, size and type of the light inlet does not significantly affect the photon flux inside the photoreactor. The photon fluxes determined in this study are the average value of at least three measurements at each intensity. The average error of the measurements was found to be lower than $0.002 \mu\text{mol s}^{-1}$.

DCA was chosen as the reactant in the experimental runs since its self-oxidation is negligible and it is photocatalytically mineralized yielding CO_2 and Cl^- which do not undergo further reaction²¹. Furthermore, DCA is easily quantified using ion chromatography (HPIC). A single photon is considered to be required in the degradation of one DCA molecule. The experimental runs were performed holding the pH and the ionic strength of the suspension almost constant (pH 3, 10 mM KNO_3). It has recently been shown by us, that the rate of the DCA degradation reaction and consequently the quantum yield was not affected by varying the initial DCA concentration between 2.5 mM and 20 mM and the mass concentration of the photocatalyst between 1 g L^{-1} and 7 g L^{-1} .

4. Determination of the Quantum Yield of a Heterogeneous Photocatalytic Reaction Employing a Black Body Photoreactor

L^{-1} employing light inlet type 1 and a photon flux of approximately $2 \mu\text{mol s}^{-1}$. The kinetics of the photocatalytic DCA degradation was found to obey a zero order rate law under these experimental conditions. Quantum yields of 0.17 ± 0.02 and 0.08 ± 0.01 have been calculated for the photocatalytic degradation of DCA in the presence of Hombikat UV 100 and Aeroxide P25, respectively¹⁷. Therefore, an initial DCA concentration of 10 mM and a catalyst mass concentration of 5 g L^{-1} were chosen. It should be emphasized that zero order kinetics was observed for the light-induced DCA degradation in all experimental runs performed in the present study.

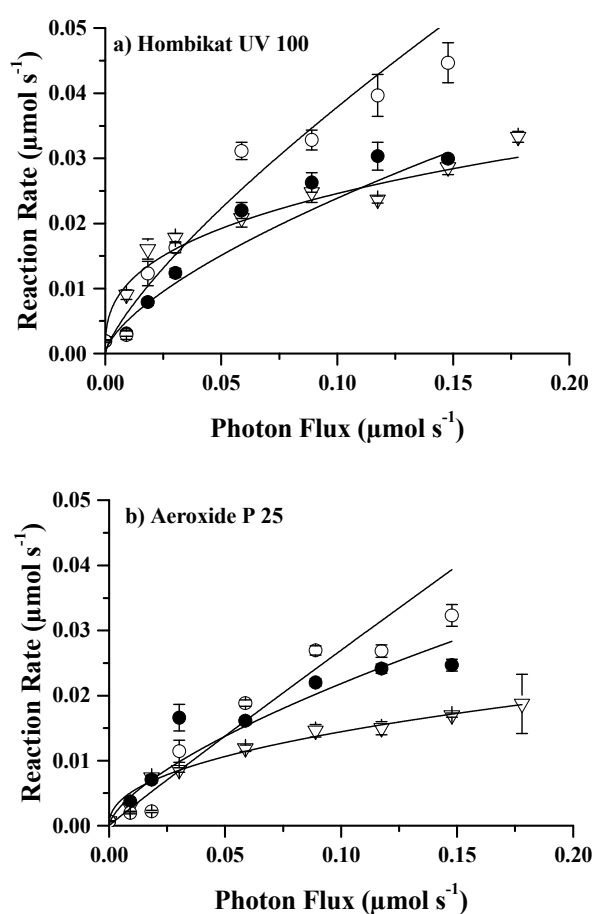


Figure 4.4. Reaction rate of the photocatalytic DCA degradation in the presence of Hombikat UV100 and Aeroxide P25 photocatalysts versus the photon flux for light inlet type 1 (∇), type 2 (\circ), and type 3 (\bullet).

The lines are to guide the eyes only.

Figure 4.4 shows the experimentally obtained reaction rates of DCA in suspensions containing Hombikat UV100 and Aeroxide P25 versus the photon flux for the three different light inlet types. Since the measurements have been carried out in a black body

4. Determination of the Quantum Yield of a Heterogeneous Photocatalytic Reaction Employing a Black Body Photoreactor

reactor, it is assumed that all photons which have entered the reactor were finally absorbed by the photocatalyst particles. Consequently, the amount of photons absorbed by the photocatalyst per unit time is equal to the photon flux determined by actinometry. The reaction rates as well as the photon fluxes are reported on an amount basis ($\mu\text{mol s}^{-1}$). It becomes obvious that the degradation rates measured in the presence of P25 are always smaller than the rates measured in suspensions containing UV100 as the photocatalyst. The reaction rate increases with increasing photon flux. However, the rate depends in a non-linear way on the photon flux. **Figure 4.4** also shows that for a given photocatalyst, the rate of the DCA degradation does not depend only on the photon flux but also on the geometry of the light inlet. The reaction rate was higher when the suspension was irradiated through the light inlet type 2 than under irradiation through the other two inlets. The reaction rate was lowest when the suspension was irradiated through inlet type 1. This suggests that the reaction rate depends not only on the photon flux but also on the light distribution (photon flux density) which in turn rely on the light inlet type.

4.8. Discussion

It is well-known that semiconductor photocatalysts absorb light with specific wavelength which results in the excitation of electrons from the valence band to the conduction band. Generally, after generating the excited electrons a large amount of the electrons and holes recombine and dissipate the received energy in form of heat or emitted light. The surviving electron and holes migrate to the photocatalyst surface and independently participate in different chemical reactions acting as reductant and oxidant^{7,8}. The rate of a photocatalytic reaction is generally given by a Langmuir-Hinshelwood type rate law

$$R = k_r I^n \frac{K(I)C}{1+K(I)C} \quad (4.2)$$

where k_r is the rate constant, $K(I)$ is considered to be a light-intensity dependant adsorption coefficient of the probe compound, and $I = dn_p/dt$ is the amount of photons being absorbed by the photocatalyst per unit time^{22,23}. Here, I is assumed to be equal the photon flux emitted by the LED light source.

As proposed for quantum yield measurements,²⁴ the reaction rate was studied here at zero order kinetic conditions regarding the probe compound concentration C and the catalyst loading. Therefore, at $K(I)C \gg 1$, the reaction rate can be written as:

4. Determination of the Quantum Yield of a Heterogeneous Photocatalytic Reaction Employing a Black Body Photoreactor

$$R = k_r I^n \quad (4.3)$$

Since charge carrier recombination demonstrates second order kinetics at high photon flux conditions, the reaction rate has a square root correlation with the light intensity ($R = k_r I^{0.5}$) and the quantum yield

$$\Phi = \frac{R}{I} = k_r I^{n-1} \quad (4.4)$$

becomes proportional to $I^{-0.5}$ ²⁵⁻²⁹. On the other hand, the light limited reaction rate follows $R = k_r I$ at low intensities^{26,28,30}. Hence, assuming the rate constant k_r to be independent from the photon flux, the quantum yield will be constant and independent from the photon flux ($\Phi = k_r$).

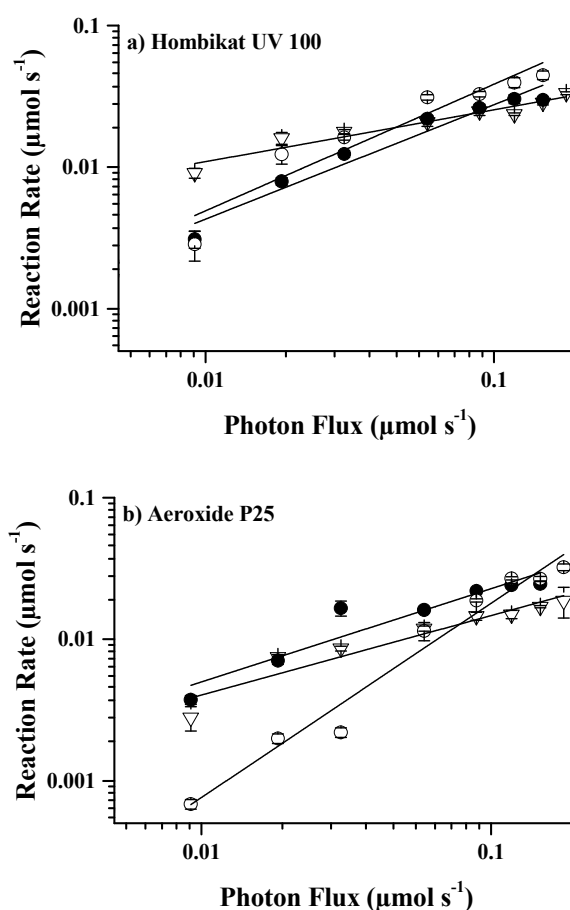


Figure 4.5. Log-log plot of the DCA degradation rates (R) versus the number of absorbed photons per unit time (I) in irradiated suspensions containing a) Hombikat UV 100, and b) Aeroxide P25 with light inlet type 1 (∇), type 2 (\circ), and type 3 (\bullet).

4. Determination of the Quantum Yield of a Heterogeneous Photocatalytic Reaction Employing a Black Body Photoreactor

To determine the dependence of the reaction rate on the photon flux the data given in **Figure 4.4** have been plotted in a log-log plot (**Figure 4.5**). As becomes obvious from this Figure the slopes of the graphs strongly depend on the type of light inlet and thus on the photon flux density at the interface between the suspension and the inlet window. In the case of UV100 the exponents n in **Equation 4.3** were calculated to be 0.37 ± 0.04 , 0.90 ± 0.13 , and 0.81 ± 0.08 for light inlet type 1, 2, and 3, respectively. When P25 was employed as the photocatalysts, the reaction rate decreased with decreasing photon flux with a slope of 0.56 ± 0.07 , 1.16 ± 0.19 , and 0.66 ± 0.10 for light inlet type 1, 2, and 3, respectively.

Figure 4.6 shows plots of the quantum yield values for the photocatalytic DCA degradation versus the photon flux. The quantum yields were calculated using **Equation 4.4**. In accordance with the data obtained from **Figure 4.4**, **Figure 4.6** indicates that the quantum yield of the photocatalytic DCA degradation in the presence of UV100 decreases for light inlets with spheres (type 2 and 3) with $I^{-0.10}$ and $I^{-0.19}$. However, in case of the smaller light inlet (type 1), it drops down with $I^{-0.63}$. When P25 is applied as a photocatalyst, the quantum yield changes with $I^{-0.44}$, $I^{0.16}$ and $I^{-0.34}$ for light inlet type 1, type 2 and type 3, respectively.

The observed non-linear dependence of the reaction rate (and consequently the quantum yield) on the amount of photons absorbed per unit time by the photocatalyst is in accordance with published results. Several authors have observed that depending on the irradiance intensity, the reaction rate can follow a linear or a square root trend in photoreactors²⁵⁻²⁸. A non-linear correlation between the reaction rate and the incident photon flux was reported for the photocatalytic degradation of phenol by Serpone *et al.*³¹ and of chloroform by Kormann *et al.*²⁶. Lindner *et al.* have reported that the photonic efficiency of the light induced DCA degradation in the presence of UV100 decreases by increasing the light intensity and the reaction rate does not have a linear relationship with the number of photons impinging on the entrance window per unit time. At a low intensity the photonic efficiency correlated with $I^{-0.12}$, while at a high intensity it changed with $I^{-0.31}$ ³². Bahnemann *et al.* reported a light intensity independent photonic efficiency for the mineralization of DCA in the presence of P25 at pH = 2.6, 7, and 11. Nevertheless, at pH 5 the photonic efficiency showed a non-linear behavior ($I^{-0.5}$) with respect to the light intensity³³. In another publication, Bahnemann *et al.* claimed a linear

4. Determination of the Quantum Yield of a Heterogeneous Photocatalytic Reaction Employing a Black Body Photoreactor

correlation between the reaction rate of the photocatalytic degradation of DCA and the light intensity applying P25 at low intensities²¹.

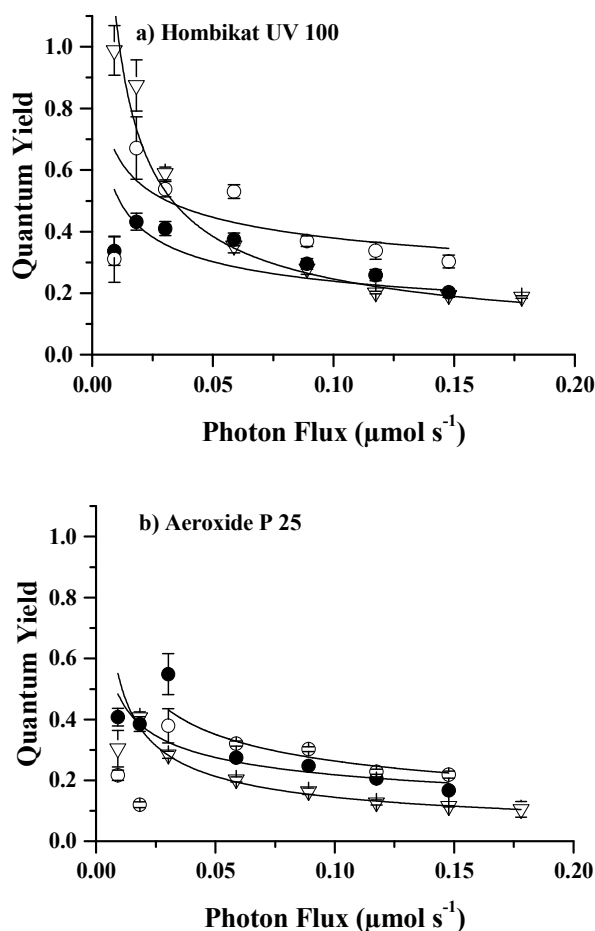


Figure 4.6. Quantum yields Φ of the photocatalytic DCA degradation versus the number of absorbed photons per unit time (I) in irradiated suspensions containing a) Hombikat UV 100, and b) Aeroxide P 25 with light inlet type 1 (∇), type 2 (\circ), and type 3 (\bullet). The lines are to guide the eyes only.

The observed differences in the light intensity dependence of the reaction rate (or the photonic efficiency or the quantum yield) between UV100 and P25 are possibly due to the different particle sizes. According to Gerischer, the quantum yield of a heterogeneous photocatalytic reaction increases by decreasing the particle size at a constant light intensity.³⁴ Hence, considering the smaller particle sizes of UV100 (8 nm) in comparison with P25 (22 nm anatase and 35 nm rutile), it can be concluded that the P25 particles near the light inlet absorb a higher number of photons per unit time than UV100. This results in multiple excitations, a large number of electron-hole pairs in one photocatalyst particle, and consequently in a high recombination rate. Therefore, the recombination rate of

4. Determination of the Quantum Yield of a Heterogeneous Photocatalytic Reaction Employing a Black Body Photoreactor

charge carriers is significantly higher in case of P25 than in UV100. In other words, the probability of the recombination reaction is lower in photocatalysts consisting small particles in comparison with photocatalysts having bigger particles.

However, as the results shown in **Figures 4.3** and **4.4** and the numerical values given in the text suggest, a high recombination rate appears to be the result of a high local photon flux density, as stipulated by the light inlet type 1. By increasing the area of the light inlet, the photon flux density is reduced, which becomes apparent in an approximation to a linear relationship between the reaction rate (or the quantum yield) and the amount of the photons being adsorbed per unit time. As mentioned above, the photon flux density at the same photon flux emitted by the LED is about 50 % lower with the light inlet type 2 than with the type 1 due to geometric reasons. The rate of the photocatalytic DCA degradation in the presence of both UV100 and P25 shows a linear dependence on the photon flux ($R \approx I^{0.90 \pm 0.13}$ [$\Phi \approx I^{-0.10}$] and $R \approx I^{1.16 \pm 0.19}$ [$\Phi \approx I^{+0.16}$]) within the limits of experimental error.

A small light inlet without a light-distributing sphere results in a non-uniform photon distribution inside the photoreactor. This type of light inlet causes regions in which photon flux densities are high, while other points inside the photoreactor have very low photon flux densities. This means that the reaction rate in regions of high photon flux densities exhibit a square root dependence upon the irradiance³⁵. Hence, it can be concluded that a light inlet of bigger size with a hollow sphere is suitable to distribute the light properly in comparison to a small light inlet without sphere that focuses the light at some points of the reactor. Therefore, the rate of electron hole recombination decreases and the efficiency of the photocatalytic reactions becomes higher, and the quantum yield of DCA photodegradation increases^{36,37}. The quantum yield of the photocatalytic DCA degradation in the presence of a given photocatalyst was found to be not a constant value but to depend on both the photon flux into the photoreactor and the photon distribution inside the photoreactor.

4.9. Conclusions

A black body like photoreactor has successfully applied to determine the quantum yield of the photocatalytic DCA degradation in aqueous titanium dioxide suspensions. Contrary to experimental results on the quantum yield of the photocatalytic phenol oxidation reported by Emeline *et al.*,¹⁵ a dependence of the quantum yield on the type of light inlet

4. Determination of the Quantum Yield of a Heterogeneous Photocatalytic Reaction Employing a Black Body Photoreactor

was observed. The quantum yield of the photocatalytic DCA degradation seems to depend not only on the photon flux but also on the photon flux density. Only the low flux density resulting from a large surface area of the light inlet seems to allow the determination of a quantum yield as a photocatalyst-inherent property.

4.10. Acknowledgements

L.M. gratefully acknowledges a scholarship of the Deutscher Akademischer Austauschdienst (DAAD). Financial support from the Global Research Laboratory program (2014 K1 A1 A2041044), Korea government (MSIP) through NRF is gratefully acknowledged.

4.11. Reference

- (1) Fujishima, A.; Zhang, X.; Tryk, D. Heterogeneous photocatalysis: From water photolysis to applications in environmental cleanup. *Int. J. Hydrogen Energy* **2007**, *32*, 2664–2672.
- (2) Nakata, K.; Fujishima, A. TiO₂ photocatalysis: Design and applications. *J. Photochem. Photobiol. C: Photochem. Rev.* **2012**, *13*, 169–189.
- (3) Li, J.; Wu, N. Semiconductor-based photocatalysts and photoelectrochemical cells for solar fuel generation: a review. *Catal. Sci. Technol.* **2015**, *5*, 1360–1384.
- (4) Marschall, R. Semiconductor Composites: Strategies for Enhancing Charge Carrier Separation to Improve Photocatalytic Activity. *Adv. Funct. Mater.* **2014**, *24*, 2421–2440.
- (5) Bagheri, S.; Mohd Hir, Z. A.; Yousefi, A. T.; Abdul Hamid, S. B. Progress on mesoporous titanium dioxide: Synthesis, modification and applications. *Microporous Mesoporous Mater.* **2015**, *218*, 206–222.
- (6) Nursam, N. M.; Wang, X.; Caruso, R. A. High-Throughput Synthesis and Screening of Titania-Based Photocatalysts. *ACS Comb. Sci.* **2015**, *17*, 548–569.
- (7) Hoffmann, M. R.; Martin, S. T.; Choi, W.; Bahnemann, D. W. Environmental Applications of Semiconductor Photocatalysis. *Chem. Rev.* **1995**, *95*, 69–96.
- (8) Tong, H.; Ouyang, S.; Bi, Y.; Umezawa, N.; Oshikiri, M.; Ye, J. Nanophotocatalytic materials: possibilities and challenges. *Adv. Mater.* **2012**, *24*, 229–251.
- (9) Serpone, N. Relative photonic efficiencies and quantum yields in heterogeneous photocatalysis. *J. Photochem. Photobiol. A: Chem.* **1997**, *104*, 1–12.
- (10) Serpone, N.; Salinaro, A. Terminology, relative photonic efficiencies and quantum yields in heterogeneous photocatalysis. Part I: Suggested protocol. *Pure Appl. Chem.* **1999**, *71*, 303–320.

4. Determination of the Quantum Yield of a Heterogeneous Photocatalytic Reaction Employing a Black Body Photoreactor

- (11) Minero, C.; Vione, D. A quantitative evaluation of the photocatalytic performance of TiO₂ slurries. *Appl. Catal. B: Environ.* **2006**, *67*, 257–269.
- (12) Kisch, H. On the problem of comparing rates or apparent quantum yields in heterogeneous photocatalysis. *Angew. Chem. Int. Ed. Engl.* **2010**, *49*, 9588–9589.
- (13) Kisch, H.; Bahnemann, D. Best Practice in Photocatalysis: Comparing Rates or Apparent Quantum Yields? *J. Phys. Chem. Lett.* **2015**, *6*, 1907–1910.
- (14) Schiavello, M.; Augugliaro, V.; Palmisano, L. An experimental method for the determination of the photon flow reflected and absorbed by aqueous dispersions containing polycrystalline solids in heterogeneous photocatalysis. *J. Catal.* **1991**, *127*, 332–341.
- (15) Emeline, A. V.; Zhang, X.; Jin, M.; Murakami, T.; Fujishima, A. Application of a "black body" like reactor for measurements of quantum yields of photochemical reactions in heterogeneous systems. *J. Phys. Chem. B* **2006**, *110*, 7409–7413.
- (16) Qureshi, M.; Takanabe, K. Insights on Measuring and Reporting Heterogeneous Photocatalysis: Efficiency Definitions and Setup Examples. *Chem. Mater.* **2017**, *29*, 158–167.
- (17) Megatiff, L.; Dillert, R.; Bahnemann, D. W. A Method to Compare the Activities of Semiconductor Photocatalysts in Liquid–Solid Systems. *ChemPhotoChem* **2018**, *2*, 948–951.
- (18) Cassano, A. E.; Martin, C. A.; Brandi, R. J.; Alfano, O. M. Photoreactor Analysis and Design: Fundamentals and Applications. *Ind. Eng. Chem. Res.* **1995**, *34*, 2155–2201.
- (19) Parker, C. A. A new sensitive chemical actinometer. I. Some trials with potassium ferrioxalate. *Proc. R. Soc. Lond. A: Math. Phys. Sci.* **1953**, *220*, 104–116.
- (20) Kuhn, H. J.; Braslavsky, S. E.; Schmidt, R. Chemical actinometry (IUPAC Technical Report). *Pure Appl. Chem.* **2004**, *76*, 2105–2146.
- (21) Bahnemann, D. W.; Bockelmann, D.; Goslich, R.; Hilgendorff, M.; Weichgrebe, D. Photocatalytic detoxification: Novel catalysts, mechanisms and solar applications. In *Photocatalytic purification and treatment of water and air: Proceedings of the 1st International Conference on TiO₂ Photocatalytic Purification and Treatment of Water and Air, London, Ontario, Canada, 8 - 13 November, 1992*; Ollis, D. F., Al-Ekabi, H., Eds.; Trace metals in the environment 3; Elsevier: Amsterdam, 1993; pp 301–319.
- (22) Ollis, D. F. Kinetics of Photocatalyzed Reactions: Five Lessons Learned. *Front. Chem.* **2018**, *6*, 378.
- (23) Mills, A.; O'Rourke, C.; Moore, K. Powder semiconductor photocatalysis in aqueous solution: An overview of kinetics-based reaction mechanisms. *J. Photochem. Photobiol. A: Chem.* **2015**, *310*, 66–105.

4. Determination of the Quantum Yield of a Heterogeneous Photocatalytic Reaction Employing a Black Body Photoreactor

- (24) Serpone, N.; Emeline, A. V. Suggested terms and definitions in photocatalysis and radiocatalysis. *Int. J. Photoenergy* **2002**, *4*, 91–131.
- (25) Ollis, D. F. Solar-Assisted Photocatalysis for Water Purification: Issues, Data, Questions. In *Photochemical Conversion and Storage of Solar Energy: Proceedings of the Eighth International Conference on Photochemical Conversion and Storage of Solar Energy, IPS-8, held July 15-20, 1990, in Palermo, Italy*; Pelizzetti, E., Schiavello, M., Eds.; Springer Science/Kluwer Academic Publishers: Dordrecht, Boston, 1991; pp 593–622.
- (26) Kormann, C.; Bahnemann, D. W.; Hoffmann, M. R. Photolysis of chloroform and other organic molecules in aqueous titanium dioxide suspensions. *Environ. Sci. Technol.* **1991**, *25*, 494–500.
- (27) Bahnemann, D.; Bockelmann, D.; Goslich, R. Mechanistic studies of water detoxification in illuminated TiO₂ suspensions. *Sol. Energy Mater.* **1991**, *24*, 564–583.
- (28) Okamoto, K.-i.; Yamamoto, Y.; Tanaka, H.; Itaya, A. Kinetics of Heterogeneous Photocatalytic Decomposition of Phenol over Anatase TiO₂ Powder. *Bull. Chem. Soc. Jpn.* **1985**, *58*, 2023–2028.
- (29) Meng, Y.; Huang, X.; Wu, Y.; Wang, X.; Qian, Y. Kinetic study and modeling on photocatalytic degradation of para-chlorobenzoate at different light intensities. *Environ. Pollut.* **2002**, *117*, 307–313.
- (30) Salaices, M.; Serrano, B.; Lasa, H. I. de. Photocatalytic Conversion of Organic Pollutants Extinction Coefficients and Quantum Efficiencies. *Ind. Eng. Chem. Res.* **2001**, *40*, 5455–5464.
- (31) Serpone, N.; Sauvé, G.; Koch, R.; Tahiri, H.; Pichat, P.; Piccinini, P.; Pelizzetti, E.; Hidaka, H. Standardization protocol of process efficiencies and activation parameters in heterogeneous photocatalysis: relative photonic efficiencies ζ_r . *J. Photochem. Photobiol. A: Chem.* **1996**, *94*, 191–203.
- (32) Lindner, M.; Bahnemann, D. W.; Hirthe, B.; Griebler, W.-D. Solar Water Detoxification: Novel TiO₂ Powders as Highly Active Photocatalysts. *Environ. Sci. Technol.* **1997**, *119*, 120–125.
- (33) Bahnemann, D. W.; Bockelmann, D.; Goslich, R.; Hilgendorff, M. Photocatalytic Detoxification of Polluted Aquifers: Novel Catalysts and Solar Applications. In *Aquatic and Surface Photochemistry*; Helz, G. R., Zepp, R. G., Crosby, D. G., Eds.; CRC Press: Milton, 1994; pp 349–367.
- (34) Gerischer, H. Photocatalysis in aqueous solution with small TiO₂ particles and the dependence of the quantum yield on particle size and light intensity. *Electrochim. Acta* **1995**, *40*, 1277–1281.
- (35) Romero, R. L.; Alfano, O. M.; Cassano, A. E. Cylindrical Photocatalytic Reactors. Radiation Absorption and Scattering Effects Produced by Suspended Fine Particles in an Annular Space. *Ind. Eng. Chem. Res.* **1997**, *36*, 3094–3109.

4. Determination of the Quantum Yield of a Heterogeneous Photocatalytic Reaction Employing a Black Body Photoreactor

- (36) Ohko, Y.; Hashimoto, K.; Fujishima, A. Kinetics of Photocatalytic Reactions under Extremely Low-Intensity UV Illumination on Titanium Dioxide Thin Films. *J. Phys. Chem. A* **1997**, *101*, 8057–8062.
- (37) Rideh, L.; Wehrer, A.; Ronze, D.; Zoulalian, A. Photocatalytic Degradation of 2-Chlorophenol in TiO₂ Aqueous Suspension: Modeling of Reaction Rate. *Ind. Eng. Chem. Res.* **1997**, *36*, 4712–4718.

5. Reaction Rate Study of Photocatalytic Degradation of Dichloroacetic Acid in a Black Body Reactor

5.1. Foreword

This chapter includes the article *Reaction Rate Study of Photocatalytic Degradation of Dichloroacetic Acid in a Black Body Reactor* by Lena Megatif, Ralf Dillert, and Detlef W. Bahnemann, submitted for publication to *Catalysts*. Herein, the kinetics of the photocatalytic dichloroacetic acid degradation in a black body reactor have been studied. In particular, the optimal experimental conditions for the determination of the rate of conversion and of the quantum yield employing Hombikat UV 100 as photocatalyst are discussed and the validity of utilizing a black body photoreactor for the quantum yield determination and the comparison of various photocatalysts is confirmed. To select the operating conditions or to design a suitable photoreactor, it is convenient to work in terms of the volume-averaged quantum yield value. Thus, the intrinsic kinetic constants have been examined and the reaction rate and consequently the quantum yield as a function of the photocatalyst loading, the probe compound concentration, and the reaction volume have been studied. The obtained optimum values of the mentioned parameters are among the key factors for the photocatalytic reactor design as well as for its operation. The optimum value of the photocatalyst loading is essential for providing the minimum optical thickness giving the highest fractional use of photons to drive a reaction. The optimal reaction volume is also significant in order to avoid dark areas inside the photoreactor to minimize the extra construction costs. Moreover, performing the reaction at an optimal probe molecule concentration can ensure that this parameter is not the rate limiting factor.

5.2. Abstract

The light-induced degradation of dichloroacetic acid in aqueous suspensions containing the TiO₂ photocatalyst Hombikat UV 100 was investigated. The reactions were performed in a black body reactor where the rate of conversion, defined as the time derivative of the extent of conversion, is not affected by the light scattering properties of the photocatalysts. At sufficiently high concentrations of both the probe compound and the photocatalyst the rate of conversion was found to be unswayed by the initial concentration of the probe compound, the mass concentration of the photocatalyst, and

5. Reaction Rate Study of Photocatalytic Degradation of Dichloroacetic Acid in a Black Body Reactor

the suspension volume. Thus, the chosen experimental conditions enable the determination of the rate of conversion and the quantum yield of the light induced degradation of dichloroacetic acid in aqueous photocatalyst suspension with sufficiently good reproducibility. The experimental procedure employed here seems to be generally applicable to determine rates of conversion and quantum yields that possibly allow a comparison of the activities of photocatalysts in aqueous suspensions.

5.3. Keywords

Black body photoreactor, Dichloroacetic acid, Heterogeneous photocatalysis, Quantum yield, Rate of conversion, Titanium dioxide.

5.4. Introduction

Heterogeneous photocatalysis in solid-liquid systems is considered as an effective method to harvest photons for the oxidative degradation of organic water pollutants, the generation of molecular hydrogen by water splitting or reforming of organic compounds, the fixation of carbon dioxide or molecular nitrogen, and the synthesis of organic compounds. Therefore, new photocatalysts and photocatalytically active composites are being synthesized and investigated with respect to possible applications in heterogeneous photocatalysis. Technically applicable photocatalysts must meet a number of requirements. It is crucial that the photocatalytically active solid is stable under the conditions of the desired light-induced chemical reaction, and that it has a high photocatalytic activity. Inevitably, the comparative assessment of the activities of semiconductors and composites designated as photocatalysts is required.

Several methods have been proposed for this comparative assessment of photocatalytic activities in suspensions. For details on the proposed methods, the curious reader is referred to the recently published papers of Kisch and Bahnemann¹, Qureshi and Takanabe², Hoque and Guzman³, and the references given therein. Usually, the reaction rate at which a probe compound is photocatalytically converted, is used as the measure of the photocatalytic activity of the considered photocatalyst. The activities of different photocatalysts are then assessed by comparing these numerical values of the respective rates. Reaction rates are usually reported on a volume basis (converted amount of the probe compound per unit time and unit suspension volume), a mass basis (converted

5. Reaction Rate Study of Photocatalytic Degradation of Dichloroacetic Acid in a Black Body Reactor

amount per unit time and unit mass of photocatalyst), or an area basis (converted amount per unit time and unit area of photocatalyst). A photocatalytic reaction, however, takes place only in the small volume inside a photoreactor that is located directly in front of the light entrance. In this volume element, the photon flux decreases with increasing the distance from the entrance window. This, of course, is accompanied by a decrease in the reaction rate. So that at the most distant layers of the suspension, which are not penetrated by photons, the reaction rate becomes equal to zero. A reported reaction rate is therefore always a volume-averaged value. A prerequisite for the comparison of reaction rates is that the values were determined under identical reaction conditions¹. However, most often the comparison of published values is impeded due to the lack of detailed information on the geometry of the photoreactor, the size of the entrance window, and the characteristics of the irradiation conditions.

To avoid this draw-back, it has been proposed to calculate the ratio between the amounts of the probe compound reacted in a time interval and the photons impinging on the outer wall of the light entrance in this time interval. However, objections have been raised against this ratio, which is called the photonic efficiency (also known as quantum efficiency), as a measure of the photocatalytic activity of a material. In almost all published papers reporting comparative studies of photocatalysts in suspensions, experimental setups were used, in which the slurries were irradiated by an external light source through a window in the outer wall of the photoreactor. In such arrangement of photoreactor and light source (positive irradiation geometry), a fraction of the photons entering the suspension is not absorbed, but back-scattered out of the slurry and the reactor⁴⁻⁷. This undesired loss of photons can vary between 13 % and 76 % of the incoming light⁴. The ratio between absorbed and out-scattered photons depends, *inter alia*, on the photocatalyst composition, its particle size, and its mass concentration⁸⁻¹⁰. A reaction rate determined with an experimental set-up having positive irradiation geometry and, consequently, the resulting photonic efficiency thus also reflects the optical properties of the suspension and is, therefore, not a measure of the intrinsic activity of the photocatalyst under consideration.

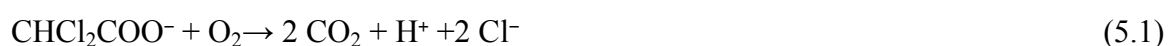
Recently, Emeline and co-authors have proposed a particular design of a reactor with negative irradiation geometry in which the light entrance is surrounded by the suspension in all three spatial directions (as far as technically feasible)¹¹. The design of this

5. Reaction Rate Study of Photocatalytic Degradation of Dichloroacetic Acid in a Black Body Reactor

photoreactor ensures that almost all out-scattered photons re-enter the suspension elsewhere. Provided that no photons are transmitted through the suspension, all the photons with appropriate energy to excite the photocatalyst are absorbed inside the suspension. Although the reactor filled with the suspension behaves like a black body only in a finite wavelength range, it was termed as a black body-like reactor by Emeline *et al.*¹¹.

Provided that the photocatalyst is the only light absorbing species and that the suspension is optically dense for photons having an energy greater than the band gap energy of the photocatalyst (i.e., no photons are transmitted through the reactor), all the photons with appropriate energy emitted by the light source are absorbed by the photocatalyst. All photons emitted by the light source are therefore available to initiate a photocatalytic reaction. The rate of a photocatalytic reaction as a measure of the photocatalytic activity is thus diminished only by the recombination of the photogenerated charge carriers and is independent from the scattering properties of the photocatalyst. The amount of photons emitted by the light source and entering the black body like photoreactor can easily be determined by chemical actinometry. When using a monochromatic light source, a quantum yield, as is usual for homogeneous photochemical reactions, can thus be calculated¹¹. However, it must be emphasized that the quantum yield will only be meaningful if the photocatalyst is the only species that absorbs the photons entering the suspension. Therefore, in order to determine the quantum yield of a light-induced reaction in a photocatalyst suspension, the probe compound must be optically transparent. In addition, the photocatalytic conversion of the probe compound must not yield intermediates and products which could absorb the incoming light.

Dichloroacetic acid (DCA) is an organic compound that meets these requirements when irradiated with visible and UV(A) light. DCA presents some additional advantages for laboratory studies due to its low vapor pressure and high water solubility¹². It also speaks for the use of DCA as the probe compound that the photocatalytic reaction according to



can be monitored not only by measuring the DCA concentration but also by¹²⁻¹⁶, the concentration of organic carbon (TOC)^{12,13,17}, as well as the evolved amounts of CO₂¹⁸,

5. Reaction Rate Study of Photocatalytic Degradation of Dichloroacetic Acid in a Black Body Reactor

Cl^- ^{12,13,18,19}, and H^+ (employing e.g. a pH-stat technique¹⁹⁻²²). However, for the direct comparison of the rates obtained by the measurements of these analytes, it is recommendable to use the rates of conversion as defined by the IUPAC²³. The rate of conversion of species i is defined as the time derivative of the extent of reaction $\zeta(i)$

$$d\zeta(i)/dt = (1/\nu(i))(dn(i)/dt) = (V/\nu(i))(dC(i)/dt) \quad (5.2)$$

where $n(i)$ and $C(i)$ are the amount and the amount concentration (molarity), respectively, of this species at any time t , $\nu(i)$ is its stoichiometric coefficient, and V is the volume of the suspension.

Equation 5.1 requires that $d\zeta(\text{DCA})/dt = d\zeta(\text{CO}_2)/dt = d\zeta(\text{Cl}^-)/dt$. However, the evaluation of published data employing the rates of conversion suggests that the numerical values are slightly different for the different analytes^{12,13,18}. Such differences in the rates of conversion would then have to be taken into account when comparing published data for one reactant but obtained with different analytes.

This article reports on the photocatalytic oxidation of dichloroacetic acid in acidic aqueous suspensions employing a black body like reactor. The initial concentration of the dichloroacetic acid, the mass concentration of the photocatalyst TiO_2 Hombikat UV 100, and the volume of the suspension were varied. The experimental conditions were chosen in such a way that the kinetics of the photocatalytic degradation of DCA could be described by a zero order rate law. This work was performed to answer two scientific questions: (i) How reproducible are the results of photocatalytic degradation experiments performed in a black body photoreactor? (ii) Are the rates of conversion for the reactant and the reaction product (here DCA and Cl^-) the same within the limits of experimental error?

5.5. Materials

Dichloroacetic acid (DCA) was purchased from Sigma-Aldrich, while potassium hydroxide (KOH) and potassium nitrate were purchased from Fluka and Merck, respectively. All mentioned chemicals were of analytical grade and used without further purification. Hombikat UV 100 (Sachtleben Chemie, now *Venator* Germany GmbH), an

5. Reaction Rate Study of Photocatalytic Degradation of Dichloroacetic Acid in a Black Body Reactor

anatase TiO₂ with a BET surface area of 280 m² g⁻¹ was used as the photocatalysts. Ultrapure water (≥ 18.2 M Ω cm) was applied in all experimental runs.

5.6. Experimental Procedure

Stock solutions were prepared by dissolving potassium nitrate and DCA in water resulting in solutions with 10 mmol L⁻¹ potassium nitrate and varying DCA concentrations (2 mmol L⁻¹ to 20 mmol L⁻¹). Required amounts of TiO₂ were added to these solutions resulting in mass concentrations of the photocatalyst varying between 1 g L⁻¹ and 10 g L⁻¹. The pH of the suspensions was adjusted at 3 by addition of potassium hydroxide. The photocatalytic runs were performed in glass bottles of suitable size containing different suspension volumes (80 mL, 100 mL, 250 mL, 400 mL, 600 mL and 900 mL) with a monochromatic light source (Omicron Laserage Laserprodukte GmbH, $\lambda_{\text{max}} = 365$ nm with full width at half maximum = 10 nm as determined with a B&W Tek Spectra RadS Xpress, photon flux = 10.7 $\mu\text{mol min}^{-1}$ as determined by ferrioxalate actinometry²⁴) equipped with a suitable wave guide within a glass tube (outer diameter = 11 mm, inner diameter = 9 mm). The outlet of the wave guide was placed in the centre of the suspension to ensure that the light entrance is surrounded by the suspension in all three spatial directions.

In all experimental runs, the suspension was magnetically stirred for 2 h in the dark in order to establish the adsorption equilibrium. Subsequently, the light source was switched on and the stirred suspension was irradiated for 3 h. Samples were taken every 30 min and centrifuged for 5 min at 13000 rpm. The supernatant solutions were filtered through syringe filters with 0.2 μm pore size and then diluted 1:20. Quantitative analysis of DCA and chloride was performed by high performance ion chromatography (HPIC) employing a DIONEX ICS-1000 instrument equipped with an anion exchange column (Ion Pac AS9-HC 2V 250 mm) in combination with a guard column (Ion Pac AG9-HC 2V 50 mm). The column temperature was set to 35 °C. The mobile phase (flow rate = 0.3 mL min⁻¹) consisted of an aqueous solution of Na₂CO₃ (8 mmol L⁻¹) and NaHCO₃ (1.5 mmol L⁻¹).

5.7. Results

The light induced degradation of dichloroacetic acid (DCA) in the presence of Hombikat UV 100 as the photocatalyst was studied varying the initial concentration of the probe

5. Reaction Rate Study of Photocatalytic Degradation of Dichloroacetic Acid in a Black Body Reactor

compound ($2 \text{ mmol L}^{-1} \leq C_s \leq 20 \text{ mmol L}^{-1}$), the mass concentration of the photocatalyst ($2 \text{ g L}^{-1} \leq \gamma \leq 20 \text{ g L}^{-1}$), and the suspension volume ($80 \text{ mL} \leq V \leq 900 \text{ mL}$). The photon flux into the suspension as well as the temperature, the concentration of dissolved oxygen, the pH, and the ionic strength was kept (almost) constant. After adding the photocatalyst to the aqueous DCA solution and pH adjustment, the suspensions were stirred in the dark for two hours prior to irradiation. In all experimental runs the DCA concentration was found to decrease during this dark period, *i.e.*, the DCA concentration C_0 at the time when the light source was switched on ($t = 0$) was always found to be lower than the DCA concentration C_s of the stock solution.

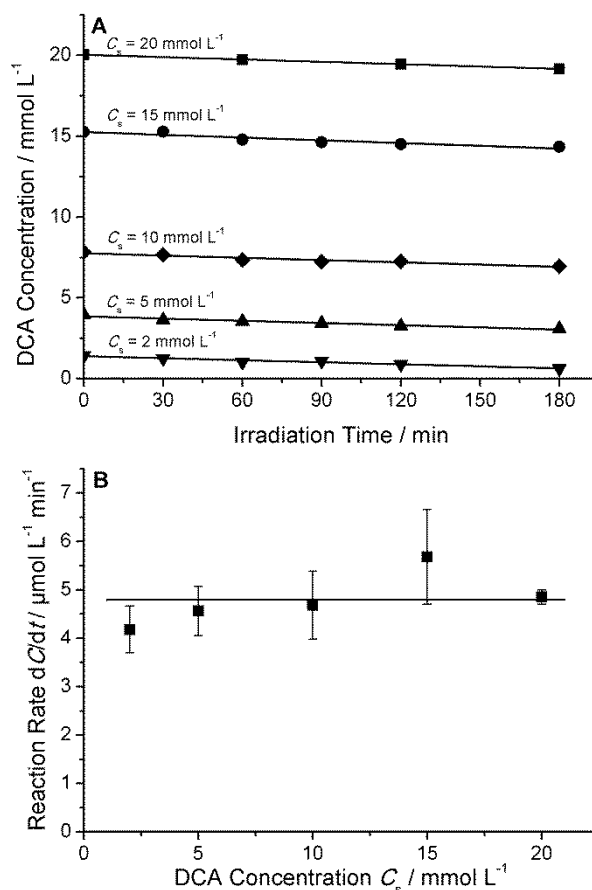


Figure 5.1. Photocatalytic degradation of dichloroacetic acid (DCA) varying the initial concentration: (A) Concentration vs. time profile, (B) Reaction rates dC/dt (calculated from the slopes of the plots in (A)) vs. the concentration of the stock solution C_s . The line in (B) represents the average of the five data points.

Experimental conditions: Hombikat UV 100, $\gamma = 5 \text{ g L}^{-1}$, $V = 400 \text{ mL}$, photon flux = $10.7 \mu\text{mol min}^{-1}$, pH 3, $10 \text{ mmol L}^{-1} \text{ KNO}_3$, air saturated, ambient temperature.

5. Reaction Rate Study of Photocatalytic Degradation of Dichloroacetic Acid in a Black Body Reactor

In a first set of experimental runs the impact of the amount concentration of DCA on the reaction rate was investigated. For that matter, the initial concentration of DCA was varied at a constant mass concentration of the photocatalyst ($\gamma = 5 \text{ g L}^{-1}$) and a constant suspension volume ($V = 400 \text{ mL}$). **Figure 5.1A** illustrates the change of the DCA concentration as determined by HPIC during UV(A) irradiation for experimental runs with DCA concentrations C_s varying between 2 mmol L^{-1} and 20 mmol L^{-1} . It becomes obvious from this Figure, that the DCA concentration decreased linearly with time during UV(A) irradiation. The degradation rate defined as the time derivative of the amount concentration (dC/dt) is directly obtained from the slope of the graphs. The numerical values of the thus calculated degradation rates are given in **Figure 5.1B**. The rates were found to be constant within the limits of experimental error ($dC/dt = 4.79 \pm 0.56 \text{ } \mu\text{mol L}^{-1} \text{ min}^{-1}$) and not affected by the initial concentration of DCA at the experimental conditions employed here. The rate of conversion was calculated inserting the reaction rate, the suspension volume V , and the stoichiometric coefficient $\nu(\text{DCA}) = 1$ into **Equation 5.2**. A mean value $d\xi(\text{DCA})/dt = 1.92 \pm 0.22 \text{ } \mu\text{mol min}^{-1}$ was obtained.

In a second set of experimental runs the impact of the mass concentration of the photocatalyst on the DCA degradation rate was investigated. The initial concentration of DCA ($C_s = 10 \text{ mmol L}^{-1}$) and the suspension volume ($V = 400 \text{ mL}$) were kept constant during these experimental runs. The measured DCA concentrations are plotted *versus* the irradiation time in **Figure 5.2A**. Again linear concentration-time plots were obtained enabling the determination of the DCA degradation rates from the slopes of these plots. The degradation rates were found to be constant ($dC/dt = 5.54 \pm 0.43 \text{ } \mu\text{mol L}^{-1} \text{ min}^{-1}$) and not affected by the mass concentration γ of the photocatalyst Hombikat UV 100 (**Figure 5.2B**). With this reaction rate, a mean rate of conversion $d\xi(\text{DCA})/dt = 2.22 \pm 0.17 \text{ } \mu\text{mol min}^{-1}$ is calculated employing **Equation 5.2**.

5. Reaction Rate Study of Photocatalytic Degradation of Dichloroacetic Acid in a Black Body Reactor

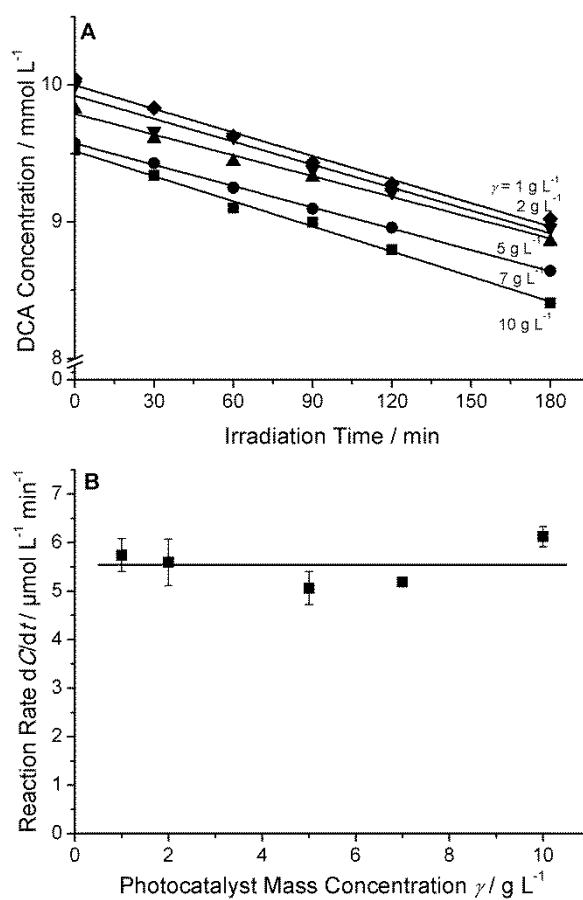


Figure 5.2. Photocatalytic degradation of dichloroacetic acid (DCA) varying the mass concentration of the photocatalyst Hombikat UV 100: (A) Concentration vs. time profile, (B) Reaction rates dC/dt (calculated from the slopes of the plots in (A)) vs. mass concentration γ . The line in (B) represents the average of the five data points. *Experimental conditions:* $C_s = 10 \text{ mmol L}^{-1}$, $V = 400 \text{ mL}$, photon flux = $10.7 \mu\text{mol min}^{-1}$, pH 3, $10 \text{ mmol L}^{-1} \text{ KNO}_3$, air saturated, ambient temperature.

5. Reaction Rate Study of Photocatalytic Degradation of Dichloroacetic Acid in a Black Body Reactor

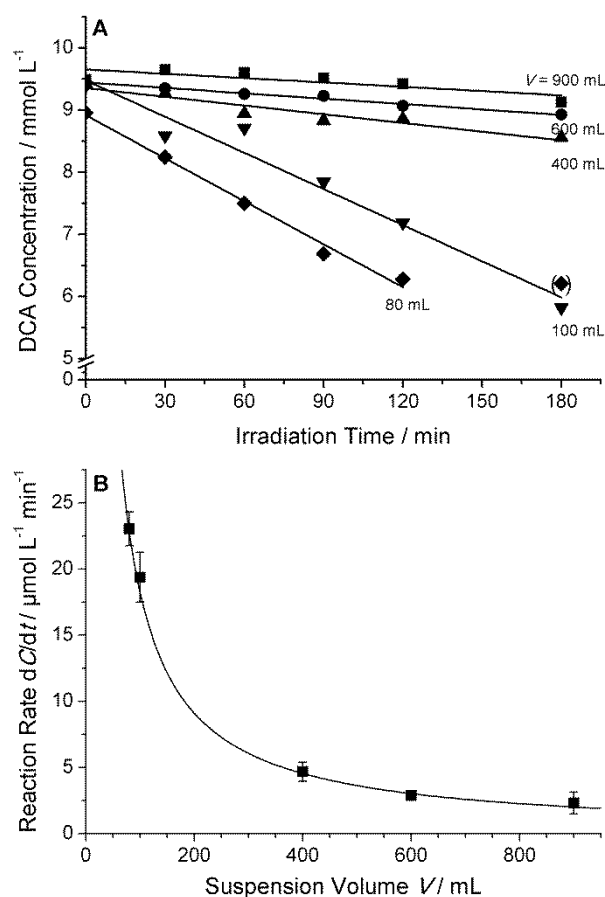


Figure 5.3. Photocatalytic degradation of dichloroacetic acid (DCA) varying the suspension volume: (A) Concentration vs. time profile, (B) Reaction rates dC/dt (calculated from the slopes of the plots in (A)) vs. the suspension volume V . The line in (B) was calculated with $dC/dt = k/V$ and $k = 1.82 \mu\text{mol min}^{-1}$.

Experimental conditions: Hombikat UV 100, $\gamma = 5 \text{ g L}^{-1}$, $C_s = 10 \text{ mmol L}^{-1}$, photon flux = $10.7 \mu\text{mol min}^{-1}$, pH 3, $10 \text{ mmol L}^{-1} \text{ KNO}_3$, air saturated, ambient temperature.

In a third set of experimental runs the suspension volume was varied at constant initial concentration of DCA ($C_s = 10 \text{ mmol L}^{-1}$) and constant mass concentration of the photocatalyst ($\gamma = 5 \text{ g L}^{-1}$). Again, linear concentration-time plots were obtained (**Figure 5.3A**). However, when the degradation rates determined from the slopes of these concentration-time plots are plotted *versus* the suspension volume, a non-linear decrease is observed (**Figure 5.3B**) as expected for the photocatalytic degradation of a probe compound in suspension. The reaction rates have been fitted using a regression curve $dC/dt = k/V$ with $k = 1.82 \pm 0.04 \mu\text{mol min}^{-1}$. Since the stoichiometric coefficient of DCA is unity, this value k corresponds directly to the rate of conversion $d\zeta(\text{DCA})/dt$ defined by **Equation 5.2**. The good agreement between the experimental and the fitted values clearly

5. Reaction Rate Study of Photocatalytic Degradation of Dichloroacetic Acid in a Black Body Reactor

indicate the independence of the rate of conversion from the suspension volume within the limits of experimental error. This also clearly demonstrates that the experimental set-up employed here behaves like a black body reactor: with a given photocatalyst and under the condition of zero order kinetics with respect to the organic solute, constant photon fluxes result in constant rates of conversion!

Finally, the impact of the photon flux was investigated employing varying the fluxes ($0.54 \mu\text{mol min}^{-1} \leq dn_p/dt \leq 10.7 \mu\text{mol min}^{-1}$). The initial concentration of DCA ($C_s = 10 \text{ mmol L}^{-1}$), the mass concentration of the photocatalyst ($\gamma = 5 \text{ g L}^{-1}$), and the suspension volume (400 mL) were kept constant. The measured DCA concentrations are plotted *versus* the photon flux in **Figure 5.4A**. Linear concentration-time plots were obtained at all photon fluxes in the range mentioned above, thus indicating that the photon flux is not affecting the kinetics of the DCA degradation reaction. The rates calculated from the slopes of these plots are presented in **Figure 5.4B**. A non-linear relation between the calculated degradation rates and the photon fluxes becomes obvious.

5. Reaction Rate Study of Photocatalytic Degradation of Dichloroacetic Acid in a Black Body Reactor

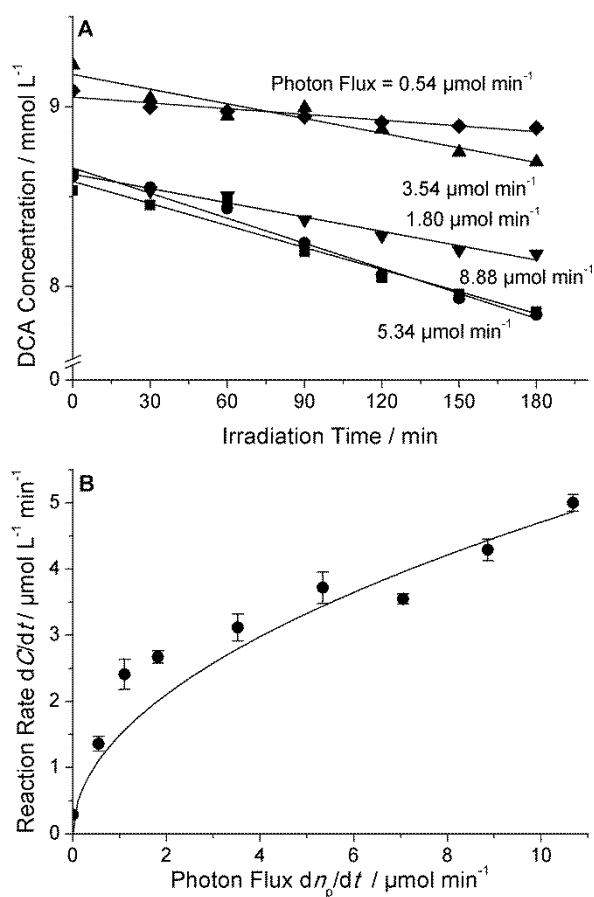


Figure 5.4. Photocatalytic degradation of dichloroacetic acid (DCA) at varying photon fluxes: (A) Concentration vs. time profile, (B) Reaction rates dC/dt (calculated from the slopes of the plots in (A)) vs. the photon flux. The line in (B) was calculated with assuming a square root dependence of the reaction rate on the photon flux. *Experimental conditions:* Hombikat UV 100, $\gamma = 5 \text{ g L}^{-1}$, $C_s = 10 \text{ mmol L}^{-1}$, $V = 400 \text{ mL}$, pH 3, $10 \text{ mmol L}^{-1} \text{ KNO}_3$, air saturated, ambient temperature.

5.8. Discussion

In all experimental runs performed here, a decrease of the DCA concentration with a simultaneous increase of the Cl^- concentration was observed during UV(A) irradiation of aqueous DCA- TiO_2 slurries. No change in the concentrations was observed when irradiating homogeneous DCA solutions with UV(A) light as well as stirring DCA-containing TiO_2 suspensions in the dark (data not shown). Therefore, the observed changes in the DCA and Cl^- concentrations in UV(A) irradiated Hombikat UV 100 suspensions can only be attributed to a photocatalytic degradation of the organic solute. A

5. Reaction Rate Study of Photocatalytic Degradation of Dichloroacetic Acid in a Black Body Reactor

possible reaction pathway for the photocatalytic DCA degradation at the acidic pH of the suspension employed here (pH 3) is given in **Table 5.1**.

Table 5.1. Main reaction steps during the photocatalytic DCA degradation at pH 3 (adapted from Ref. 12 and 13).

Reaction step	
$TiO_2 + O_2 \rightleftharpoons TiO_2-O_{2\ ads}$	(5.3)
$TiO_2 + CHCl_2COO^- \rightleftharpoons TiO_2-CHCl_2COO^-_{\ ads}$	(5.4)
$TiO_2-CHCl_2COO^-_{\ ads} + h^+ \rightarrow TiO_2-CHCl_2COO^\bullet_{\ ads}$	(5.5)
$CHCl_2COO^\bullet_{\ ads} \rightarrow \bullet CHCl_2_{\ ads} + CO_2$	(5.6)
$O_{2\ ads} + \bullet CHCl_2_{\ ads} \rightarrow \bullet O_2CHCl_2_{\ ads}$	(5.7)
$2 \bullet O_2CHCl_2_{\ ads} \rightarrow 2 COCl_2 + H_2O_2$	(5.8)
$COCl_2 + H_2O \rightarrow CO_2 + 2 H^+ + 2 Cl^-$	(5.9)

At pH 3, DCA is mainly present dissociated in its constituting ions ($pK_a(DCA) = 1.06$)²⁵ resulting in the adsorption of negatively charged dichloroacetate ions at the positively charged TiO_2 surface. The reaction pathway given in **Table 5.1** takes into account that adsorbed dichloroacetate is attacked directly by a hole that is produced upon light excitation of a photocatalyst particle. The mechanism thus considers that, in acidic TiO_2 suspensions, direct attack of the organic adsorbate by holes is significantly more important than oxidation by OH radicals as clearly demonstrated in previous publications reporting the photocatalytic degradation of carboxylic acids^{12,13,26-36}. The dichloroacetoxy radical formed by direct hole oxidation of adsorbed DCA (**Equation 5.5**) decarboxylates yielding a carbon-centered radical (photo-Kolbe reaction, **Equation 5.6**) which reacts with molecular oxygen in a subsequent reaction step (**Equation 5.7**). Two of the intermediate radicals react in a bimolecular reaction yielding hydrogen peroxide and phosgene (**Equation 5.8**) which is immediately hydrolyzed into CO_2 and Cl^- (**Equation 5.9**). According to this reaction mechanism the absorption of one photon by a photocatalyst particle is required to initiate the complete mineralization of one DCA yielding CO_2 , H^+ , and Cl^- . If this mechanistic scheme is valid, then $d\zeta(DCA)/dt = d\zeta(Cl^-)/dt$ must hold.

5. Reaction Rate Study of Photocatalytic Degradation of Dichloroacetic Acid in a Black Body Reactor

The kinetics of light-induced reactions of organic compounds in photocatalyst suspensions have been analyzed using a variety of different rate laws³⁷. Some of these rate laws can be mathematically expressed by a Langmuir–Hinshelwood-type rate law, which is written here as

$$dC/dt = \chi_1 C / (\chi_2 C + \chi_3) \quad (5.10)$$

Depending on the underlying mechanistic assumptions, the physical meaning of the kinetic parameters χ_1 , χ_2 , and χ_3 are different in the different rate laws³⁸⁻⁴³.

It became obvious from the **Figures 5.1A, 5.2A, and 5.3A** that the kinetics of the photocatalytic DCA degradation can be described by a zero order rate law under the experimental conditions employed in this work. This suggests that the condition $\chi_2 C \gg \chi_3$ holds. Consequently, **Equation 5.11** simplifies resulting in

$$dC/dt = \chi_1 / \chi_2 = r_{\max} \quad (5.11)$$

with the maximum reaction rate r_{\max} which depends on the time derivative of the adsorbed amount of photons $dn_{p,abs}/dt$.

It is known that the adsorption of carboxylic acids, such as acetic acid and dichloroacetic acid, from acidic aqueous solutions on TiO₂ surfaces can be described by Langmuir adsorption isotherms⁴⁴⁻⁴⁶. This suggests that **Equation 5.10** can be written as

$$dC/dt = r_{\max} KC / (1 + KC) \quad (5.12)$$

and the condition $KC \gg 1$ holds, thus indicating the saturation of all adsorption sites on the TiO₂ surface by adsorbed DCA molecules, *i.e.*, the surface coverage $\theta = KC / (1 + KC)$ is unity. The amount of adsorbed DCA per unit mass of the adsorbent $q = (C_s - C_0) / \gamma$, which was calculated from the difference of the DCA amount concentrations C_s and C_0 , and the mass concentration γ of the photocatalyst, was found to be almost constant, thus supporting the latter proposition. However, the obtained value $q = 150 \mu\text{mol g}^{-1}$ is surprisingly low when compared with data published by Boehm and co-authors who have determined the amounts of OH groups being present on the amphoteric surface of anatase TiO₂^{44,45}. For samples having surface areas of $56 \text{ m}^2 \text{ g}^{-1}$ and $200 \text{ m}^2 \text{ g}^{-1}$ values of $7.8 \mu\text{mol m}^{-2}$ and $7.3 \mu\text{mol m}^{-2}$, respectively, have been reported. Approximately half of

5. Reaction Rate Study of Photocatalytic Degradation of Dichloroacetic Acid in a Black Body Reactor

these OH groups are basic and suitable to interact with anions at acidic pH. From the Langmuir adsorption isotherm of acetic acid adsorbed at the surface of a TiO₂ sample with a surface area of 56 m² g⁻¹ the number of basic OH groups per unit mass was calculated to be 190 μmol g⁻¹⁴⁴, which corresponds to 3.4 μmol m⁻². Using this value and the surface area of the photocatalyst employed in the present study (280 m² g⁻¹), a DCA loading of 950 μmol g⁻¹ is expected. However, Hufschmidt *et al.* reported DCA loadings of 45–60 μmol g⁻¹ and 70–90 μmol g⁻¹ for platinized anatase-rutile mixtures (Degussa P 25, 50 m² g⁻¹) and platinized anatase (Hombikat UV 100, 300 m² g⁻¹), respectively, in aqueous suspensions at pH 3⁴⁷. From data published by Czili and Horváth for the adsorption of DCA at pH 3, values of ≈ 50 μmol g⁻¹, ≈ 20 μmol g⁻¹, and ≈ 20 μmol g⁻¹ are estimated for the anatase-rutile composite Degussa P25 (50 m² g⁻¹), anatase (9.6 m² g⁻¹), and rutile (9.7 m² g⁻¹), respectively⁴⁸. Krivec *et al.* investigated the adsorption of DCA on Degussa P25 at pH 3 and observed Langmuir adsorption with a maximum amount of adsorbed DCA of 43 μmol g⁻¹. The maximum amount of adsorbed DCA decreased to 22 μmol g⁻¹ in the presence of 0.5 mmol L⁻¹ Cl⁻. They reported a Langmuir adsorption constant for DCA of 1.64 mmol L⁻¹ unaffected by the presence of Cl⁻⁴⁶. It seems likely that the significantly lower *q* obtained for DCA compared to acetate is due to the larger area required by the bulky DCA on the TiO₂ surface. The length of the C–H and C–Cl bonds are ≈ 0.11 nm and ≈ 0.18 nm, respectively⁴⁹. The assumption of a larger space requirement of DCA compared to acetic acid is also supported by experimental observations. Thus, Czili and Horváth found that the loading of titanium dioxide surfaces with an adsorbate decreases in the order monochloroacetic acid > dichloroacetic acid > trichloroacetic acid⁴⁸. The above comparison with published data should have shown that there are no reasons against the assumption of complete coverage of the Hombikat UV 100 surface with adsorbed DCA at the experimental conditions employed in this study. Complete coverage of all adsorption sites at the photocatalyst surface then results in zero order kinetics ($dC/dt = r_{\max}$) as observed here (*cf.* **Figure 5.1A, 5.2A, 5.3A, and 5.4A**). As already mentioned above, the maximum reaction rate r_{\max} depends on the time derivative of the amount of absorbed photons $dn_{p,\text{abs}}/dt$, and thus on the photon flux $dn_{p,\text{em}}/dt$ emitted by the light source. For a black body photoreactor as used here, to a good approximation, the photon flux emitted by the light source is equal to the photon

5. Reaction Rate Study of Photocatalytic Degradation of Dichloroacetic Acid in a Black Body Reactor

flux absorbed by the photocatalyst particles in the suspension ($dn_{p,em}/dt \cong dn_{p,abs}/dt$). Following a suggestion by Turchi and Ollis⁵⁰, the relation between the observed reaction rates and the employed photon fluxes is given by $r_{max} = k(dn_{p,em}/dt)^m \cong k(dn_{p,abs}/dt)^m$. The power term m has values of 1 and 0.5 at low and high $dn_{p,abs}/dt$ values., respectively. Here, a non-linear dependence of r_{max} on the photon flux was observed (**Figure 5.4B**), which, however, can not be described by a power term $m = 0.5$. The non-linear regression of the experimental data presented in **Figure 5.4B** with two adjustable parameters gave $m < 0.5$ (data not shown), which is not within the mechanistic assumptions used to derive the rate law. The RODA model, recently proposed by Mills and co-authors³⁷ and applied here in the modified form $dC/dt = k_1[-1 + \{1 + k_2(dn_p/dt)\}^{0.5}]$ to apply to zero order kinetics, also did not fit the experimental data (not shown). Salvador and co-workers have emphasised that photocatalytic reactions at solid surfaces always occur by direct electron transfer from the organic solute to valance band holes and by indirect reaction between the organic solute and surface-trapped holes⁴¹⁻⁴³. Both reactions proceed in parallel. Thus, the observed reaction rate is the sum of the reaction rates of the direct and the indirect reaction, i.e., $dC/dt = (dC/dt)_{direct} + (dC/dt)_{indirect}$. The analysis of the experimental data depicted in **Figure 5.4** was based on the rate law for the direct-indirect mechanism as derived by Mills and co-authors³⁷. Since zero order kinetics was observed in all experimental runs, it was possible to simplify the rate law given by Mills *et al.* resulting in $dC/dt = [k_3^2 + k_4(dn_p/dt)]^{0.5} - k_3 + k_5(dn_p/dt)$. A good agreement between the experimental data and the calculated curve was obtained (data not shown). However, the numerical values of the three adjustable kinetic parameters were found to be physically meaningless. These results indicate that additional reactions of the organic solute (DCA) occur at the surface of the excited photocatalyst or inside the surrounding electrolyte, which are not considered in the discussed rate laws and the underlying reaction mechanisms. Here, the reduction reaction of adsorbed DCA by conduction band reactions as well as reactions between secondarily formed OH radicals and DCA in the aqueous phase should be considered.

As discussed in the Introduction, the reaction rate dC/dt of a photocatalytic reaction in suspension is a volume-averaged value. Consequently, the values $dC/dt = r_{max}$ reported in the **Figure 5.1B**, **5.2B**, and **5.3B** are also volume-averaged values. The absorbed photons result in the formation of electron-hole pairs. A fraction of the formed electrons and holes

5. Reaction Rate Study of Photocatalytic Degradation of Dichloroacetic Acid in a Black Body Reactor

recombine in a fast process. However, the remaining holes react with adsorbed dichloroacetate in a single electron transfer reaction according to **Equation 5.5**. The following equation applies

$$dn_{p,em}/dt \cong dn_{p,abs}/dt = \Phi^{-1}(d\zeta(\text{DCA})/dt) \quad (5.13)$$

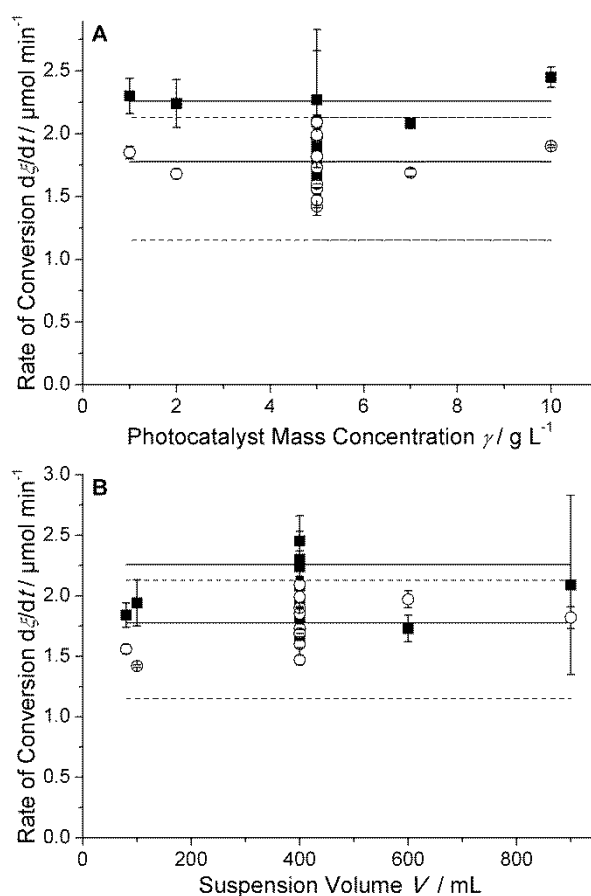


Figure 5.5. Rates of conversion $d\zeta(\text{DCA})/dt$ and $d\zeta(\text{Cl}^-)/dt$ vs. (A) the photocatalyst mass concentration γ and (B) the suspension volume V . The lines represent the limits of experimental errors (= mean rate \pm standard deviation) for DCA (solid lines) and Cl^- (dotted lines).

The parameter $\Phi = d\zeta(\text{DCA})/dn_{p,abs}$ corresponds to the quantum yield of the photocatalytic degradation reaction under consideration²³. In **Figure 5.5**, the rates of conversion $d\zeta(\text{DCA})/dt$ for all experimental runs at a photon flux of $10.7 \mu\text{mol min}^{-1}$ are plotted *versus* both the mass concentration γ of the photocatalyst and the suspension

5. Reaction Rate Study of Photocatalytic Degradation of Dichloroacetic Acid in a Black Body Reactor

volume V . The average rate of DCA conversion was calculated as $d\zeta(\text{DCA})/dt = 2.02 \pm 0.24 \mu\text{mol min}^{-1}$ ($N = 13$). With this average rate of conversion and the photon flux of $10.7 \mu\text{mol min}^{-1}$ emitted by the light source and determined by actinometry, the average quantum yield Φ of the photocatalytic DCA oxidation in the presence of Hombikat UV 100 is calculated to be 0.189 ± 0.023 .

For the purpose of comparison, the rates of conversion of Cl^- are included in **Figure 5.5**. The average rate of conversion was calculated to be $d\zeta(\text{Cl}^-)/dt = 1.64 \pm 0.48 \mu\text{mol min}^{-1}$ ($N = 13$) which corresponds to an average quantum yield $\Phi = 0.153 \pm 0.046$ for the photocatalytic DCA oxidation in acidic suspension containing Hombikat UV 100.

It becomes obvious from the data presented in **Figure 5.4** that chloride is released slower than DCA is photocatalytically oxidized. The rate $d\zeta(\text{Cl}^-)/dt$ was found to be almost 20 % lower than $d\zeta(\text{DCA})/dt$. Obviously, the relation $d\zeta(\text{DCA})/dt = d\zeta(\text{Cl}^-)/dt$, whose validity is mandatory if the DCA degradation follows the reaction path proposed in **Table 5.1**, does not hold. Chloride is known to be adsorbed on a TiO_2 surface at acidic pH^{20,46}. A Langmuir adsorption constant of 0.69 mmol L^{-1} was reported for the adsorption of Cl^- on a Degussa P25 surface at pH 3⁴⁶. Certainly, the adsorbed fraction of the photocatalytically generated Cl^- is not available for the quantification by HPIC. Losses due to the evolution of molecular chlorine, which might be formed *via* hole oxidation of adsorbed Cl^- and subsequent dimerization of two Cl^\bullet , seems to be unlikely⁴⁶. However, the formation of chloro-organic intermediates cannot be excluded. One possible reaction is the formation of tetrachloroethane by dimerization of two dichloromethyl radicals. The analogous formation of ethane by dimerization of two methyl radicals was demonstrated to occur during the photocatalytic reaction of acetic acid in O_2 -free^{33,34,51,52} and in O_2 -containing TiO_2 suspensions⁵². It should be mentioned that Chemseddine and Boehm, who have investigated the photocatalytic DCA degradation in aqueous slurries of Degussa P25 TiO_2 , reported a rate of CO_2 evolution significantly lower than the rate of Cl^- formation. They emphasized, however, that almost all the chlorine bound in the reactant was released as chloride¹⁸. On the other hand, Ballari and co-authors, who have investigated the DCA degradation in the presence of an anatase TiO_2 , reported that 2 moles of Cl^- are generated from 1 mole of degraded DCA, and that the

5. Reaction Rate Study of Photocatalytic Degradation of Dichloroacetic Acid in a Black Body Reactor

chromatographically determined DCA concentrations were almost equal to the concentrations calculated from corresponding TOC measurements. They concluded that no stable organic intermediates are formed during the photocatalytic degradation of DCA¹². Zalazar *et al.* reported small differences between the measured concentrations of organic carbon (TOC) and Cl^- and the values expected from the measured DCA concentrations in the initial phase of the experimental runs. However, they claim that a statistical test does not indicate these deviations to be significant¹³.

The rates of conversion $d\zeta(\text{DCA})/dt$ and $d\zeta(\text{Cl}^-)/dt$ were found to be constant within the limits of experimental error and not affected by the initial concentration of the probe compound dichloroacetic acid, C_s , the mass concentration of the photocatalyst Hombikat UV 100, γ , and the suspension volume V , when C_s and γ are larger than 2.5 mmol L^{-1} and 1 g L^{-1} , respectively. The deviations from the average values of $d\zeta(\text{DCA})/dt$ and $d\zeta(\text{Cl}^-)/dt$ were found to be about 12 % and 30 %, respectively. The larger experimental error in the determination of $d\zeta(\text{Cl}^-)/dt$ is attributed to the significantly lower concentrations of chloride formed during the photocatalytic degradation of DCA. Employing a black body photoreactor, rates of conversion can thus be determined with sufficiently good reproducibility.

5.9. Conclusions

The experimental results presented here clearly evince that the rate of a photocatalytic reaction in suspension can be determined unaffected by the scattering properties of the photocatalyst when a black body photoreactor is employed. It was shown that experimental conditions can be achieved under which the rate of the photocatalytic degradation reaction, defined as the time derivative of the extent of reaction, is constant within the limits of experimental error. It is assumed that the observed variance of the rates of conversion is due to inhomogeneities of the commercial Hombikat UV 100, as had already been reported for Degussa P25 (now Aeroxide TiO_2 P25, Evonik)⁵³. Employing a black body photoreactor, rates of conversion and quantum yields can thus be determined with sufficiently good reproducibility.

Finally, some remarks (platitudes) on the comparative assessment of different photocatalysts may be given:

5. Reaction Rate Study of Photocatalytic Degradation of Dichloroacetic Acid in a Black Body Reactor

- (i) For comparative measurements in suspensions, it should be ensured that the photocatalyst is the only light-absorbing species. The probe compound as well as intermediates and products formed during the photocatalytic reaction must therefore be optically transparent at the wavelength used for the excitation of the photocatalyst.
- (ii) The experimental conditions should allow the determination of the amount of photons absorbed by the photocatalyst.
- (iii) Comparative activity measurements with a set of photocatalysts should be performed under conditions of zero order kinetics with respect to the probe compound. This ensures the observed differences in rates of conversion or quantum yields are not due to differences in the coverage of the photocatalyst surface with the sample compound.
- (iv) As the measure of the activity of a solid photocatalyst, it is advisable to indicate the quantum yield or the rate of conversion of the probe compound obtained under the conditions of zero order kinetics. This enables the direct comparison of reported data without any necessary conversions of volume, mass or area related reaction rates.
- (v) It seems doubtful that rates of conversion that differ by less than 10 % indicate differences in photocatalytic activities. If necessary, a sufficiently high number of replicate measurements are to be performed demonstrating that differences between the determined activities of photocatalysts of less than 10 % are statistically significant.

5.10. Acknowledgements

L.M. gratefully acknowledges a scholarship of the Deutscher Akademischer Austauschdienst (DAAD). Financial support from the Global Research Laboratory program (2014 K1 A1 A2041044), Korea government (MSIP) through NRF is gratefully acknowledged.

5.11. References

- (1) Kisch, H.; Bahnemann, D. Best practice in photocatalysis: Comparing rates or apparent quantum yields? *J. Phys. Chem. Lett.* **2015**, *6*, 1907–1910.
- (2) Qureshi, M.; Takanabe, K. Insights on measuring and reporting heterogeneous photocatalysis: Efficiency definitions and setup examples. *Chem. Mater.* **2017**, *29*, 158–167.

5. Reaction Rate Study of Photocatalytic Degradation of Dichloroacetic Acid in a Black Body Reactor

- (3) Hoque, M.A.; Guzman, M.I. Photocatalytic activity: Experimental features to report in heterogeneous photocatalysis. *Materials (Basel)***2018**, *11*, 1990.
- (4) Schiavello, M.; Augugliaro, V.; Palmisano, L. An experimental method for the determination of the photon flow reflected and absorbed by aqueous dispersions containing polycrystalline solids in heterogeneous photocatalysis. *J. Catal.***1991**, *127*, 332–341.
- (5) Brandi, R.J.; Alfano, O.M.; Cassano, A.E. Evaluation of radiation absorption in slurry photocatalytic reactors. 1. Assessment of methods in use and new proposal. *Environ. Sci. Technol.***2000**, *34*, 2623–2630.
- (6) Brandi, R.J.; Citroni, M.A.; Alfano, O.M.; Cassano, A.E. Absolute quantum yields in photocatalytic slurry reactors. *Chem. Eng. Sci.***2003**, *58*, 979–985.
- (7) Satuf, M.L.; Brandi, R.J.; Cassano, A.E.; Alfano, O.M. Experimental method to evaluate the optical properties of aqueous titanium dioxide suspensions. *Ind. Eng. Chem. Res.***2005**, *44*, 6643–6649.
- (8) Cabrera, M.I.; Alfano, O.M.; Cassano, A.E. Absorption and scattering coefficients of titanium dioxide particulate suspensions in water. *J. Phys. Chem.***1996**, *100*, 20043–20050.
- (9) Loddo, V.; Addamo, M.; Augugliaro, V.; Palmisano, L.; Schiavello, M.; Garrone, E. Optical properties and quantum yield determination in photocatalytic suspensions. *AIChE J.***2006**, *52*, 2565–2574.
- (10) Yurdakal, S.; Loddo, V.; Bayarri Ferrer, B.; Palmisano, G.; Augugliaro, V.; Giménez Farreras, J.; Palmisano, L. Optical properties of TiO₂ suspensions: Influence of pH and powder concentration on mean particle size. *Ind. Eng. Chem. Res.***2007**, *46*, 7620–7626.
- (11) Emeline, A.V.; Zhang, X.; Jin, M.; Murakami, T.; Fujishima, A. Application of a "black body" like reactor for measurements of quantum yields of photochemical reactions in heterogeneous systems. *J. Phys. Chem. B***2006**, *110*, 7409–7413.
- (12) Ballari, M.d.I.M.; Alfano, O.O.; Cassano, A.E. Photocatalytic degradation of dichloroacetic acid. A kinetic study with a mechanistically based reaction model. *Ind. Eng. Chem. Res.***2009**, *48*, 1847–1858.
- (13) Zalazar, C.S.; Romero, R.L.; Martín, C.A.; Cassano, A.E. Photocatalytic intrinsic reaction kinetics I: Mineralization of dichloroacetic acid. *Chem. Eng. Sci.***2005**, *60*, 5240–5254.
- (14) Zalazar, C.S.; Martín, C.A.; Cassano, A.E. Photocatalytic intrinsic reaction kinetics. II: Effects of oxygen concentration on the kinetics of the photocatalytic degradation of dichloroacetic acid. *Chem. Eng. Sci.***2005**, *60*, 4311–4322.
- (15) Megatiff, L.; Dillert, R.; Bahnemann, D.W. A method to compare the activities of semiconductor photocatalysts in liquid–solid systems. *ChemPhotoChem***2018**, *2*, 948–951.

5. Reaction Rate Study of Photocatalytic Degradation of Dichloroacetic Acid in a Black Body Reactor

- (16) Megatiff, L.; Dillert, R.; Bahnemann, D.W. Determination of the quantum yield of a heterogeneous photocatalytic reaction employing a black body photoreactor. *Catal. Today***2019**, in the press, doi:10.1016/j.cattod.2019.06.008.
- (17) Sakthivel, S.; Hidalgo, M.C.; Bahnemann, D.W.; Geissen, S.-U.; Murugesan, V.; Vogelpohl, A. A fine route to tune the photocatalytic activity of TiO₂. *Appl. Catal. B: Environ.***2006**, *63*, 31–40.
- (18) Chemseddine, A.; Boehm, H.P. A study of the primary step in the photochemical degradation of acetic acid and chloroacetic acids on a TiO₂ photocatalyst. *J. Mol. Catal.***1990**, *60*, 295–311.
- (19) Bahnemann, D.W.; Kholuiskaya, S.N.; Dillert, R.; Kokorin, A.I. Photodestruction of dichloroacetic acid catalyzed by nano-sized TiO₂ particles. *Appl. Catal. B: Environ.***2002**, *36*, 161–169.
- (20) Lindner, M.; Bahnemann, D.W.; Hirthe, B.; Griebler, W.-D. Solar water detoxification: Novel TiO₂ powders as highly active photocatalysts. *J. Sol. Energy Eng.***1997**, *119*, 120–125.
- (21) Lindner, M.; Theurich, J.; Bahnemann, D. Photocatalytic degradation of organic compounds: Accelerating the process efficiency. *Water Sci. Technol.***1997**, *35*, 79–86.
- (22) Lindner, M. Optimierung der photokatalytischen Wasserreinigung mit Titandioxid: Festkörper- und Oberflächenstruktur des Photokatalysators. Dissertation; Universität, Hannover, 1997.
- (23) Laidler, K.J. A glossary of terms used in chemical kinetics, including reaction dynamics (IUPAC Recommendations 1996). *Pure Appl. Chem.***1996**, *68*, 149–192.
- (24) Hatchard, C.G.; Parker, C.A.; Bowen, E.J. A new sensitive chemical actinometer - II. Potassium ferrioxalate as a standard chemical actinometer. *Proc. R. Soc. Lond. A***1956**, *235*, 518–536.
- (25) Szakács, Z.; Hägele, G. Accurate determination of low pK values by H NMR titration. *Talanta***2004**, *62*, 819–825.
- (26) Kraeutler, B.; Bard, A.J. Heterogeneous photocatalytic decomposition of saturated carboxylic acids on titanium dioxide powder. Decarboxylative route to alkanes. *J. Am. Chem. Soc.***1978**, *100*, 5985–5992.
- (27) Kraeutler, B.; Bard, A.J. Heterogeneous photocatalytic synthesis of methane from acetic acid - new Kolbe reaction pathway. *J. Am. Chem. Soc.***1978**, *100*, 2239–2240.
- (28) Kraeutler, B.; Jaeger, C.D.; Bard, A.J. Direct observation of radical intermediates in the photo-Kolbe reaction - heterogeneous photocatalytic radical formation by electron spin resonance. *J. Am. Chem. Soc.***1978**, *100*, 4903–4905.
- (29) Kaise, M.; Kondoh, H.; Nishihara, C.; Nozoye, H.; Shindo, H.; Nimura, S.; Kikuchi, O. Photocatalytic reactions of acetic acid on platinum-loaded TiO₂: ESR

5. Reaction Rate Study of Photocatalytic Degradation of Dichloroacetic Acid in a Black Body Reactor

- evidence of radical intermediates in the photo-Kolbe reaction. *J. Chem. Soc., Chem. Commun.***1993**, 395–396.
- (30) Kaise, M.; Nagai, H.; Tokuhashi, K.; Kondo, S.; Nimura, S.; Kikuchi, O. Electron spin resonance studies of photocatalytic interface reactions of suspended M/TiO₂ (M = Pt, Pd, Ir, Rh, Os, or Ru) with alcohol and acetic acid in aqueous media. *Langmuir***1994**, *10*, 1345–1347.
- (31) Nosaka, Y.; Koenuma, K.; Ushida, K.; Kira, A. Reaction mechanism of the decomposition of acetic acid on illuminated TiO₂ powder studied by means of in situ electron spin resonance measurements. *Langmuir***1996**, *12*, 736–738.
- (32) Nosaka, Y.; Kishimoto, M.; Nishino, J. Factors governing the initial process of TiO₂ photocatalysis studied by means of in-situ electron spin resonance measurements. *J. Phys. Chem. B***1998**, *102*, 10279–10283.
- (33) Hamid, S.; Ivanova, I.; Jeon, T.H.; Dillert, R.; Choi, W.; Bahnemann, D.W. Photocatalytic conversion of acetate into molecular hydrogen and hydrocarbons over Pt/TiO₂: pH dependent formation of Kolbe and Hofer-Moest products. *J. Catal.***2017**, *349*, 128–135.
- (34) Hamid, S.; Dillert, R.; Bahnemann, D.W. Photocatalytic reforming of aqueous acetic acid into molecular hydrogen and hydrocarbons over co-catalyst-loaded TiO₂: Shifting the product distribution. *J. Phys. Chem. C***2018**, *122*, 12792–12809.
- (35) Wolff, K. Mechanistische Untersuchungen zum Oxidationsprozess an der belichteten Titandioxid/Wasser-Grenzfläche. Dissertation; Universität, Hannover, 1993.
- (36) Wolff, K.; Bockelmann, D.; Bahnemann, D.W. Mechanistic aspects of chemical transformations in photocatalytic systems. In *Symposium on electronic and ionic properties of silver halides. Common trends with photocatalysis [Proc. IS&T 44th annual conference].*; Levy, B., Ed.; IS&T: Springfield, Virginia, 1991; pp 259–267.
- (37) Mills, A.; O'Rourke, C.; Moore, K. Powder semiconductor photocatalysis in aqueous solution: An overview of kinetics-based reaction mechanisms. *J. Photochem. Photobiol. A: Chem.***2015**, *310*, 66–105.
- (38) Turchi, C.S.; Ollis, D.F. Photocatalytic degradation of organic water contaminants: Mechanisms involving hydroxyl radical attack. *J. Catal.***1990**, *122*, 178–192.
- (39) Ollis, D.F. Kinetics of liquid phase photocatalyzed reactions: An illuminating approach. *J. Phys. Chem. B***2005**, *109*, 2439–2444.
- (40) Emeline, A.V.; Ryabchuk, V.; Serpone, N. Factors affecting the efficiency of a photocatalyzed process in aqueous metal-oxide dispersions. *J. Photochem. Photobiol. A: Chem.***2000**, *133*, 89–97.

5. Reaction Rate Study of Photocatalytic Degradation of Dichloroacetic Acid in a Black Body Reactor

- (41) Illarreal, T.L.; Gómez, R.; González, M.; Salvador, P. A kinetic model for distinguishing between direct and indirect Interfacial hole transfer in the heterogeneous photooxidation of dissolved organics on TiO₂ nanoparticle suspensions. *J. Phys. Chem. B***2004**, *108*, 20278–20290.
- (42) Monllor-Satoca, D.; Gómez, R.; González-Hidalgo, M.; Salvador, P. The “Direct–Indirect” model: An alternative kinetic approach in heterogeneous photocatalysis based on the degree of interaction of dissolved pollutant species with the semiconductor surface. *Catal. Today***2007**, *129*, 247–255.
- (43) Montoya, J.F.; Peral, J.; Salvador, P. Comprehensive kinetic and mechanistic analysis of TiO₂ photocatalytic reactions according to the direct–indirect model: (I) Theoretical approach. *J. Phys. Chem. C***2014**, *118*, 14266–14275.
- (44) Flaig-Baumann, R.; Herrmann, M.; Boehm, H.P. Über die Chemie der Oberfläche des Titandioxids. III. Reaktionen der basischen Hydroxylgruppen auf der Oberfläche. *Z. Anorg. Allg. Chem.***1970**, *372*, 296–307.
- (45) Boehm, H.P. Acidic and basic properties of hydroxylated metal oxide surfaces. *Discuss. Faraday Soc.***1971**, *52*, 264–275.

6. Summarizing Discussion

This chapter starts with the introduction of the possible mechanistic pathways of the photocatalytic dichloroacetic acid (DCA) degradation followed by a discussion of the kinetic study and the obtained reaction rates during the photocatalytic dichloroacetic acid (DCA) degradation in a black body reactor using anatase TiO_2 nanoparticles (Hombikat UV 100) as photocatalyst upon UV irradiation. Hereby, the effect of the model compound concentration, the catalyst loading and the reaction volume on the reaction rate will be discussed in detail. Based on the kinetics of the DCA degradation and the Cl^- formation, the respective mechanisms of the photocatalytic degradation of DCA are discussed. In the following, the quantum yield of the reaction and its dependency on the photon flux in a black body reactor are discussed. Furthermore, the role of the light density in a black body reactor and its effect on the reaction rate and the quantum yield is described. Finally, the activities of various photocatalysts measured in a black body reactor are compared and a new standard method for the comparison of the photocatalytic activities in heterogeneous systems is introduced.

As mentioned in **Chapter 1**, the proper design of a photoreactor necessitates the determination of the volume-averaged quantum yield. Consequently, in addition to the reaction rates, the volume-averaged amount of photons that are absorbed by the photocatalyst per unit time is required. Therefore, an integration of the local volumetric rate of the photon absorption (LVRPA) for all possible positions inside the reactor is required. In turn, the LVRPA is calculated by solving the radiative transfer equation (RTE). To solve this equation, the scattering effects of solid particles in the reaction slurry must be studied and the best phase function for radiation scattering by the photocatalyst particles must be selected. As shown in **Chapter 2**, scattering is the most challenging issue in heterogeneous systems. Unavoidable intrinsic spatial variations of this phenomenon are responsible for the majority of the difficulties associated with the photoreactor analysis and design¹. Hence, it would be a great simplification for the photoreactor design to find a way in which scattering does not have to be considered. The best solution to apply this approach is a method enabling the determination of the volume-averaged quantum yield in a system in which all the light is absorbed by the system and the light scattering is negligible.

6. Summarizing Discussion

Furthermore, as discussed in **Chapter 1**, the lack of a standard method to measure the activity of different photocatalysts in heterogeneous systems makes it difficult to compare the photocatalytic activity of various materials. Although it is recommended by the IUPAC to compare the activity of photocatalysts based on their respective quantum yield², in most of the studies the activity is reported in terms of the reaction rate. The main obstacle in the quantum yield determination of heterogeneous systems is the measurement of the number of absorbed photons by the semiconductor particles which requires sophisticated and time consuming methods^{3,4}. On the other hand, it should be taken into account that in heterogeneous photocatalytic systems, the reaction rate is always a volume-averaged value. The photocatalytic reaction only takes place in regions where light penetrates while in dark regions no photocatalytic reaction can occur. Therefore, many parameters such as the reaction volume, the reactor geometry, the catalyst loading, and the concentration of the probe molecule, have an impact on the reaction rate of the photocatalysts defined as the time derivative of the concentration.

The choice of a proper model compound is an important issue in photocatalysis in order to find a straightforward procedure for the determination of the quantum yield. Many researchers employ dye molecules (*e.g.* methylene blue) as a probe compound to evaluate the kinetics or the mechanism of a photocatalytic process⁵⁻⁷. However, it has been discussed by mills *et al.* that the photobleaching of methylene blue sensitised by TiO₂ in aqueous phase (commonly mistaken with its photocatalytic degradation), has a quite complicated mechanism. They have shown that the observed photobleaching of the dye, is not necessarily due its photocatalytic oxidation⁸. Phenol is another commonly investigated probe molecule which is not an ideal candidate for evaluation of photocatalytic systems. Upon its photocatalytic degradation, some stable intermediates such as catechol, hydroquinone, hydroxyl hydroquinone, and benzoquinone are produced⁹⁻¹¹, thus part of the incoming photons might be absorbed by the intermediates. Other popular model compounds such as chlorophenol¹² and its derivatives can be criticized with the same arguments. Therefore, DCA has been chosen in many studies as a simple compound for the comparison of different photocatalytic process¹³⁻²¹.

6.1. Mechanism of the Photocatalytic Degradation of DCA

As already mentioned, in this work DCA was chosen as a simple model compound which requires only one hole for a complete decomposition²². This compound only absorbs

radiation below 275 nm and its photocatalytic conversion does not yield intermediates, thus any unwanted absorption of the incoming light will be avoided¹⁸. Furthermore, its low vapor pressure and high water solubility make it a good choice for laboratory studies²¹.

The reaction pathway and the primary steps of the photocatalytic degradation of DCA have a significant impact on the kinetics of this photocatalytic reaction. Therefore, to have a complete understanding of the kinetics of the DCA degradation, the underlying mechanism needs to be known. The photocatalytic decomposition of DCA takes place *via* two different reaction pathways; (I) direct mineralization in which the organic adsorbate is directly attacked by holes and, (II) indirect oxidation process by OH radicals (**Figure 6.1**)²³.

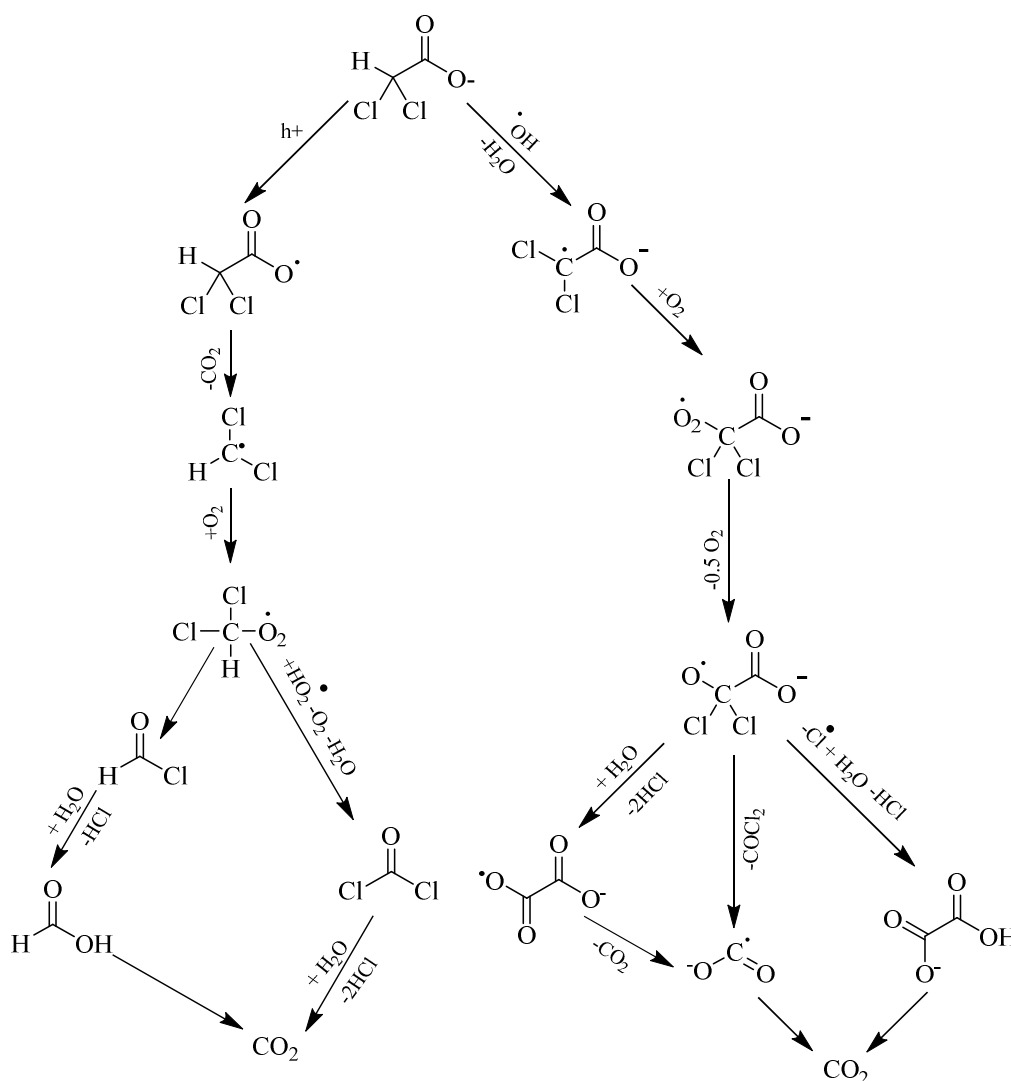


Figure 6.1. Mechanisms of DCA degradation²³

6. Summarizing Discussion

In the direct oxidation pathway, excitation of electrons from the valence band to the conduction band occurs upon light absorption of the semiconductor photocatalyst within a specific wavelength range. The promotion of an electron to the conduction band leaves a positive hole in the valence band (**Equation 6.1**)²⁴. The photo-generated electrons and holes either recombine or migrate to the photocatalyst surface, where they can act as reductants and oxidants, respectively²⁵. In the pH range applied in this work (pH 3), the DCA molecule dissociates into dichloroacetate and is adsorbed on the surface of the photocatalyst (**Equation 6.2**)¹⁹. As reported by Bahnemann *et al.*, the generated hole attacks the adsorbed DCA molecule and produces a dichloroacetate radical (**Equation 6.3**)²⁶. According to Bahnemann, this radical decomposes into carbon dioxide and a dichloro methyl radical (photo-Kolbe) which in turn reacts with adsorbed molecular oxygen producing a dichloro methyl peroxy radical (**Equations 6.4, 6.5**)²². The bimolecular reaction of two dichloro methyl peroxy radicals results in the formation of hydrogen peroxide and phosgene which hydrolyzes very fast yielding HCl and CO₂ (**Equations 6.6, 6.7**)¹⁸. According to this mechanism Zalazar *et al.* claimed that one hole is required for the complete mineralization of DCA, because during the degradation process a stable chloride reaction intermediate is not generated. Therefore, the decomposition of each mole of DCA leads to generation of stoichiometric ratios (two moles) of HCl²⁷.

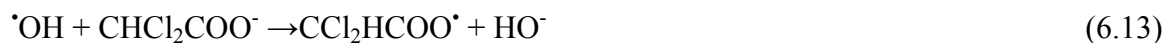


Besides the direct reaction pathway, DCA can also be decomposed through an indirect pathway involving [•]OH radicals formed at the surface of the photocatalyst. As described by Schuchmann *et al.*²⁸ for the [•]OH-induced formation of acetate, this mechanism

proceeds through a pathway which involves the following steps (**Equations 6.8-6.12**): formation of an electron-hole pair, transfer of the hole to the surface, reaction with an OH⁻ ion or an adsorbed water molecule forming an [•]OH radical (**Equation 6.8**), hydrogen abstraction and production of a [•]CCl₂COO⁻ radical (**Equation 6.9**), formation of [•]OOCCl₂COO⁻ (**Equation 6.10**), bimolecular reaction of [•]OOCCl₂COO⁻ (**Equation 6.11**)²⁹ and hydrolysis of phosgene to produce hydrochloric acid and carbon dioxide (**Equation 6.12**)²⁹.



However, besides the above mentioned mechanism, Zalazar *et.al* have proposed another pathway in which the [•]OH radical attacks the negatively charged carboxyl group of the molecule which results in a neutral radical^{29,30}.



Through the Kolbe reaction the formed radical is decarboxylated as shown in **Equation 6.4**²⁹. The formed dichloromethyl radical also reacts with molecular oxygen resulting in the formation of a dichloromethylperoxyl radical (**Equation 6.5**). In the next step, phosgene is formed by a bimolecular reaction (**Equation 6.6**). As in the first pathway, the formed phosgene is hydrolyzed in the solution (**Equation 6.7**).

Nevertheless, considering the experimental conditions presented in this work, it is experimentally not possible to differentiate between these two reaction pathways, whether measuring DCA, Cl⁻, H⁺, TOC, etc.

Furthermore, since the degradation pathway might affect the kinetics of the DCA degradation, the Cl⁻ formation rate was also studied besides the DCA degradation rate. As illustrated in **Figure 6.1**, DCA can be degraded through the initial abstraction of the H atom or *via* the photo-Kolbe reaction pathway forming CO₂ as reported by Lindner²³.

6. Summarizing Discussion

Accordingly, in the current study, the combination of the experimental results from the Cl^- formation and DCA^- ion degradation may provide a better understanding of the photocatalytic degradation mechanism of DCA. Interestingly, it was found that the rate of chloride formation was constant with an average value of $1.64 \pm 0.48 \mu\text{mol min}^{-1}$ (**Figure 5.5**) which was slightly lower than the DCA degradation rate ($2.02 \pm 0.24 \mu\text{mol min}^{-1}$). These differences between the reaction rate of the DCA degradation and the Cl^- formation suggest that Cl^- is released more slowly than DCA is photocatalytically oxidized. Therefore, either the direct mechanism is not the only pathway of the photodegradation of DCA or part of the generated Cl^- remains adsorbed on the photocatalyst surface.

After the formation of HCl, the chloride ions compete with DCA for adsorption sites at the catalyst surface. According to the results reported by Piscopo *et al.* and Wang *et al.*, the Cl^- ions are strongly adsorbed on the TiO_2 surface at pH 3^{31,32}. Therefore, considering that the adsorbed fraction of the generated Cl^- is not available for the quantification by HPIC, this small difference between the photocatalytic oxidation rate of DCA and the formation rate of Cl^- can be explained by the strong adsorption of Cl^- on the catalyst surface.

As shown in **Figure 6.1**, DCA can be decomposed through different pathways resulting in various intermediates. These reactive intermediates can react with each other forming some stable intermediates leading to a decrease in the amount of Cl^- in the solution. For example, according to **Equation 6.4**, the obtained dichloromethyl radical can dimerize yielding tetrachloroethene:



It has to be mentioned that this reaction only happens in the absence of molecular oxygen. The formed intermediates can result in differences between the DCA degradation rate according to the measured DCA ions and the generated chloride ions. Considering the physical properties such as volatility and low solubility of tetrachloroethene in water, this compound can evaporate after the formation. Therefore, detection of this compound is difficult in an open system. Nevertheless, the excess amount of molecular oxygen present in the system leads to a low conversion of this reaction. It should be mentioned that Zalazar *et al.* also reported lower values of Cl^- than the values expected from the

measured DCA concentrations. However, according to the performed statistical test no significant deviation was indicated¹⁸.

6.2. Reaction Rate Study of Photocatalytic Degradation of DCA

Regardless of the detailed microscopic mechanism of the photocatalyst, the rate of the photocatalytic DCA degradation is generally given by a form of the Langmuir-Hinshelwood-type rate law having the mathematical form of **(Equation 6.15)**³³⁻³⁶.

$$dC/dt = \chi_1 C / (\chi_2 C + \chi_3) \quad (6.15)$$

where the physical meaning of the kinetic parameters χ_1 , χ_2 , and χ_3 depends on the underlying mechanistic assumptions. This model is widely accepted and can fit many photocatalytic results. Although this model is just an apparent description of the photocatalytic kinetics, it is applied to interpret the kinetic data of the heterogeneous DCA degradation reaction due to a simple mathematical form³⁷. According to this model when $\chi_2 C \gg \chi_3$, the reaction rate reaches its maximum value and becomes independent from the concentration following zero order kinetics regarding the concentration of the probe molecule **(Equation 6.16)**.

$$dC/dt = \chi_1 / \chi_2 = r_{\max} \quad (6.16)$$

According to the kinetic experiments reported in **Chapter 5 (Figure 5.1, 5.2, and 5.3)**, the kinetics of the photocatalytic DCA degradation can be described by a zero order rate law under the experimental conditions employed in this work which is expressed as follows **(Equation 6.17)**.

$$r = \frac{dC}{dt} = -k \quad (6.17)$$

The kinetic parameter k is the reaction constant, which under zero order kinetic conditions is equal to the maximum reaction rate. As shown in **Figure 5.1**, similar to the Langmuir-Hinshelwood prediction, the observed rate constants for various initial concentrations of DCA (C_0) seems to initially follow first order kinetics only at low initial concentrations (lower than 2 mM). However, by increasing the concentration, zero order kinetics are observed at higher DCA concentrations. According to the results shown in **Chapter 5 in Figure 5.1**, the average value of the reaction rate for initial concentrations higher than 5 mM was $4.79 \pm 0.56 \mu\text{mol L}^{-1} \text{min}^{-1}$. The experimental runs for various catalyst

6. Summarizing Discussion

concentrations of Hombikat UV 100, illustrated in **Figure 5.2**, also showed zero order kinetics. The reaction rate linearly increased upon an increase of the catalyst loading and after reaching an optimum catalyst concentration (1 g L^{-1}), the reaction rate was found to be independent from the catalyst concentration and became constant.

Therefore, considering the advantages of a black body reactor described in **Chapter 1**, it is proposed here to measure the photocatalytic activity of semiconductors under zero order kinetic conditions regarding the mentioned parameters, utilizing a black body reactor. A black body photoreactor ensures a complete absorption of the incoming photons by the photocatalyst. The small area of the light inlet in comparison to the whole reactor area leads to negligible back reflections through the inlet and the loss of light due to transmission is also omitted by increasing the catalyst loading surrounding the light.

In the current study, in order to confirm the employed system as a real black body photoreactor, an experimental validation was performed through carrying out actinometry measurements in this system in the absence as well as in the presence of a light scattering particle (BaSO_4 powder). It was observed that the photon flux inside the reactor is identical in both cases.

However, the reaction rate defined as the time derivative of the amount concentration is a volume-averaged value. The experimental results presented in **Figure 5.3**, clearly evince that the reaction constants decrease with an increase of the reaction volume. This can be easily explained by the fact that the rate constant is defined as the change in concentration per time and as the reaction volume changes the reaction rate changes as well. In order to solve this issue, the current study recommends to convert the reaction rate to an amount based unit and to report it as a converted amount of the probe compound per time. Therefore, performing a reaction at the optimum concentration of the probe molecule and of the photocatalyst results in an independent reaction rate regarding these two parameters and by reporting the reaction rate on an amount basis, a constant reaction rate concerning the reaction volume will be achieved (as shown in **Figures 5.1B, 5.2B, 5.5**).

According to the data discussed in **Chapter 3 (Figure 3.1)**, providing a photoreactor which meets the requirements of a black body reactor, the DCA degradation rates on an amount basis (dn/dt) were found to be constant within the limits of experimental error and independent from the reaction volumes and the initial concentrations of the probe

molecule (C_0) and the photocatalyst (γ) when $C_0 \geq 2$ mM, $\gamma \geq 1$ g L⁻¹. The average value of the reaction rate was 1.98 ± 0.18 $\mu\text{mol min}^{-1}$ and the average quantum yield Φ of the photocatalytic DCA oxidation in the presence of Hombikat UV 100 was calculated to be 0.189 ± 0.023 .

6.3. Evaluation of the Quantum Yield in a Black Body Photoreactor

In order to compare the activity of different photocatalysts, in addition to the reaction rate, the number of absorbed photons should be measured to obtain the quantum yield. Therefore, to determine the photon flux of the LED-based light beam inside the black body reactor, actinometrical measurements were carried out. As the quantum yield value of potassium ferrioxalate photolysis at 365 nm is known to be independent from the light intensity ($\phi = 1.21$) and the light absorber as well as the photoproduct are thermally stable³⁸, potassium ferrioxalate was used to determine the incoming photon flux inside the reactor. After exposure of a ferrioxalate solution to UV irradiation, Fe³⁺ converts to Fe²⁺ forming a complex with 1,10-phenanthroline that absorbs light at 510 nm ($\epsilon = 1.10 \times 10^4$ M⁻¹ cm⁻¹) which can be detected³⁹. By measuring the number of converted molecules, the number of absorbed photons can be determined. According to the obtained results shown in **Figure 4.3**, the photon flux measured for various light intensities confirms a linear dependency of the photon flux on the LED power output.

The measured photon fluxes through different light inlets for various light intensities demonstrated that the shape and size of the light inlet into the black body reactor do not affect the photon flux inside the reactor. However, the light inlet types affect the photon flux density and the reaction rate inside the reactor. As can be seen in **Figure 6.2**, at a constant photon flux, the photon flux density was varied by means of three light inlets of different geometry. As an example, light inlet type 2 (hollow sphere) showed about 50 % lower photon density in comparison with type 1 (without sphere). As a result, the quantum yield of DCA decomposition revealed various correlations with the photon flux depending on the type of the light inlet.

6. Summarizing Discussion

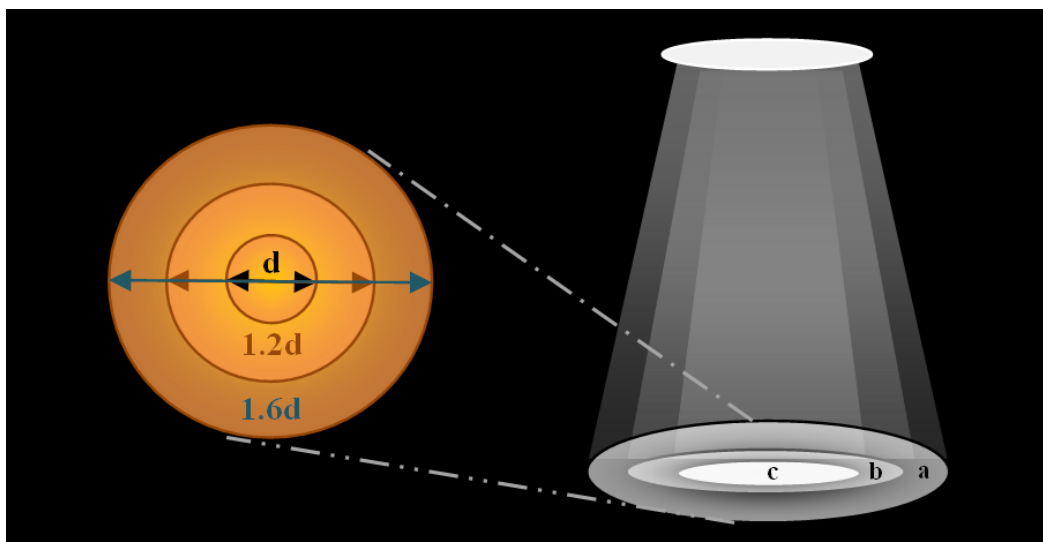


Figure 6.2. Flux density of different light inlets a) type 2, b) type 3, c) type 1

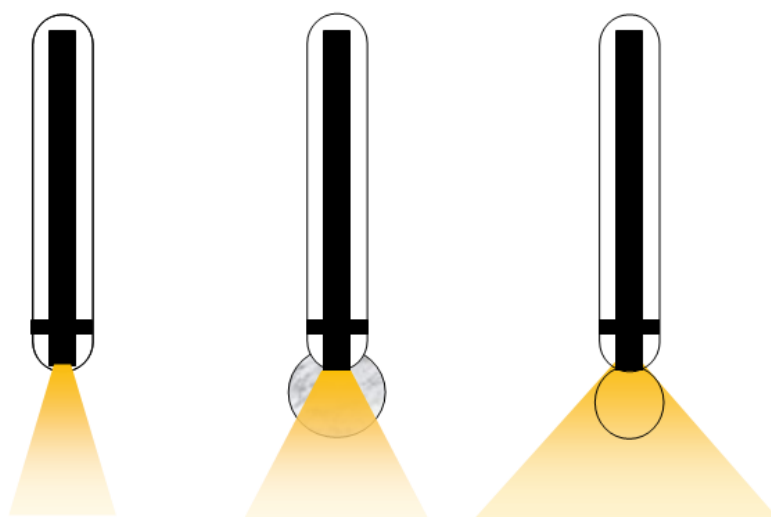


Figure 6.3. Light distribution of different light inlets: Note the lens effect of light inlet type 3. Note the lens effect of light inlet type 3

According to the results shown in **Figure 4.4**, for a light inlet in the form of a hollow sphere, the reaction rates were found to be higher in comparison with the other two light inlets. In all cases, the reaction rate decreases by a decrease of the photon flux. However, as illustrated in **Figure 4.4** a linear dependency on the photon flux could only be observed for the hollow sphere light inlet for both, Hombikat UV 100 and P25, as well as for the light inlet with a closed sphere for Hombikat UV 100. In other cases, the degradation rate

correlated with the square root of the photon flux. Assuming that the rate constant is independent from the light intensity, the rate of a photocatalytic reaction according to the Langmuir- Hinshelwood rate law is proportional to the light intensity.

$$R = k_r I^n \frac{K(I)C}{1+K(I)C} \quad (6.18)$$

in which k_r is the rate constant, $K(I)$ is the adsorption coefficient of the probe compound which is dependent on the light intensity, and $I = dn_p/dt$ is the amount of photons being absorbed by the photocatalyst per unit time^{40,41}. Here, I is assumed to be equal the photon flux emitted by the LED light source.

As proposed by Serpone *et al.*⁴², for quantum yield measurements the reaction rate was studied at zero order kinetic conditions regarding the probe compound concentration C and the catalyst loading. Therefore, at $K(I)C \gg 1$, the reaction rate can be written as:

$$R = k_r I^n \quad (6.19)$$

Upon high illumination intensities, the recombination rate of charge carriers is described by second order reaction kinetics. Thus, this recombination results in a square root correlation between the photodegradation reaction rate and the photon flux ($R = k_r I^{0.5}$) which in turn leads to a linear dependency of the quantum yield (Φ) on the inverse of the square root of the photon flux (i.e., $\Phi \propto I^{-0.5}$) according to the following equation⁴³⁻⁴⁷.

$$\Phi = \frac{R}{I} = k_r I^{n-1} \quad (6.20)$$

However, at low light intensities the light limited reaction rate follows $R = k_r I$ revealing the linear dependency of the reaction rate on the photon flux^{44,46,48}. Hence, assuming the rate constant k_r to be independent from the photon flux, the quantum yield will be constant and independent from the photon flux ($\Phi = k_r$).

Hence, the observed dependency of the quantum yield on the type of light inlet (**Figure 4.6**) can be explained by the fact that the reaction rate and consequently the quantum yield depend strongly on the light distribution inside the reactor and the photon flux density at the interface between the suspension and the inlet window (**Figure 6.3**). Providing an appropriate light distribution inside the photoreactor might decrease the recombination rate of the photogenerated electron-holes pairs being the result of a

6. Summarizing Discussion

suitable light density at each point of the black body photoreactor keeping the photon density at different positions relatively low.

Emeline *et al.* have tested cavities displaying three different shapes to confirm the independency of the quantum yield measured in a black body reactor from the light distribution in solution and thus from the irradiated surface area of the photocatalyst⁴⁹. All three corresponding values of the quantum yield were found to be almost constant and independent from the cavity shape within experimental error. In comparison with the results obtained here and shown in **Figure 4.4**, this independency can be due to sufficiently big sizes of all cavities leading to a low photon density distribution inside the reactor and consequently to constant quantum yield values.

A non-linear correlation between the reaction rate and the photon flux was also reported by Lindner *et al.*²⁰. At low photon fluxes, the photonic efficiency for the degradation of DCA over Hombikat UV 100 decreased with $(I)^{-0.12}$ and at high photon fluxes with $(I)^{-0.31}$. However, as reported by Bahnemann *et al.*⁵⁰ when P25 was used as a photocatalyst, the photonic efficiency of the DCA degradation showed an independency from the photon flux at pH = 2.6, 7, and 11. Nevertheless, at pH 5 the photonic efficiency exhibited a square root correlation with the light intensity.

Therefore, it can be concluded that applying a black body reactor with a suitable type of light inlet through which the light is distributed properly inside the reactor, thus avoiding high photon density spots in the solution, leads to a light limited reaction rate and a quantum yield which is independent from the photon flux. Since the independency of the quantum yield from the photon flux is an important condition in order to characterize the intrinsic activity of the photocatalyst, it can be concluded that the proposed method of applying a black body reactor to compare the activities of different photocatalysts has significant advantages compared to other methods.

However, it should be taken into account that for large scale applications, providing a low photon flux density throughout the whole photoreactor requires a large volume and consequently a large land area for its installation. This might result in extra costs for the photoreactor construction. Therefore, it is important to calculate the required illuminated reactor volume considering the technical and economical aspects⁵¹.

Finally, applying a light inlet with a closed sphere established a linear correlation between the photodegradation rate and the photon flux using Hombikat UV 100 as a photocatalyst. However, in case of P25 the degradation showed a square root dependency to the photon flux. These results can be explained by the dependency of the amount of absorbed photons on the solid state characteristics of the photocatalyst particles.

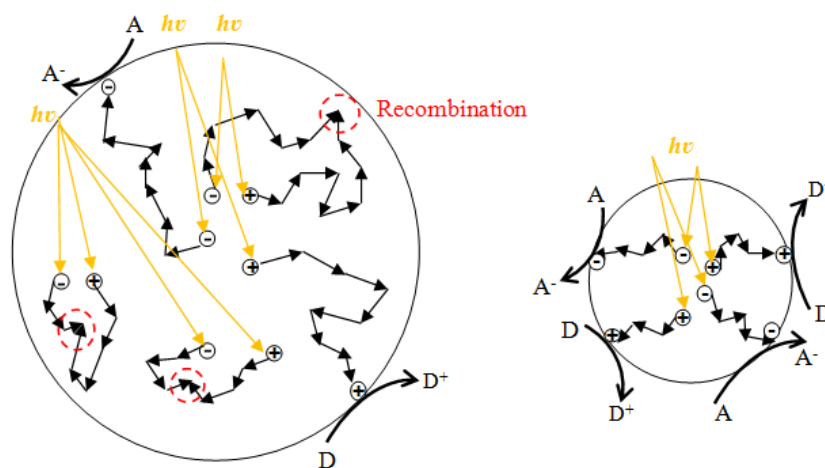


Figure 6.4. Recombination of charge carriers in a particle with different sizes during illumination

In principle, charge carriers should have average lifetimes long enough to diffuse to the surface. This can be affected by the particle size. The distance of the trapped electrons and holes to the surface of the photocatalyst in particles with smaller size is shorter. Thus, in smaller particles compared to the bigger particles the charge carriers can reach the surface more efficiently before they recombine and provided that the energetic requirements are fulfilled, they can be easily transferred to the electron and hole acceptors. As a result, the recombination rate of the photogenerated electrons and holes decreases with a decrease of the particle size and therefore, higher quantum yields compared to bigger particles are expected. The quantum yield of a photocatalytic reaction is a function of the transfer rate at the interface, the recombination rate inside the particle and the transit time⁵². Basically, the average transit time for the charge carrier trapping (τ_{tr}) within a particle with radius R is obtained from solving the Fick's law of diffusion as following⁵³:

6. Summarizing Discussion

$$\tau_{tr} = R^2/\pi^2D \quad (6.21)$$

in which D is the diffusion coefficient. The typical values of R and D are 10 nm and $0.1 \text{ cm}^2 \text{ s}^{-1}$, respectively. Considering these values, the average transit time will be about 1 ps. This value is much shorter than the recombination time of the charge carriers. Therefore, in particles with smaller size, most of the charge carriers can reach the surface before recombination⁵².

Therefore, the small particle size (8 nm) of pure anatase in Hombikat UV 100 exhibits better utilization of light in comparison with P25 which has bigger particle sizes (22 nm)⁵⁴. Smaller particle sizes of Hombikat UV 100 can also result in a balance between the bulk and surface recombination of charge carriers leading to higher photonic efficiencies⁵⁵. Zhang *et al.* have already shown that the particle size is a factor which plays a significant role for the charge carrier recombination and 10 nm seems to be an optimal size of pure TiO_2 photocatalysts in liquid phase for the decomposition of chloroform⁵⁶.

On the other hand, big particles of P25 are able to absorb a higher number of photons leading to high light intensity spots and superior recombination rates of charge carriers (**Figure 6.4**). The difference in the quantum yield of Hombikat UV 100 and P25 results from their different physicochemical properties such as the degree of crystallinity and the surface area. Hombikat UV 100 has a surface area of $280 \text{ m}^2 \text{ g}^{-1}$ which is approximately 6 times higher than that of P25. The high surface area can lead to higher adsorption of DCA on the surface. Since the rate of a surface reaction is proportional to the surface coverage⁵⁷, according to the Langmuir-Hinshelwood rate law (**Equation 6.22**), for the particles with higher surface area higher reaction rates are expected.

$$\frac{dC}{dt} = \frac{k n_{ox} n_{os}}{V} \quad (6.22)$$

C (mol L^{-1}), t (s) and V (L) are respectively, the concentration of the probe molecule in the suspension, the time, and the total reaction volume. k ($\text{mol}^{-1} \text{ s}^{-1}$) is the rate constant of the photocatalytic reaction and n_{ox} (mol) and n_{os} (mol) are the amount of oxidizing species at the photocatalyst surface and the amount of occupied sites, respectively.

Furthermore, Otalvaro-Marin *et al.* have reported the average extinction coefficient (β) values of $5.71 \times 10^4 \text{ cm}^2 \text{ g}^{-1}$ and $2.64 \times 10^4 \text{ cm}^2 \text{ g}^{-1}$ between 280 to 395 nm for Degussa P25 and Hombikat UV 100, respectively. Extinction coefficient (β) was defined as the sum of

the average values of the absorption coefficient (κ) and the scattering coefficient (σ). This parameter was used to calculate the scattering albedo coefficient ($\omega = \sigma_{\text{average}} / \beta$) which determines the fraction of dispersed energy. Hombikat UV100 was found to have a lower average absorption coefficient ($\kappa = 1.17 \times 10^3 \text{ cm}^2 \text{ g}^{-1}$) and a higher scattering albedo coefficient ($\omega = 0.96$) compared to P25. Accordingly, for Hombikat UV100 most of the photons are dispersed in a larger layer of the suspension with a photon absorption rate slower than P25⁵⁸.

6.4. A Standard Method for the Comparison of the Photocatalytic Activities of Semiconducting Materials

The validity of the proposed idea of comparing the activity of different photocatalysts in a black body reactor with the reaction rate defined as the number of converted molecules per time, is also supported by measurements of the photocatalytic activity of nine other photocatalysts namely, anatase, rutile, a mixture of rutile and anatase (P25), brookite, surface modified anatase (KRONOClean 7000), SrTiO₃, BaTiO₃, WO₃, and ZnO. The following experimental conditions were applied: I) $c_0 = 5 \text{ mM}$, $\gamma = 5 \text{ g L}^{-1}$, $V = 400 \text{ mL}$; II) $c_0 = 10 \text{ mM}$, $\gamma = 5 \text{ g L}^{-1}$, $V = 400 \text{ mL}$; III) $c_0 = 10 \text{ mM}$, $\gamma = 7 \text{ g L}^{-1}$, $V = 600 \text{ mL}$. The results confirmed that for each of these catalysts the obtained quantum yield was constant and independent from the variation of the mentioned experimental conditions (**Figure 6.5**). These investigations demonstrated that anatase (Hombikat UV 100) exhibits the highest photocatalytic activity for DCA degradation confirming the common notion of the high photocatalytic activity of anatase^{13,20}. Hombikat UV 100 enhances the photodegradation of DCA due to its high surface area which favors the adsorption of polar molecules such as DCA on the surface. The activity of this catalyst was two times higher than that of P25. Rutile exhibited a low photocatalytic activity, which is in good agreement with the literature^{25,59}. However, brookite revealed a better photocatalytic activity as compared with P25. Similar observations have been reported by Kandiel *et al.*¹⁵. KRONOClean 7000, a visible-light active carbon modified anatase TiO₂, showed almost a similar activity to P25 while SrTiO₃ and BaTiO₃ had lower activities than P25. In agreement with the obtained results, ZnO and WO₃ are also known to be non-efficient photocatalysts in comparison with P25⁶⁰⁻⁶².

The obtained reaction rate confirmed that under sufficiently high optical density of the reaction slurry and suitably large concentrations of the probe molecule, the reaction rate

6. Summarizing Discussion

being defined on an amount basis is constant for each semiconductor. This value is independent from the mass concentration of the catalyst, from the initial concentration of DCA, and from the reaction volume.

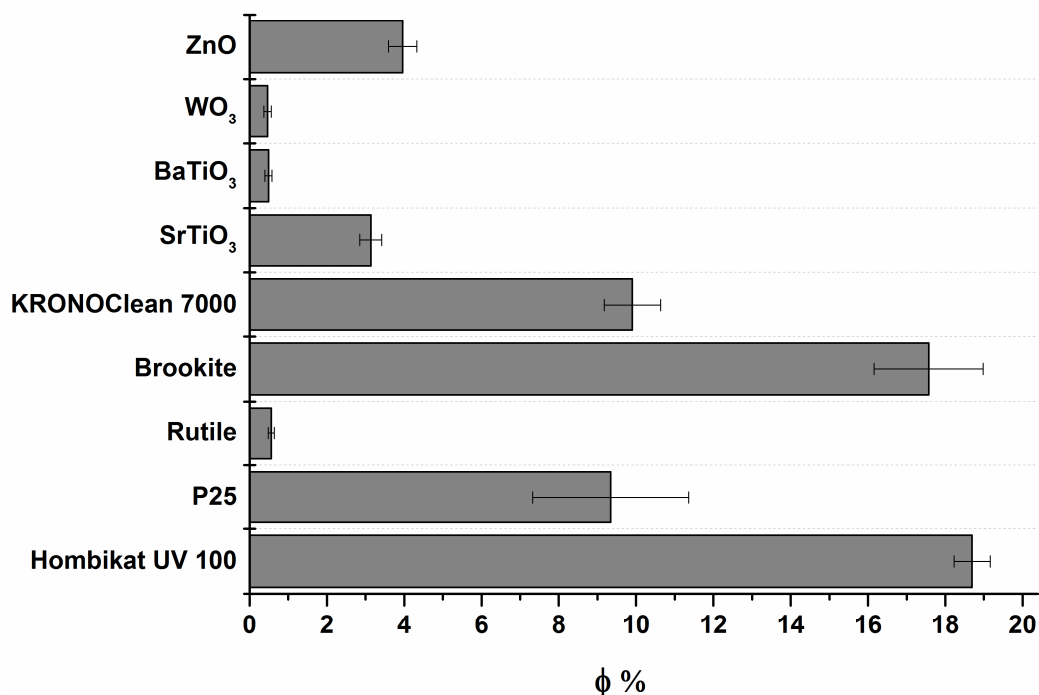


Figure 6.5. Average value of the quantum yield for different photocatalysts. Experimental conditions: A) $c_0 = 5$ mM, $\gamma = 5$ g L⁻¹, $V = 400$ mL; B) $c_0 = 10$ mM, $\gamma = 5$ g L⁻¹, $V = 400$ mL; C) $c_0 = 10$ mM, $\gamma = 7$ g L⁻¹, $V = 600$ mL. Photon flux = $10.7 \mu\text{mol min}^{-1}$, pH 3, 10 mmol L^{-1} KNO₃, air saturated, ambient temperature.

Degradation of DCA at pH 3 was also investigated by Hufschmidt *et al.*⁵⁴. Assuming zero order kinetics for the degradation of DCA, photonic efficiencies of 12.2 % and 8.1 % were reported for pure Hombikat UV100 and P25, respectively. Comparing the obtained quantum yields for Hombikat UV100 ($\Phi = 18.9$ %) and P25 ($\Phi = 9.4$ %) by applying the proposed method in the current work confirms that the incident light is utilized more efficiently by a black body reactor than in reactors having a positive irradiation geometry. This is mainly because in a black body reactor almost all the light is absorbed by the photocatalyst and the loss of light due to the back reflection is almost zero. Consequently, the quantum yield in the black body reactor is approximately equal to the photonic efficiency which has a higher value in comparison with other photoreactors. Efficient

utilization of the incident light in a black body reactor can also be proved through comparison of the reported efficiencies by Menendez-Flores *et al.* and the obtained results through the black body reactor. They have examined P25 for the photodegradation of DCA at pH 3 reporting the photonic efficiency to be 2.83 %¹⁷. However, in the current study, the obtained quantum yield for P25 in a black body reactor was found to be about 9.4 % which is approximately 3 times higher than the reported value.

Lindner *et al.* have reported the photocatalytic activity of Hombikat UV 100 in terms of photonic efficiency to be about four times higher than P25²⁰. Employing similar conditions as compared to our experimental work, the photonic efficiency of Hombikat UV 100 for DCA degradation was reported to be around 22 %, while P25 showed a maximum photonic efficiency of approximately 5 %. They also reported that in case of P25, the photonic efficiency showed constant behavior for catalyst concentrations higher than 0.5 g L⁻¹. However, in case of Hombikat UV 100 the photonic efficiency was not independent from the catalyst concentration even at high concentrations of the catalyst (10 g L⁻¹). This behavior of UV 100 is explained through aggregates of small particles of UV 100 which results in a blue shifted absorption spectrum at identical catalyst concentration due to the different absorptivity and scattering properties²⁰.

It should be mentioned that this difference between the obtained results and the reported data for DCA degradation can be due to the differences between the applied photocatalysts. Depending on the production batch of the photocatalyst and its position in a package, the reported results might differ between from different laboratories⁶³. These variations can significantly influence the number of absorbed photons and the recombination rate of the charge carriers⁶⁴.

On the other hand, Minero and Vione have investigated the degradation of phenol employing two TiO₂ photocatalysts, namely Degussa P25 and pure anatase named TiO₂ Wackherr. These authors observed a higher photocatalytic activity of pure anatase (Wackherr) by a factor of about 2 compared to the corresponding data of Degussa P25 under similar conditions⁶⁵. These observations are in good agreement with results obtained in the current work. The higher efficiency of pure anatase (Wackherr TiO₂) was explained by Minero and Vione through slower surface charge-carrier-recombination processes, different chemical reactivity and a lower scattering coefficient of the Wackherr TiO₂. An increase in radiation absorption of Wackherr TiO₂ by increasing the photocatalyst loading was reported, implying that the photocatalyst loading and the

6. Summarizing Discussion

reactor geometry strongly affect the photocatalytic efficiency⁶⁵. In contrast, in the current work, the efficiency of the photocatalyst was independent from the photocatalyst loading and the reactor geometry, since all experimental runs were performed in a black body reactor at sufficient high loadings of the photocatalyst and it revealed zero order kinetics and independent conditions.

Comparison of the results obtained in the current study with literature values confirms the validity of the proposed method. For instance, higher activity of brookite as compared to P25 for the degradation of organic compounds has also been reported by Lin *et al.*⁶⁶ A composite of brookite and rutile was also used for the photocatalytic degradation of phenol under UV-irradiation by Cao *et al.*, showing that the composite with the highest brookite content had a higher activity than composites with lower brookite content. The reaction rate of the composite with 72 % brookite was three times bigger than that of P25⁶⁷.

SrTiO₃ and BaTiO₃ catalysts are known not to be proper photocatalysts for the decomposition of organic compounds^{68,69}. According to Ahuja *et al.*, SrTiO₃ does not show a high photocatalytic activity for the degradation of phenol upon UV irradiation. Reaction rates of phenol degradation were found to be extremely low and only about 5 % of phenol was degraded within 90 minutes of irradiation⁶⁹. The photocatalytic activity of BaTiO₃ was also reported to be very low for methyl orange and methylene blue removal upon UV illumination⁷⁰. However, KRONOClean 7000 illustrated a slightly higher photocatalytic activity than P25 for degradation of hexane as reported by Moulis and Krysa⁷¹ which is similar to the observations of the current study.

According to the research carried out by Liao *et al.*, for the degradation of formaldehyde⁷², the reaction rate constant of ZnO was two orders of magnitude smaller than that of TiO₂ confirming the validity of the obtained results from the current work. The decomposition rate of 4-chlorophenol per unit mass of catalyst by ZnO and P25 was also reported by Hariharan⁶⁰. The photocatalytic activity of bulk ZnO was almost half of P25 and once again a similar result was observed in this work.

Therefore, the outcome of the present study is essential for the comparison of the photocatalytic activities of different semiconductors. It is of high importance to measure the reaction rate under zero order conditions considering the initial concentration of the model compound, the photocatalyst loading, and the reaction volume. Based on the proposed idea, using a black body reactor, all the incoming photons are absorbed by the

photocatalyst and the reaction rate on an amount basis can be easily correlated under constant photon flux. This method is a simple and applicable approach to compare the photocatalytic activities of different semiconductors and it can answer some open questions in the field of semiconductor photocatalysis.

A method proposed by Qureshi and Takanabe suggests to compare the intrinsic activities of various photocatalysts employing their photonic efficiencies considering the incident photon flux, the optimal rate, and the reaction rate⁷³. These authors also highly recommend to report a list of factors including the reactant conversion rate or the product evolution rate, the incident photon flux as a function of the wavelength, the type of lamp and filters, the activities or the partial pressures of reactants and sacrificial reagents, the type of solution, the supporting electrolyte concentration, the pH, the amount of photocatalyst, the amount of co-catalyst, the amount of solution, the flow rate inside the reactor, the reactor volume and its dimensions (with photographs)⁷³.

Buriak *et al.* have also suggested to report the quantum efficiency together with all related measurement conditions including the catalyst loading, the light source, and the wavelength distribution, the optical irradiance at the sample and the substrate concentration⁷⁴. Moreover, statistics and error analysis should also be included to provide an idea regarding the claimed materials improvements and the experimental error⁷⁴.

6.5. Photocatalytic Reactor Design

In a photocatalytic reaction the photon absorption process is the main step which is proportional to the local volumetric rate of energy absorption (LVREA). Therefore, the initiation reaction can be defined as:

$$R_{init,\lambda} = \Phi_{prim,\lambda} e_{\lambda}^a \quad (6.23)$$

in which e_{λ}^a is the spectral local volumetric rate of photon absorption which presents the absorbed photons in an elementary volume of radiation absorption as following⁷⁵:

$$e_{\lambda}^a(x, t) = \int_{\lambda_1}^{\lambda_2} k_{\lambda}(x, t) G_{\lambda}(x, t) d\lambda = \int_{\lambda_1}^{\lambda_2} \int_{\varphi_1}^{\varphi_2} \int_{\theta_1}^{\theta_2} k_{\lambda}(x, t) I_{\lambda}(x, \theta, \varphi, t) \sin\theta d\theta d\varphi d\lambda \quad (6.24)$$

6. Summarizing Discussion

where k_λ is the absorption coefficient, λ is the wavelength, x is the position, and t is the time. I_λ , the radiation field, is the amount of radiative energy per unit wavelength interval, per unit solid angle, per unit normal area, and per unit time. For a given wavelength, I is a function of position (x), direction (Ω), and time (t) and can be presented as follows⁷⁵:

$$I_\lambda(x, \Omega, t) = \frac{dE_\lambda}{dA \cos\theta d\Omega d\lambda dt} \quad (6.25)$$

G_λ is the spectral incident radiation defined by **Equation 6.26** which is a radiation property for the consideration of the radiation arriving at one point inside a photoreactor from all directions in space⁷⁵:

$$G_\lambda(x, t) = \int_\Omega I_\lambda(x, \Omega, t) d\Omega = \int_{\varphi_1}^{\varphi_2} \int_{\theta_1}^{\theta_2} I_\lambda(x, \theta, \varphi, t) \sin\theta d\theta d\varphi \quad (6.26)$$

In case of having a polychromatic radiation, an integration over the applicable range of wavelengths results in the polychromatic incident radiation G as following⁷⁵:

$$G_\lambda(x, t) = \int_{\lambda_1}^{\lambda_2} \int_{\varphi_1}^{\varphi_2} \int_{\theta_1}^{\theta_2} I_\lambda(x, \theta, \varphi, t) \sin\theta d\theta d\varphi d\lambda \quad (6.27)$$

In order to calculate the LVREA, the concept of the photon transport equation must be introduced. Assuming an elemental volume V in space with an absorbing, emitting and scattering medium, the photons with a flight path lying within the solid angle of propagation $d\Omega$ which transport radiant energy of wavelength λ are called the Ω, λ photons. Accordingly the photon transport equation can be written as⁷⁵:

$$\left[\begin{array}{l} \text{Time rate of} \\ \text{change of } \Omega, \lambda \\ \text{photons in the} \\ \text{volume } V \end{array} \right] + \left[\begin{array}{l} \text{Net flux of } \Omega, \lambda \\ \text{photons within the} \\ \text{volume } V \text{ across} \\ \text{the surface } A \end{array} \right] = \left[\begin{array}{l} \text{Net gain of } \Omega, \lambda \text{ photons} \\ \text{owing to emission, absorption,} \\ \text{inscattering and outscattering} \\ \text{in the volume } V \end{array} \right] \quad (6.28)$$

Therefore, as mentioned in **Chapter 1** the RTE equation can be written as follows⁷⁵:

$$\frac{1}{c} \frac{\partial I_{\Omega, \nu}}{\partial t} + \nabla \cdot (I_{\Omega, \nu} \Omega) = -W_{\Omega, \nu}^{\text{absorption}} + W_{\Omega, \nu}^{\text{emission}} + W_{\Omega, \nu}^{\text{in-scattering}} - W_{\Omega, \nu}^{\text{out-scattering}} \quad (6.29)$$

A simplifying assumption is that the factor $1/c$ is very low, thus the first term on the left in this equation can be neglected. Thus, at a given time the radiation field can reach the steady state instantaneously⁷⁵:

$$\frac{1}{c} \frac{\partial I_{\Omega,\lambda}}{\partial t} \cong 0 \quad (6.30)$$

Moreover, the term $W_{\Omega,\nu}^{\text{emission}}$ can also be neglected as the radiation emission is only significant at high temperatures. Therefore, the RTE can be given as^{75,76}:

$$\begin{aligned} \frac{dI_{\Omega,\lambda}(s,t)}{ds} = & [k_{\lambda}(s,t) + \sigma_{\lambda}(s,t)]I_{\Omega,\lambda}(s,t) \\ & + \frac{\sigma_{\lambda}(s,t)}{4\pi} \int_{4\pi} p_{\lambda}(\hat{\Omega} \rightarrow \Omega) I_{\hat{\Omega},\lambda}(s,t) d\hat{\Omega} \end{aligned} \quad (6.31)$$

This equation can also be presented using the two common definitions of the spectral extinction coefficient (β_{λ}) and the spectral albedo (ω_{λ}). The extinction coefficient is the sum of the absorption coefficient and the scattering coefficient (**Equation 6.32**) and the spectral albedo is the ratio of the scattering coefficient to the extinction coefficient (**Equation 6.33**)⁷⁶.

$$\beta_{\lambda}(x,t) = k_{\lambda}(x,t) + \sigma_{\lambda}(x,t) \quad (6.32)$$

$$\omega_{\lambda}(x,t) = \frac{\sigma_{\lambda}(x,t)}{\beta_{\lambda}(x,t)} \quad (6.33)$$

In a homogenous media, the radiation reaches any point in the reaction space from a light source emitting in all directions. Assuming to have no emission and no scattering, the RTE can be given as⁷⁶:

$$\frac{dI_{\lambda}(s,\Omega,t)}{ds} = -k_{\lambda}(s,t)I_{\lambda}(s,\Omega,t) \quad (6.34)$$

Under normal conditions radiation will reach a point at location (x) in the photoreactor following a light path characterized by the directional coordinate, $s(x,\theta,\phi)$. Along its path, the radiation will be reduced by absorption. Radiation from the lamp reaches the reactor wall at a point where $s = s_R$. Thus, considering this boundary condition at the entrance point⁷⁶:

$$I_{\lambda}(s_R,\Omega,t) = I_{\lambda}^0(\Omega,t) = I_{\lambda}^0(\theta,\phi,t) \quad (6.35)$$

By an integration of this equation from the entrance point at the reactor wall ($s=s_R$) to the considered point ($s=s$) the following correlation will be derived⁷⁶:

$$I_{\lambda}(x,\theta,\phi,t) = I_{\lambda}^0(\theta,\phi,t) \exp\left[-\int_{\bar{s}=s_R}^{\bar{s}=s(x,\theta,\phi)} k_{\lambda}(\bar{s},t) d\bar{s}\right] \quad (6.36)$$

6. Summarizing Discussion

Therefore, the LVREA for a homogeneous system can be given as the following equation⁷⁶:

$$e_{\lambda}^a(x, t) = k_{\lambda}(x, t) \int_{4\pi} I_{\lambda}(x, \theta, \phi, t) d\Omega \quad (6.37)$$

However, in photocatalytic heterogeneous systems, scattering is significant and cannot be neglected. Assuming that the changes in the direction of flight are the main scattering effects, a pseudo-homogeneous system can be considered⁷⁶:

$$\frac{dI_{\lambda}(s, \Omega, t)}{ds} + [k_{\lambda}(s, t) + \sigma_{\lambda}(s, t)]I_{\lambda}(s, \Omega, t) = \frac{\sigma_{\lambda}(s, t)}{4\pi} \int_{4\pi} I_{\lambda}(s, \Omega', t) p(\Omega' \rightarrow \Omega) d\Omega' \quad (6.38)$$

By an integration of this correlation from the entrance point at the reactor wall ($s=s_R$) to the considered point ($s=s$) the following equations will be derived⁷⁶:

$$I_{\lambda}(s, \Omega, t) = I_{\lambda}^0(s_R, \Omega, t) \exp\left\{-\int_{s_R}^s [k_{\lambda}(\bar{s}, t) + \sigma_{\lambda}(\bar{s}, t)] d\bar{s}\right\} + \int_{s_R}^s \left[\frac{\sigma_{\lambda}(\bar{s}, t)}{4\pi} \int_{4\pi} I_{\lambda}(\bar{s}, \Omega', t) p(\Omega' \rightarrow \Omega) d\Omega'\right] \exp\left[-\int_{\bar{s}}^s [k_{\lambda}(\bar{s}, t) + \sigma_{\lambda}(\bar{s}, t)] d\bar{s}\right] d\bar{s} \quad (6.39)$$

$$I_{\lambda}(x, \theta, \phi, t) = I_{\lambda}^0(\theta, \phi, t) \exp\left\{-\int_{s_R}^{s(x, \theta, \phi)} [k_{\lambda}(\bar{s}, t) + \sigma_{\lambda}(\bar{s}, t)] d\bar{s}\right\} + \int_{s_R}^{s(x, \theta, \phi)} \left[\frac{\sigma_{\lambda}(\bar{s}, t)}{4\pi} \int_{\phi=0}^{2\pi} d\phi \int_{\theta=0}^{\pi} \sin\theta d\theta I_{\lambda}(\bar{x}, \theta', \phi', t) p(\theta', \phi' \rightarrow \theta, \phi)\right] \exp\left\{-\int_{\bar{s}}^{s(x, \theta, \phi)} [k_{\lambda}(\bar{s}, t) + \sigma_{\lambda}(\bar{s}, t)] d\bar{s}\right\} d\bar{s} \quad (6.40)$$

The first term in **Equation 6.39** represents the extinction of the incoming radiation from the light source. The second term in this equation is the extinction of the radiation integrated into the direction Ω by in-scattering.

Finally, the LVRAP in heterogeneous photocatalytic systems can be written as⁷⁶:

$$e_{\lambda}^a(x, t) = k_{\lambda}(x, t) \left\{ \int_{\Omega_s} I_{\lambda}^0(s_R, \Omega, t) \exp\left[-\int_{s_R}^{s(x, \theta, \phi)} (k_{\lambda} + \sigma_{\lambda}) d\bar{s}\right] d\Omega \right\} + k_{\lambda}(x, t) \int_{4\pi} \left\{ \int_{s_R}^{s(x, \theta, \phi)} \frac{\sigma_{\lambda}}{4\pi} \left[\int_{4\pi} \int_{\theta=0}^{\pi} I_{\lambda}(\bar{x}, \Omega', t) p(\Omega' \rightarrow \Omega) d\Omega' \right] \exp\left[-\int_{\bar{s}}^{s(x, \theta, \phi)} (k_{\lambda} + \sigma_{\lambda}) d\bar{s}\right] d\bar{s} \right\} d\Omega \quad (6.41)$$

$$\begin{aligned}
e_{\lambda}^a(x, t) = & k_{\lambda}(x, t) \int_{\phi_1}^{\phi_2} d\phi \int_{\theta_1(\phi)}^{\theta_2(\phi)} d\theta \sin\theta I_{\lambda}^0(\theta, \phi, t) \exp \left\{ - \int_{s_R}^{s(x, \theta, \phi)} [k_{\lambda}(\bar{s}, t) + \sigma_{\lambda}(\bar{s}, t)] d\bar{s} \right\} \\
& + k_{\lambda}(x, t) \int_{\phi=0}^{2\pi} d\phi \int_{\theta=0}^{\pi} \sin\theta d\theta \left\{ \int_{s_R}^{s(x, \theta, \phi)} \frac{\sigma_{\lambda}(\bar{s}, t)}{4\pi} \left[\int_{\phi'=0}^{2\pi} d\phi' \int_{\theta'=0}^{\pi} \sin\theta' d\theta' I_{\lambda}(\bar{x}, \theta', \phi', t) p(\theta', \phi' \rightarrow \right. \right. \\
& \left. \left. \theta, \phi \exp -s(x, \theta, \phi) s(x, \theta, \phi) k_{\lambda} s, t + \sigma_{\lambda} s, t ds ds \right. \right. \quad (6.42)
\end{aligned}$$

For solving the RTE, several methods have been proposed such as the two-flux method, the exponential kernel approximation, the spherical harmonics method, and the six-flux method. However, the most common numerical techniques of solving the RTE are the discrete ordinate (DO) method, the Monte Carlo (MC) method and the finite volume (FV) method⁷⁵.

A simplified one-dimensional description with detailed calculations, gives a better idea for the understanding of the complex three-dimensional radiation field inside a photoreactor. Herein, the two-flux approximation is applied. The two-flux approximation method includes scattering and absorption phenomena. Nevertheless, it simplifies the related calculations by considering the scattering only in one direction, which is the direction opposite to the incident light.

In this case the RTE can be solved considering the forward and backward light intensity as follows⁷⁷:

$$e_a = \beta I_0 a (b e^{\beta x} + c e^{-\beta x}) \quad (6.43)$$

$$a = [(1 + u)\omega]^{-1} \quad (6.44)$$

$$b = u[1 - \omega + (1 - \omega^2)^{1/2}] \quad (6.45)$$

$$c = -1 + \omega + (1 - \omega^2)^{1/2} \quad (6.46)$$

In these equations, a , b , and c are dimensionless coefficients dependent on the scattering albedo (ω) and the optical thickness (τ). This dependency is described as follows:

$$u = e^{-2\tau} [-1 + (1 - \omega^2)^{1/2}] / [1 + (1 - \omega^2)^{1/2}] \quad (6.47)$$

The optical thickness defined as $\tau = \beta L$ is a dimensionless parameter. The possible amount of scattering and absorption through the whole length of the reactor in the direction of incident photons (L) can be signified through this parameter. The light penetration outside the reactor (to the opposite side of the light source) is negligible in

6. Summarizing Discussion

case of having a thick reactor⁷⁸. Therefore the term u and consequently the term b in **Equation 6.43** will be approximately zero. Thus the resulting correlation resembles the common Lambert–Beer exponential decay.

On the other hand, in a thin reactor the light not only scatters back to the light source but also scatters out to the opposite side of the light source through transmitting out of the reactor. Therefore the term b does not tend to zero and the equation will be more complicated.

In a black body photoreactor, the back reflection of photons through the light inlet, as well as the transmitted light outside the photoreactor are negligible. Therefore, the Lambert–Beer law for the calculation of local volumetric rate of energy absorption in a black body photoreactor can be applied.

For the development of kinetic analysis, in addition to the quantum yield, the rate of photon absorption per volume is also required (i.e., $r = \Phi e_{\lambda}^a$). By using the volume-averaged values of these parameters, the rate of the reaction can be derived from the experimental data. However, the gradient in rate of photon absorption inside the reactor has to be also taken into account. Therefore, the volume-averaged quantum yield value inside the photoreactor can be used for calculating the reaction rate in every position of the reactor volume.

6.6. Conclusions

For the development of new and highly active photocatalytic materials, a standard approach to evaluate their activities is essential. The results presented in this work describe a newly developed method for the comparison of the photoactivity of different photocatalysts in heterogeneous systems. Obviously, the common comparison methods are not only unable to measure the number of photons absorbed by the photocatalyst, but also require too many information and values to be reported. However, applying a black body photoreactor for the photocatalytic comparison, in addition to the simplicity and the sufficient utilization of the incident light, does not need so many further information since it is independent from effecting parameters such as the initial concentration of the model compound, the catalyst loading, the reaction volume, the reactor geometry, and the photon flux provided that the photon density inside the reactor is low. To summarize, in

order to compare the intrinsic activity of various photocatalyst materials between different laboratories, the following key factors are suggested to be considered:

- Constant values of temperature, pH, ionic strength, and photon flux
- Utilizing a black body reactor
- Adequate loading of the catalyst providing no light transmission out of the reactor and reaction rates independent from the catalyst concentration
- High enough initial concentrations of the probe molecule leading to zero order kinetics
- Comparison of the reaction rates defined on an amount basis

In case of a known photon flux, the quantum yield of various materials can also be easily evaluated.

The purpose of this work was to provide a method with simple guidelines to be able to properly measure kinetic data and the absorbed amount of photons in photoreactors in order to determine the quantum yield. In contrast to the kinetic data of photoreactors that is usually leveled out by mixing, the rate of photon absorption is non-homogeneous and requires the time consuming calculation of RTE. Solving the RTE is complicated when the possibility of scattering in every direction at each position should be considered. However, considering the properties of the black body photoreactor suggested in this work, the amount of backscattered light out of the photoreactor is almost zero. Moreover, in this photoreactor almost no photons are transmitted out of the photoreactor. As a result, the Lambert–Beer (L–B) law adequately describes the local light intensity in the photoreactor, from which local volumetric rate of photon absorption is readily obtained as the gradient of light intensity in its direction of propagation.

In all the photoreactors, the photon absorption in the area near to the light source is high and it decreases with increasing distance from the light source. These gradients are the main obstacles to use simple kinetic interpretations of the data. However, using the volume-averaged value of photon absorption is a useful simplification. Therefore, the optical reactor characteristics and the operation procedures which are appropriate for the measurement of the quantum yield and the development of kinetic expressions are needed.

6. Summarizing Discussion

Determination of quantum yields through the methods suggested in the present work, simplifies the design of photoreactors. Accordingly, the reaction rate at any position of the reactor can be calculated. This is possible by employing the volume-averaged quantum yield and the local volumetric rate of photon absorption. The local volumetric rate of photon absorption has to be computed through the resolution of the RTE, by having the optical properties of the semiconductor inside the reactor. The values of the quantum yield of the photocatalytic process are of high importance in optimization of the photoreactor. Therefore, the proposed method in this work contributes to the development of efficient photoreactor designs with further perspective of large applications.

6.7. References

- (1) Cassano, A. E.; Alfano, O. M. Design and Analysis of Homogeneous and Heterogeneous Photoreactors. In *Chemical Engineering: Trends and Developments*; Galán, M. A., Valle, E. M. del, Eds.; John Wiley & Sons, Inc., 2005; Vol. 4, pp 125–169.
- (2) Braslavsky, S. E.; Braun, A. M.; Cassano, A. E.; Emeline, A. V.; Litter, M. I.; Palmisano, L.; Parmon, V. N.; Serpone, N. Glossary of Terms Used in Photocatalysis and Radiation Catalysis (IUPAC Recommendations 2011). *Pure Appl. Chem.* **2011**, *83*, 931–1014.
- (3) Pareek, V.; Adesina, A. Light Intensity Distribution in Photocatalytic Reactors Using a Finite Volume Method. *AIChE J.* **2004**, *50*, 1273–1288.
- (4) Brandi, R. J.; Alfano, O. M.; Cassano, A. E. Evaluation of Radiation Absorption in Slurry Photocatalytic Reactors. 2. Experimental Verification of the Proposed Method. *Environ. Sci. Technol.* **2000**, *34*, 2631–2639.
- (5) Matos, J.; Ocares-Riquelme, J.; Poon, P. S.; Montaña, R.; García, X.; Campos, K.; Hernández-Garrido, J. C.; Titirici, M. M. C-Doped Anatase TiO₂: Adsorption Kinetics and Photocatalytic Degradation of Methylene Blue and Phenol, and Correlations with DFT Estimations. *J. Colloid Interface Sci.* **2019**, *547*, 14–29.
- (6) Luo, S.; Xu, J.; Li, Z.; Liu, C.; Chen, J.; Min, X.; Fang, M.; Huang, Z. Bismuth Oxyiodide Coupled with Bismuth Nanodots for Enhanced Photocatalytic Bisphenol A Degradation: Synergistic Effects and Mechanistic Insight. *Nanoscale* **2017**, *9*, 15484–15493.
- (7) Nair, R. G.; Mazumdar, S.; Modak, B.; Bapat, R.; Ayyub, P.; Bhattacharyya, K. The Role of Surface O-Vacancies in the Photocatalytic Oxidation of Methylene Blue by Zn-Doped TiO₂: A Mechanistic Approach. *J. Photochem. Photobiol. A Chem.* **2017**, *345*, 36–53.
- (8) Mills, A.; Wang, J. Photobleaching of Methylene Blue Sensitised by TiO₂: An Ambiguous System? *J. Photochem. Photobiol. A Chem.* **1999**, *127*, 123–134.
- (9) Hosseini, S. N.; Borghei, S. M.; Vossoughi, M.; Taghavinia, N. Immobilization of TiO₂ on Perlite Granules for Photocatalytic Degradation of Phenol. *Appl. Catal. B Environ.* **2007**, *74*, 53–62.
- (10) Wang, X.; Sun, Y.; Yang, L.; Shang, Q.; Wang, D.; Guo, T.; Guo, Y. Novel Photocatalytic System Fe-Complex/TiO₂ for Efficient Degradation of Phenol and Norfloxacin in Water. *Sci. Total Environ.* **2019**, *656*, 1010–1020.
- (11) Wu, C.; Liu, X.; Wei, D.; Fan, J.; Wang, L. Photosonochemical Degradation of Phenol in Water. *Water Res.* **2001**, *35*, 3927–3933.
- (12) Kim, D.; Lee, D.; Monllor-Satoca, D.; Kim, K.; Lee, W.; Choi, W. Homogeneous Photocatalytic Fe³⁺/Fe²⁺ Redox Cycle for Simultaneous Cr(VI) Reduction and Organic Pollutant Oxidation: Roles of Hydroxyl Radical and Degradation

6. Summarizing Discussion

- Intermediates. *J. Hazard. Mater.* **2019**, *372*, 121–128.
- (13) Lindner, M.; Theurich, J.; Bahnemann, D. W. Photocatalytic Degradation of Organic Compounds: Accelerating the Process Efficiency. *Water Sci. Technol.* **1997**, *35*, 79–86.
 - (14) Dillert, R.; Cassano, A. E.; Goslich, R.; Bahnemann, D. Large Scale Studies in Solar Catalytic Wastewater Treatment. *Catal. Today* **1999**, *54*, 267–282.
 - (15) Kandiel, T. A.; Feldhoff, A.; Robben, L.; Dillert, R.; Bahnemann, D. W. Tailored Titanium Dioxide Nanomaterials: Anatase Nanoparticles and Brookite Nanorods as Highly Active Photocatalysts. *Chem. Mater.* **2010**, *22*, 2050–2060.
 - (16) Pupo Nogueira, R. F.; Guimarães, J. R. Photodegradation of Dichloroacetic Acid and 2,4-Dichlorophenol by Ferrioxalate/H₂O₂ System. *Water Res.* **2000**, *34*, 895–901.
 - (17) Menéndez-Flores, V. M.; Friedmann, D.; Bahnemann, D. W. Durability of Ag-TiO₂ Photocatalysts Assessed for the Degradation of Dichloroacetic Acid. *Int. J. Photoenergy* **2008**, *2008*, 11 pages.
 - (18) Zalazar, C. S.; Romero, R. L.; Martín, C. A.; Cassano, A. E. Photocatalytic Intrinsic Reaction Kinetics I: Mineralization of Dichloroacetic Acid. *Chem. Eng. Sci.* **2005**, *60*, 5240–5254.
 - (19) Bahnemann, D. W.; Kholuiskaya, S. N.; Dillert, R.; Kulak, A. I.; Kokorin, A. I. Photodestruction of Dichloroacetic Acid Catalyzed by Nano-Sized TiO₂ Particles. *Appl. Catal. B Environ.* **2002**, *36*, 161–169.
 - (20) Lindner, M.; Bahnemann, D. W.; Hirthe, B.; Griebler, W.-D. Solar Water Detoxification: Novel TiO₂ Powders as Highly Active Photocatalysts. *J. Sol. Energy Eng.* **1997**, *119*, 120–125.
 - (21) Ballari, M. M. D. L.; Alfano, O. O.; Cassano, A. E. Photocatalytic Degradation of Dichloroacetic Acid. A Kinetic Study with a Mechanistically Based Reaction Model. *Ind. Eng. Chem. Res.* **2009**, *48*, 1847–1858.
 - (22) Bahnemann, D. W. Current Challenges in Photo Catalysis: Improved Photocatalysts and Appropriate Photoreactor Engineering. *Res. Chem. Intermed.* **2000**, *26*, 207–220.
 - (23) Lindner, M. Optimierung Der Photokatalytischen Wasserreinigung Mit Titan-Dioxid: Festkörper- Und Oberflächenstruktur Des Photokatalysators, Hannover University, 1997.
 - (24) Mills, A.; Le Hunte, S. An Overview of Semiconductor Photocatalysis. *J. Photochem. Photobiol. A Chem.* **1997**, *108*, 1–35.
 - (25) Hoffmann, M. R.; Martin, S. T.; Choi, W.; Bahnemann, D. W. Environmental Applications of Semiconductor Photocatalysis. *Chem. Rev.* **1995**, *95*, 69–96.
 - (26) Bahnemann, D. W.; Hilgendorff, M.; Memming, R. Charge Carrier Dynamics at

- TiO₂ Particles: Reactivity of Free and Trapped Holes. *J. Phys. Chem. B* **1997**, *101*, 4265–4275.
- (27) Zalazar, C. S.; Martin, C. A.; Cassano, A. E. Photocatalytic Intrinsic Reaction Kinetics. II: Effects of Oxygen Concentration on the Kinetics of the Photocatalytic Degradation of Dichloroacetic Acid. *Chem. Eng. Sci.* **2005**, *60*, 4311–4322.
- (28) Schuchmann, M. N.; Zegota, H.; Sonntag, C. von. Acetate Peroxyl Radicals, ·O₂CH₂CO₂⁻: A Study on the γ -Radiolysis and Pulse Radiolysis of Acetate in Oxygenated Aqueous Solutions. *Zeitschrift für Naturforsch. B* **1985**, *40*, 215–221.
- (29) Zalazar, C. S.; Labas, M. D.; Brandi, R. J.; Cassano, A. E. Dichloroacetic Acid Degradation Employing Hydrogen Peroxide and UV Radiation. *Chemosphere* **2007**, *66*, 808–815.
- (30) Chemseddine, A.; Boehm, H. P. A Study of the Primary Step in the Photochemical Degradation of Acetic Acid and Chloroacetic Acids on a TiO₂ Photocatalyst. *J. Mol. Catal.* **1990**, *60*, 295–311.
- (31) Piscopo, A.; Robert, D.; Weber, J. V. Influence of pH and Chloride Anion on the Photocatalytic Degradation of Organic Compounds: Part I. Effect on the Benzamide and Para-Hydroxybenzoic Acid in TiO₂ Aqueous Solution. *Appl. Catal. B Environ.* **2001**, *35*, 117–124.
- (32) Wang, K. H.; Hsieh, Y. H.; Wu, C. H.; Chang, C. Y. The pH and Anion Effects on the Heterogeneous Photocatalytic Degradation of O-Methylbenzoic Acid in TiO₂ Aqueous Suspension. *Chemosphere* **2000**, *40*, 389–394.
- (33) Turchi, C. S.; Ollis, D. F. Mixed Reactant Photocatalysis: Intermediates and Mutual Rate Inhibition. *J. Catal.* **1989**, *119*, 483–496.
- (34) Turchi, C. S.; Ollis, D. F. Photocatalytic Degradation of Organic Water Contaminants: Mechanisms Involving Hydroxyl Radical Attack. *J. Catal.* **1990**, *122*, 178–192.
- (35) Sagawe, G.; Satuf, M. L.; Brandi, R. J.; Muschner, J. P.; Federer, C.; Alfano, O. M.; Bahnemann, D.; Cassano, A. E. Analysis of Photocatalytic Reactors Employing the Photonic Efficiency and the Removal Efficiency Parameters: Degradation of Radiation Absorbing and Nonabsorbing Pollutants. *Ind. Eng. Chem. Res.* **2010**, *49*, 6898–6908.
- (36) Sagawe, G.; Brandi, R.; Bahnemann, D.; Cassano, A. Photocatalytic Reactors for Treating Water Pollution with Solar Illumination. I: A Simplified Analysis for Flow Reactors. *Chem. Eng. Sci.* **2003**, *58*, 2587–2599.
- (37) Liu, B.; Zhao, X.; Terashima, C.; Fujishima, A.; Nakata, K. Thermodynamic and Kinetic Analysis of Heterogeneous Photocatalysis for Semiconductor Systems. *Phys. Chem. Chem. Phys.* **2014**, *16*, 8751–8760.
- (38) Hatchard, C. G.; Parker, C. A. A New Sensitive Chemical Actinometer. II. Potassium Ferrioxalate as a Standard Chemical Actinometer. *Proc. R. Soc. A Math.*

6. Summarizing Discussion

- Phys. Eng. Sci.* **1956**, *235*, 518–536.
- (39) Hasegawa, Y.; Takahashi, K.; Kume, S.; Nishihara, H. Complete Solid State Photoisomerization of Bis(Dipyrzolylstyrylpyridine) Iron(II) to Change Magnetic Properties. *Chem. Commun.* **2011**, *47*, 6846–6848.
- (40) Ollis, D. F. Kinetics of Photocatalyzed Reactions: Five Lessons Learned. *Front. Chem.* **2018**, *6*, 1–7.
- (41) Mills, A.; O'Rourke, C.; Moore, K. Powder Semiconductor Photocatalysis in Aqueous Solution: An Overview of Kinetics-Based Reaction Mechanisms. *J. Photochem. Photobiol. A Chem.* **2015**, *310*, 66–105.
- (42) Serpone, N.; Emeline, A. V. Suggested Terms and Definitions in Photocatalysis and Radiocatalysis. *Int. J. Photoenergy* **2002**, *4*, 91–131.
- (43) Meng, Y.; Huang, X.; Wu, Y.; Wang, X.; Qian, Y. Kinetic Study and Modeling on Photocatalytic Degradation of Para-Chlorobenzoate at Different Light Intensities. *Environ. Pollut.* **2002**, *117*, 307–313.
- (44) Okamoto, K.; Yamamoto, Y.; Tanaka, H.; Itaya, A. Kinetics of Heterogeneous Photocatalytic Decomposition of Phenol over Anatase TiO₂ Powder. *Bulletin of the Chemical Society of Japan*. 1985, pp 2023–2028.
- (45) Bahnemann, D.; Bockelmann, D.; Goslich, R. Mechanistic Studies of Water Detoxification in Illuminated TiO₂ Suspensions. *Sol. Energy Mater.* **1991**, *24*, 564–583.
- (46) Kormann, C.; Bahnemann, D. W.; Hoffmann, M. R. Photolysis of Chloroform and Other Organic Molecules in Aqueous TiO₂ Suspensions. *Environ. Sci. Technol.* **1991**, *25*, 494–500.
- (47) Ollis, D. F. Photochemical Conversion and Storage of Solar Energy, IPS-8. In *Solar-assisted photocatalysis for water purification: Issues, data, questions*; Pelizzetti, E., Schiavello, M., Eds.; Palermo, Italy, 1990; pp 593–622.
- (48) Salaiques, M.; Serrano, B.; de Lasa, H. I. Photocatalytic Conversion of Organic Pollutants Extinction Coefficients and Quantum Efficiencies. *Ind. Eng. Chem. Res.* **2001**, *40*, 5455–5464.
- (49) Emeline, A. V.; Zhang, X.; Jin, M.; Murakami, T.; Fujishima, A. Application of a “Black Body” like Reactor for Measurements of Quantum Yields of Photochemical Reactions in Heterogeneous Systems. *J. Phys. Chem. B* **2006**, *110*, 7409–7413.
- (50) Bahnemann, D. W.; Bockelmann, D.; Goslich, R.; Hilgendorff, M.; Weichgrebe, D. Photocatalytic Detoxification: Novel Catalysts, Mechanisms and Solar Applications. *Photocatalytic Purif. Treat. Water Air* **1993**, 301–319.
- (51) Alfano, O.; Bahnemann, D.; Cassano, A.; Dillert, R.; Goslich, R. Photocatalysis in Water Environments Using Artificial and Solar Light. *Catal. today* **2000**, *58*, 199–230.

- (52) Memming, R. Photoreactions at Semiconductor Particles. In *Semiconductor Electrochemistry*; WILEY-VCH Verlag GmbH: Weinheim, 2000; pp 264–299.
- (53) Graetzel, M.; Frank, A. J. Interfacial Electron-Transfer Reactions in Colloidal Semiconductor Dispersions. Kinetic Analysis. *J. Phys. Chem.* **1982**, *86*, 2964–2967.
- (54) Hufschmidt, D.; Bahnemann, D.; Testa, J. J.; Emilio, C. A.; Litter, M. I. Enhancement of the Photocatalytic Activity of Various TiO₂ Materials by Platinisation. *J. Photochem. Photobiol. A Chem.* **2002**, *148*, 223–231.
- (55) Alonso-Tellez, A.; Masson, R.; Robert, D.; Keller, N.; Keller, V. Comparison of Hombikat UV100 and P25 TiO₂ Performance in Gas-Phase Photocatalytic Oxidation Reactions. *J. Photochem. Photobiol. A Chem.* **2012**, *250*, 58–65.
- (56) Zhang, Z.; Wang, C.; Zakaria, R.; Ying, J. Y. Role of Particle Size in Nanocrystalline TiO₂ -Based Photocatalysts. *J. Phys. Chem. B* **1998**, *102*, 10871–10878.
- (57) Friedmann, D.; Mendive, C.; Bahnemann, D. TiO₂ for Water Treatment: Parameters Affecting the Kinetics and Mechanisms of Photocatalysis. *Appl. Catal. B Environ.* **2010**, *99*, 398–406.
- (58) Otalvaro-Marin, H. L.; Mueses, M. A.; Machuca-Martinez, F. Boundary Layer of Photon Absorption Applied to Heterogeneous Photocatalytic Solar Flat Plate Reactor Design. *Int. J. Photoenergy* **2014**, *2014*, 8 pages.
- (59) Karakitsou, K. E.; Verykios, X. E. Effects of Altrivalent Cation Doping of Titania on Its Performance as a Photocatalyst for Water Cleavage. *J. Phys. Chem.* **1993**, *97*, 1184–1189.
- (60) Hariharan, C. Photocatalytic Degradation of Organic Contaminants in Water by ZnO Nanoparticles: Revisited. *Appl. Catal. A Gen.* **2006**, *304*, 55–61.
- (61) Chantes, P.; Jarusutthirak, C.; Danwittayakul, S. Internation Conference on Biological, Environmental and Food Engineering. In *A Comparison Study of Photocatalytic Activity of TiO₂ and ZnO on the Degradation of Real Batik Wastewater*; 2015; pp 8–12.
- (62) Mrowetz, M.; Selli, E. Photocatalytic Degradation of Formic and Benzoic Acids and Hydrogen Peroxide Evolution in TiO₂ and ZnO Water Suspensions. *J. Photochem. Photobiol. A Chem.* **2006**, *180*, 15–22.
- (63) Ohtani, B.; Prieto-Mahaney, O. O.; Li, D.; Abe, R. What is Degussa (Evonic) P25? Crystalline Composition Analysis, Reconstruction from Isolated Pure Particles and Photocatalytic Activity Test. *J. Photochem. Photobiol. A Chem.* **2010**, *216*, 179–182.
- (64) Satuf, M. L.; Brandi, R. J.; Cassano, A. E.; Alfano, O. M. Experimental Method to Evaluate the Optical Properties of Aqueous Titanium Dioxide Suspensions. *Ind. Eng. Chem. Res.* **2005**, *44*, 6643–6649.

6. Summarizing Discussion

- (65) Minero, C.; Vione, D. A Quantitative Evaluation of the Photocatalytic Performance of TiO₂ Slurries. *Appl. Catal. B Environ.* **2006**, *67*, 257–269.
- (66) Lin, H.; Li, L.; Zhao, M.; Huang, X.; Chen, X.; Li, G.; Yu, R. Synthesis of High-Quality Brookite TiO₂ Single-Crystalline Nanosheets with Specific Facets Exposed: Tuning Catalysts from Inert to Highly Reactive. *J. Am. Chem. Soc.* **2012**, *134*, 8328–8331.
- (67) Cao, Y.; Li, X.; Bian, Z.; Fuhr, A.; Zhang, D.; Zhu, J. Highly Photocatalytic Activity of Brookite/Rutile TiO₂ Nanocrystals with Semi-Embedded Structure. *Appl. Catal. B Environ.* **2016**, *180*, 551–558.
- (68) Suri, R. P. S.; Liu, J.; Hand, D. W.; Crittenden, J. C.; Perram, D. L.; Mullins, M. E. Heterogeneous Photocatalytic Oxidation of Hazardous Organic Contaminants in Water. *Water Environ. Res.* **1993**, *65*, 665–673.
- (69) Ahuja, S.; Kutty, T. R. N. Nanoparticles of SrTiO₃ Prepared by Gel to Crystallite Conversion and Their Photocatalytic Activity in the Mineralization of Phenol. *J. Photochem. Photobiol. A Chem.* **1996**, *97*, 99–107.
- (70) Lin, X.; Xing, J.; Wang, W.; Shan, Z.; Xu, F. Photocatalytic Activities of Heterojunction Semiconductors Bi₂O₃ / BaTiO₃: A Strategy for the Design of Efficient Combined Photocatalysts. *J. Phys. Chem. B* **2007**, *111*, 18288–18293.
- (71) Moulis, F.; Krysa, J. Photocatalytic Degradation of Several VOCs (n-Hexane, n-Butyl Acetate and Toluene) on TiO₂ Layer in a Closed-Loop Reactor. *Catal. today* **2013**, *209*, 153–158.
- (72) Liao, Y.; Xie, C.; Liu, Y.; Chen, H.; Li, H.; Wu, J. Comparison on Photocatalytic Degradation of Gaseous Formaldehyde by TiO₂, ZnO and Their Composite. *Ceram. Int.* **2012**, *38*, 4437–4444.
- (73) Qureshi, M.; Takanabe, K. Insights on Measuring and Reporting Heterogeneous Photocatalysis: Efficiency Definitions and Setup Examples. *Chem. Mater.* **2017**, *29*, 158–167.
- (74) Buriak, J. M.; Kamat, P. V.; Schanze, K. S. Best Practices for Reporting on Heterogeneous Photocatalysis. *ACS Appl. Mater. Interfaces* **2014**, *6*, 11815–11816.
- (75) Alfano, O. M.; Cassano, A. E.; Marugan, J.; Grieken, R. van. Fundamentals of Radiation Transport in Absorbing Scattering Media. In *Photocatalysis Fundamentals and perspectives*; Schneider, J., Bahnemann, D., Ye, J., Puma, G. L., Dionysiou, D. D., Eds.; The Royal Society of Chemistry, 2016; pp 351–366.
- (76) Cassano, A. E.; Martin, C. A.; Brandi, R. J.; Alfano, O. M. Photoreactor Analysis and Design: Fundamentals and Applications. *Ind. Eng. Chem. Res.* **1996**, *34*, 2155–2201.
- (77) Brucato, A.; Rizzuti, L. Simplified Modeling of Radiant Fields in Heterogeneous Photoreactors. 2. Limiting “Two-Flux” Model for the Case of Reflectance Greater Than Zero. *Ind. Eng. Chem. Res.* **1997**, *36*, 4748–4755.

- (78) Motegh, M.; Cen, J.; Appel, P. W.; van Ommen, J. R.; Kreutzer, M. T. Photocatalytic-Reactor Efficiencies and Simplified Expressions to Assess Their Relevance in Kinetic Experiments. *Chem. Eng. J.* **2012**, 207–208, 607–615.

6. Summarizing Discussion

Publications

Journal Publications

Megatif, L.; Dillert, R.; Bahnemann, D. W., Reaction Rate Study of Photocatalytic Degradation of Dichloroacetic Acid in a Black Body Reactor, *Catalysts* **2019**, Submitted

Megatif, L.; Dillert, R.; Bahnemann, D. W., Determination of the Quantum Yield of Heterogeneous Photocatalytic Reactions Employing a Black Body Photoreactor, *Catalysis Today* **2019**, in the press, doi:10.1016/j.cattod.2019.06.008

Megatif, L.; Dillert, R.; Bahnemann, D. W., A Method to Compare the Activities of Semiconductor Photocatalysts in Liquid-Solid Systems, *Chemphotochem*, **2018**, 2, 948-951

Arimi, A.; Megatif, L.; Granone, L. I.; Dillert, R.; Bahnemann, D. W., Visible-light Photocatalytic Activity of Zinc Ferrites, *Journal of Photochemistry and Photobiology A: Chemistry* **2018**, 366,118-126

Megatif, L.; Ghozatloo, A.; Arimi, A.; Shariati-Niasar, M., Investigation of Laminar Convective Heat Transfer of TiO₂-CNT Hybrid Water Base Nano Fluid, *Experimental Heat Transfer Journal* **2016**, 29 (1), 124-138

Megatif, L.; Ghozatloo, A.; Shojaiee, M.; Shariati-Niasar, M., Comparison of Different Methods for the Synthesis of TiO₂-CNT Hybrid Nanoparticles, *Journal of Nanomeghias (in Persian)*, **2015**, 1(4), 231-238

Book Chapter

Megatif, L.; Arimi, A.; Dillert, R.; Bahnemann, D. W., Reactors for Artificial Photosynthesis in Heterogeneous Systems, In *Artificial Photosynthesis*, World Scientific Series in Current Energy Issues: Solar Energy, Volume 6, Submitted

Oral Presentations

L. Megatif, R. Dillert, D.W. Bahnemann, “Method to Compare the Activities of Semiconductor Photocatalysts in Liquid Systems”, Russian-German Workshop, National University of St. Petersburg, October 2017, St. Petersburg, Russia.

L. Megatif, R. Dillert, D.W. Bahnemann, “Comparison of the Photocatalytic Activity of Different Photocatalysts by Applying a “Black Body” Reactor”, 6th International

Publications

Conference on Semiconductor Photochemistry (SP6), Carl von Ossietzky University, September 2017, Oldenburg, Germany.

L. Megatif, R. Dillert, D.W. Bahnemann, “Photocatalytic Degradation of Dichloroacetic Acid in a Black Body Reactor as a Standard Method to Compare the Activities of Photocatalysts”, New Photocatalytic Materials for Environment, Energy and Sustainability 2 (NPM-2), July 2017, Ljubljana, Slovenia.

L. Megatif, R. Dillert, D.W. Bahnemann, “Photocatalytically Active Adsorbent for Water Treatment”, Russian-German Workshop, Laboratorium für Nano- und Quantenengineering (LNQE), Leibniz University Hannover, November 2016, Hannover, Germany.

Poster Presentations

L. Megatif, R. Dillert, D.W. Bahnemann, “A Standard Method to Compare the Activities of Photocatalysts”, Nanoday 2017, Laboratorium für Nano- und Quantenengineering (LNQE), Leibniz University Hannover, September 2017, Hannover, Germany.

L. Megatif, R. Dillert, D.W. Bahnemann, “Comparison of the Photocatalytic Activity of Different Photocatalysts by Applying a “Black Body” Reactor”, 6th International Conference on Semiconductor Photochemistry (SP6), Carl von Ossietzky University, September 11-14, 2017, Oldenburg, Germany.

A. Arimi; L. Megatif; L.I. Granone, R. Dillert, D.W. Bahnemann, “Ferrites for Photoelectrochemical Water Splitting”, DFG SPP 1613 Summer School, Hotel Teikyo, September 2016, Berlin-Schmoeckwitz, Germany.

Curriculum Vitae

Personal data

Name **Megatif, Lena**

Address **Podbielskistrasse. 116, 30177 Hannover**

Date of birth **11.12.1986**

Place of birth **Shiraz, Iran**

Education

Since 10/2015 PhD Student at the Leibniz University of Hannover, Institute of Technical Chemistry, Hannover, Germany
 PhD Thesis: “Development of New Reactors for the Solar Treatment of Polluted Aquifers by Photocatalytic Treatment”

10/2010 – 02/2013 Master of Science in Chemical Engineering (M.Sc.Eng) at College of Engineering, University of Tehran, Tehran, Iran
 Major: Design of separation processes
 Master Thesis: “Fabrication of Nano-Fluids by Synthesis of Metal Oxide-Carbon Nanotube Hybrids”

10/2006 – 09/2010 Bachelor of Science in Chemical Engineering (B.Sc.Eng) at School of Chemical and Petroleum Engineering, Shiraz University, Shiraz, Iran
 Major: Refinery, Petrochemical and Gas Industries
 Bachelor Thesis: “Enhance oil recovery (EOR) by CO₂ injection”

06/2005 Diploma and Pre-University at Haj Bahador (Grashi) High School (National Organization for Development of Exceptional Talents (NODET))
 Major: Mathematical Sciences

Work Experience

11/2014 – 01/2015 Process engineer, Wastewater Treatment Plant of Sepahan Oil Company, Isfahan, Iran

10/2013 – 10/2014 Adviser, Supervision of Master degree Thesis (Fabrication and characterization of the mixed matrix gas separation membranes containing carbon nanotubes-metal hybrids), University of Tehran, Tehran, Iran

09/2012 – 12/2012 Intern, Federal Institute for Material Research and Testing (BAM), Berlin, Germany

07/2010 – 09/2010 Intern, Petrochemical Industries Design & Engineering Company, Shiraz, Iran

